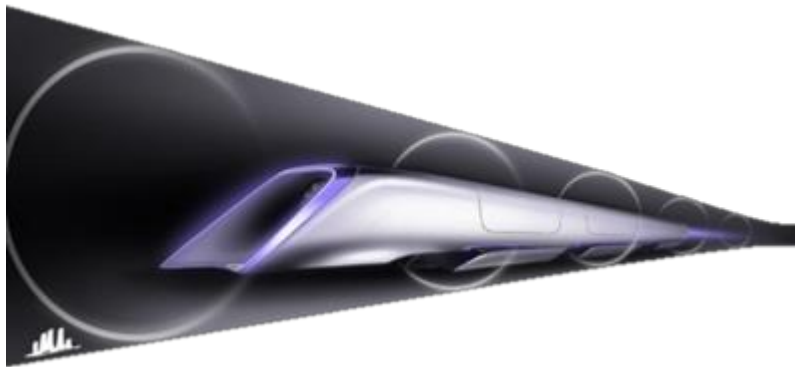




An Experiment on Compliant Air Skates

June 2016

FINAL DESIGN REPORT



"Flick & Swish"

Sam Feldtkeller sfeldtke@calpoly.edu

Cody Anderson cander43@calpoly.edu

Kevin Daily kddaily@calpoly.edu

Eliana Stefani estefani@calpoly.edu

Statement of Disclaimer

Since this project is a result of a class assignment, it has been graded and accepted as fulfillment of the course requirements. Acceptance does not imply technical accuracy or reliability. Any use of information in this report is done at the risk of the user. These risks may include catastrophic failure of the device or infringement of patent or copyright laws. California Polytechnic State University at San Luis Obispo and its staff cannot be held liable for any use or misuse of the project.

Table of Contents

List of Tables

List of Figures

Abstract

Chapters

1 Introduction

- 1.1 Project Management
- 1.2 Specifications

2 Background

3 Design Development

- 3.1 Discussion of Conceptual Designs
- 3.2 Concept Selection
- 3.3 Supporting Preliminary Analysis
- 3.4 Any proof of concept analysis or testing

4 Description of the Final Design

- 4.1 Overall Description/Layout with labeled solid model
- 4.2 Detailed Design Description
- 4.3 Analysis Results (Details in Appendix)
- 4.4 Cost Breakdown (prototype, mass manufacturing)
- 4.5 Material, Geometry, Component Selection
- 4.6 Flowcharts, Schematics, Pseudo Code, Wiring Diagrams
- 4.7 Refer to any manufacturing drawings in appendix!
- 4.8 Any special safety considerations
- 4.9 Any maintenance and repair considerations

5 Product Realization

- 5.1 Description of the various manufacturing processes employed (with photos).
- 5.2 Description of how your prototype might differ from your planned design.
- 5.3 Recommendations for future manufacturing of your design

6 Design Verification (Testing)

- 6.1 Test Descriptions with photos
- 6.2 Specification Verification checklist or DVPR

7 Conclusions and Recommendations

Appendices

- Appendix A: QFD, Decision Matrices etc. (As appropriate)
- Appendix B: Final Drawings (Assemblies with Bill of Materials, detailed part drawings)
- Appendix C: Detailed Supporting Analysis
- Appendix D: Operators Manual with Safety Guidelines
- Appendix E: Elon Musk's Hyperloop White Paper
- Appendix F: SpaceX Hyperloop Competition Rules as of 10/20/2015
- Appendix G: SpaceX Hyperloop Competition Tube Specifications as of 10/20/2015

TABLES

Table 1: List of Air Skate Requirements
Table 3A: FEA mesh convergence data
Table 3B: FEA mesh quality analysis results
Table 3C: FEA bending stress and deflection results
Table 3D: FEA model and hand calculation comparison
Table 3E: Bill of Materials and Cost for Concept
Table 4A: Bill of Materials and Cost for Prototype
Table C: Quantity, Vendors and Pricing

FIGURES

Figure 2A: Demonstration of Airflow
Figure 2B: Porous Air Bearing
Figures 3A, 3B: Concept Sketches
Figures 3D, 3E, 3F, 3G, 3H: Pod Dimensions
Figures 3I, 3J: Air Skate Concept models
Figures 3K: Flowrate as a function of air gap
Figures 3L: FEA boundary conditions
Figure 3M: FEA depiction of Mesh on model
Figures 3N, 3O: Proof of Concept
Figure 4A: Air Supply & Regulation
Figure 5A: Top and bottom half of skirt molds.
Figure 7A: Testing in Progress
Figure A: Quality Function Development
Figure B1: Assembly of Prototype
Figure B2: Bill of Materials
Figure B3: Top Plate Drawing
Figure B4: Bottom Plate Drawing
Figure B5: Routed mold model
Figures C1, C2, C3, C4: Example flowrate calculations
Figure C5: EES Code
Figure C6: Parametric study results
Figure C7: Example calculations for maximum plate bending stress and deflection
Figures C8, C9: Additional FEA boundary conditions
Figures C10, C11: Mesh convergence studies
Figures C12, C13: Mesh quality control
Figures C14, C15, C16, C17: Results for maximum bending stress and deflection

ABSTRACT

There is currently a gap in the market of train levitation systems: wheeled trains and MagLev trains exist, but none utilize the low friction and high efficiency aspect of trains levitated by air skates. An air skate, is an air bearing that uses a pressure difference along its annular body to create a thin flow of air which is strong enough to "levitate" the weight of the skate. We have designed a compliant air skate that can glide over 0.04[in] defects in surfaces without touching down. After having made compliant skirts out of fiberglass and silicone, our setup of three air skates was easily capable of levitating 300[lb] while maintaining 3[psi] evenly split at the skates with an equivalent air flowrate of 3 [ft³/min].

Chapter 1: INTRODUCTION

On August 12, 2013, Elon Musk released a white paper on the Hyperloop, his concept of high-speed ground transportation. His idea of the Hyperloop is a near-frictionless interface train contained inside a vacuum tube. Musk envisioned a train levitating on air bearings to create the frictionless interface. The tube would be evacuated by pumps spaced out along the length of the tube to create a low pressure system that would reduce drag at high speeds. Elon states that, "If we are going to make a massive investment into a new transportation system, the return should by rights be equally massive. Compared to the alternatives, it should ideally be: safer, faster, lower cost, more convenient, immune to weather, resistant to earthquakes, and not disruptive to those along the route." The idea of the Hyperloop has the potential to revolutionize the world of travel. Imagine living in San Francisco and having the option of commuting to Los Angeles every day for work in under an hour. While the idea of the Hyperloop sounds like a dream, there are many technical challenges that need to be solved before this idea can become a reality. In order to accelerate the development of a functional prototype and to encourage student innovation, SpaceX hosted a competition to design and build a half-scale Hyperloop Pod. SpaceX has plans to build a 1-mile test track to test these prototypes by the summer of 2016. Specifically, our team has chosen to focus on what we think is the most challenging and innovative concept: the levitation subsystem, the enabling technology of the pod. Our team began by following the structure laid out by the Hyperloop challenge as well as the formal design process for senior project. Our goal was to design, build, and test a functional high speed levitation subsystem that satisfies the criteria in table

1.1 Project Management

Fall 2015: Meet, Greet, and Define

Our group is composed of four mechanical engineers, two of which have a general concentration, the other two have a mechatronics concentration. With this in mind, group responsibilities and tasks were delegated based on interests. For example, when investigating modes of levitation, all members chose an area of interest to delve into, feasibility calculations were then done on the various levitation mechanisms. Once these calculations were analyzed, our final choice was made

as a group on which to follow through with. Task delegations proceeded much in this manner for the majority of the project.

Because the scope of this project is so large, our team spent substantial time understanding the big picture of what the Hyperloop is about. We read over the literature provided by SpaceX which included: Elon Musk's white paper on the Hyperloop, Hyperloop challenge rules and guidelines, and the tube specifications which were released as a draft to illicit feedback on October 7th and then updated to a working draft on October 20th (all of which can be seen in Appendices E-G). This was important in order to understand the design criteria as well as any previous design ideas. There was also a forum hosted by Blackboard where teams could post questions to SpaceX or other competitors. Reading through this forum was important to broaden the team's understanding of the scope of the project as well as see what other competitors were considering for solutions and what problems they were running into.

Winter 2016: Conceptualize and Prove

Sam and Kevin worked on the majority of the analysis for sizing the air skate components, understanding the flow field generating lift, and tolerance analysis for the type surface that the air skate would be able to accommodate. In order to understand and verify some of the calculations, the group built and tested proof of concept builds. This information helped finalize the design. Eliana focused on compiling the information to be delivered to the sponsor as well as cost analysis and overall group organization. Cody researched different manufacture methods as well as current products on the market.

Spring 2016: Build and Test

The entire team worked on machining the plates for the three air skates. This was done in multiple shifts over the course of two weeks. After the steel was machined, the mold for the skirt was made. Kevin and Sam worked from Solidworks to generate a toolpath. Polyurethane foam was used for the mold and was routed out using a ShopBot CNC router. Once the mold was routed, Kevin sanded, smoothed, and waxed the surfaces down. Once the mold was prepared, Sam and Kevin molded three skirts over the course of two weeks and multiple attempts. Assembly was done by the team. Cody and Eliana worked on the poster for Exposition. Testing was performed by Kevin and Sam.

1.2 Design Requirements and Specifications

After thorough reading of the competition guidelines, adjusting for feasibility throughout the project, and working around \$0 in funding, we came up with a set of requirements based on what we felt was necessary and feasible. Our qualitative objectives were:

- Must be stable and balanced on its own
- Won't burn or rip if compliant air-skate touches down

Our qualitative objectives were:

Table 1: Listed are the requirements for the air bearing

Spec #	Parameter	Requirement/Target	Tolerance
1	Weight	200 [lbs/ft ²]	max
2	Lift (load)	250 [lbs/ft ²]	min
3	Ride Height	0.005 [in]	0.005
4	Compliance	0.04 [in] roughness	max
5	Operating Pressure	5 [psi]	max
6	Supply Pressure	100 [psi]	max
7	Cost Estimate	\$500	max

Chapter 2: BACKGROUND

In our efforts to focus on levitation as a means to support the pod on its journey, we turned our attention to some existing methods. For instance, there are already a number of high and low speed trains that are able to travel in nearly frictionless conditions on the ground by way of Magnetic Levitation. We came across two main forms of Magnetic Levitation: Electromagnetic Levitation uses magnets on the train to attract to passive metal on the tracks; Electrodynamic Levitation uses electromagnets on the track to repel and pull forward permanent magnets on the train. The team also began to explore the use of fluid bearings. The idea of fluid bearings can be seen in journal bearings in cars, sculptures of large heavy objects being supported on a stream of water, and more simplistically, a hockey table. The example of a hockey table most closely represents Elon Musk's proposed method of support and would be the lowest friction option of fluid bearings, but little research is published on the performance of air bearings at high speeds or in a partial vacuum.

Looking into air bearings further we found that the two main types of air bearings are aerodynamic and aerostatic bearings. Aerostatic air bearings use pressurized supplied air to create a film between the bearing surfaces. Aerodynamic air bearings require at least one surface to be operating at a high speed. It is this fast movement that forces a lubricating layer of air flow along its own surface much like a journal bearing. By nature, these air bearings cannot exist at low speeds. Aerostatic air bearings are able to operate even when the bearing is not in motion hence, aero "static". We decided to pursue aerostatic bearings since our final result would need to be able support weight while not moving as well as while moving at high speeds.

Different types of aerostatic air bearings can be simplified into rigid, compliant, and skirted. Based on our objectives, rigid bearings would be preferable as they can support the largest load, but they would not be able to handle the roughness requirement. Skirted bearings, such as a traditional

hovercraft, would be able to very easily handle the roughness, but not the load. This leaves us with the compliant air bearings which provide the best of both worlds.



Figure 2A: Example of air flow in a compliant air bearing. The bearing is compliant because when the skirt meets a fluctuation in the ground surface, it can deflect to accommodate the step.

As seen in Figure 2A, compliant air bearings levitate a mass based on air entering into a pliable air membrane, or skirt. This skirt slightly inflates as air enters from the top and then exists through holes into a middle chamber formed by the skirt and the ground. The air then follows along the path of least resistance out the bottom between the contact surface and the pliable membrane. The resultant air gap between these surfaces is what creates our desired frictionless levitation mechanism. Other choices included bearings such as porous air bearings as seen in Figure 2B. These bearings provide more lift with respect to the airflow that they require, however they fall into the rigid category and will not tolerate fluctuations in a surface.

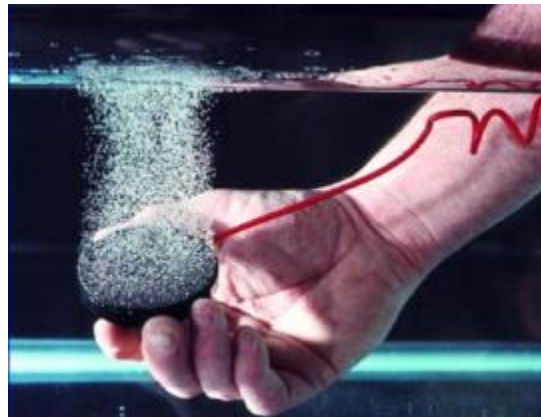


Figure 2B: Porous Media air bearing from New Way Air Bearings

Picture source:

http://www.newwayairbearings.com/sites/default/files/new_way_application_and_design_guide_%20Rev_E_2006-01-18.pdf

Airfloat is a company that uses state of the art air-bearing technology for moving heavy loads across industrial floors. Airfloat uses circular compliant air-skates at low speeds. In our attempt at a high-speed application, we used their design for inspiration for the initial shape of a compliant air bearing.

Chapter 3: DESIGN DEVELOPMENT

We wanted to be as innovative and creative as possible even though the technical aspects limited most of our options. Funding was also a large limiting factor as we did not have a direct sponsor. SpaceX made it a requirement that a team must present preliminary designs in Texas at design weekend to be eligible for any grants, and even then money was not guaranteed. Funding would have come from individual sponsors that were encouraged to fund full pod designs. Initially we were planning on building an entire levitation system, able to operate without a wall tether, but since traveling to Texas was not practical and did not guarantee sponsorship, we narrowed the scope to an experiment in air-bearings to better match our budget. The feasibility of the scope of the entire pod being built was greatly diminished when three quarters of the extracurricular team backed out.

We did however begin our designing process using the structure and specifications released by SpaceX regarding tube design and final pod requirements in order to be competitive. Even though we eventually branched away from the SpaceX competition, and those specifications were no longer necessarily a driving factor, we chose to keep as many of the SpaceX parameters as possible to give our project shape and direction. We ended up performing an experiment in air bearings in the hope of designing a bearing that could be incorporated into a Hyperloop competition pod. This change of scope not only made this project more feasible financially, but it also allowed us to delve deeper into the heart of the project and gave us sufficient time to focus on the most important aspect - the air-skate itself. Ultimately, our goal became to demonstrate an air-skate capable of floating across the floor in the engineering building with a single push, as a proof of concept.

3.1 Full Pod Concept Sketches

While still working with SpaceX on the Hyperloop, we were designing concepts for a full pod. The following sketches, 3A-3C represent these pod designs.

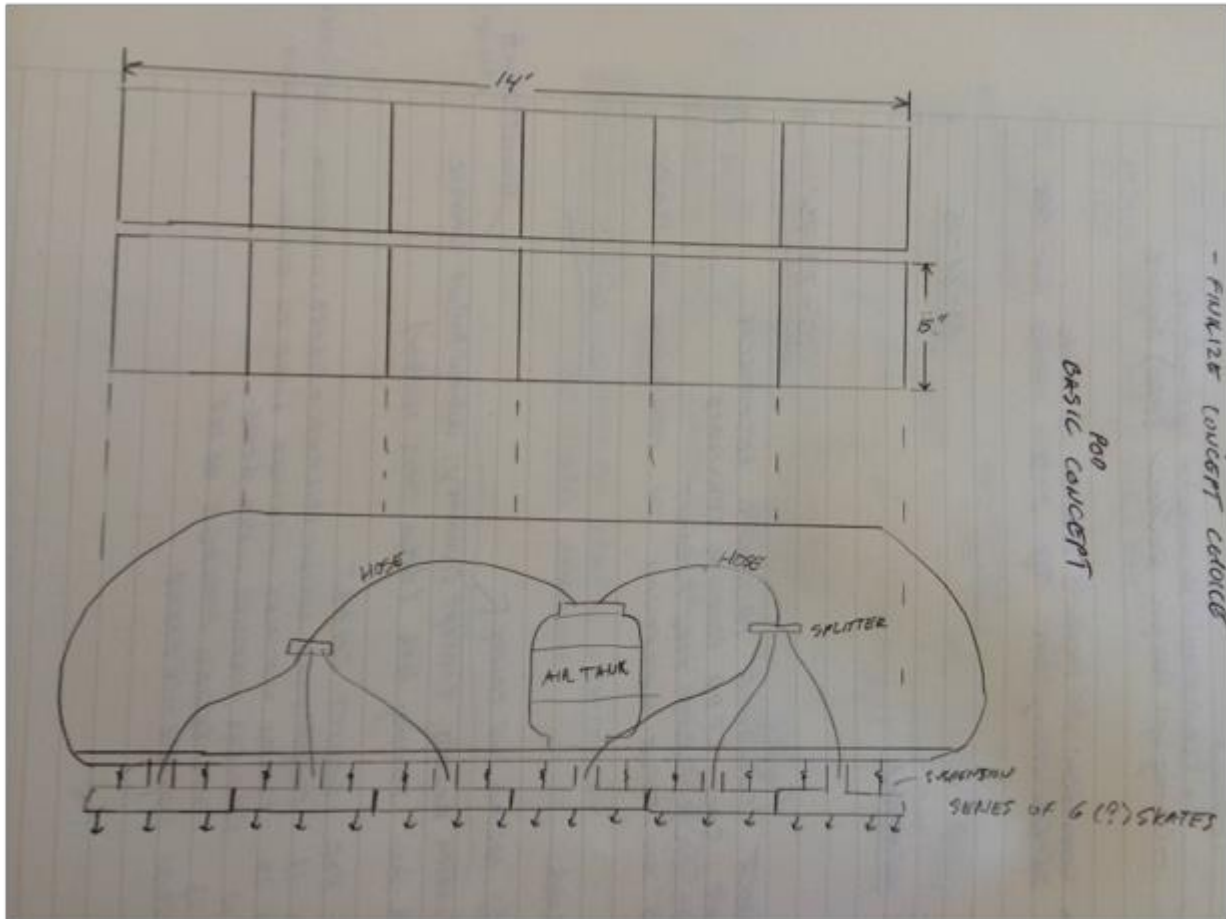


Figure 3A: Basic pod layout visual. A series of skates using compressed air in two rows travel along the aluminum rails.

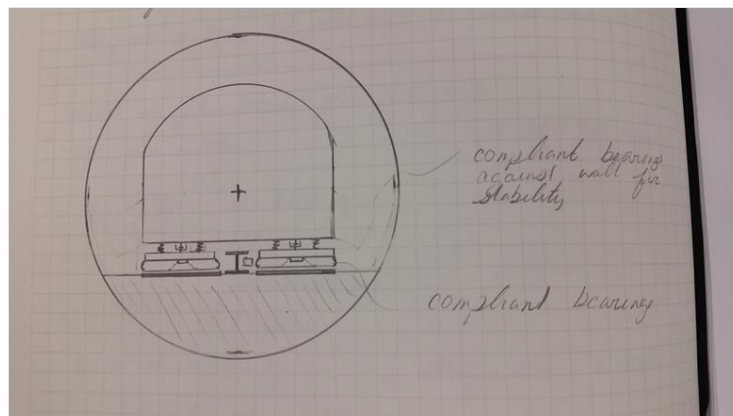


Figure 3B: Section view of pod. Compliant air bearings work in correlation with aluminum sub-track. Option for lateral air bearings against tube or center rail.

Pod dimensions for Figures 3D-3H: 14[ft] long; 50[in] wide; 50[in] tall. This design had three oblong compliant air-skates per side, totaling 6 skates per pod; skates were 12[in] wide and 24[in] long. See below for pod sketches.

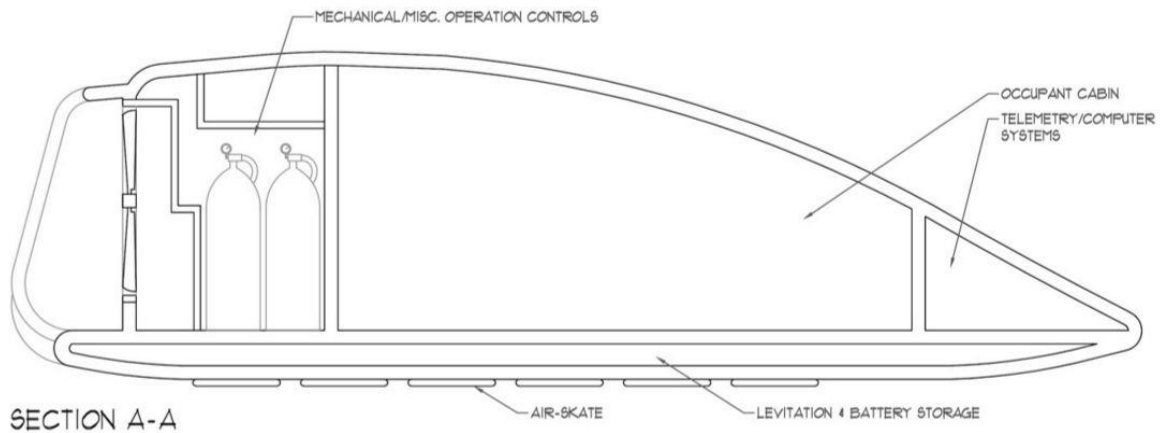


Figure 3D: Sketch of possible pod interior side profile. There will be up to 8 tanks of compressed air, and instead of the 6 skates shown on the side, there will be 3 oval shaped skates.

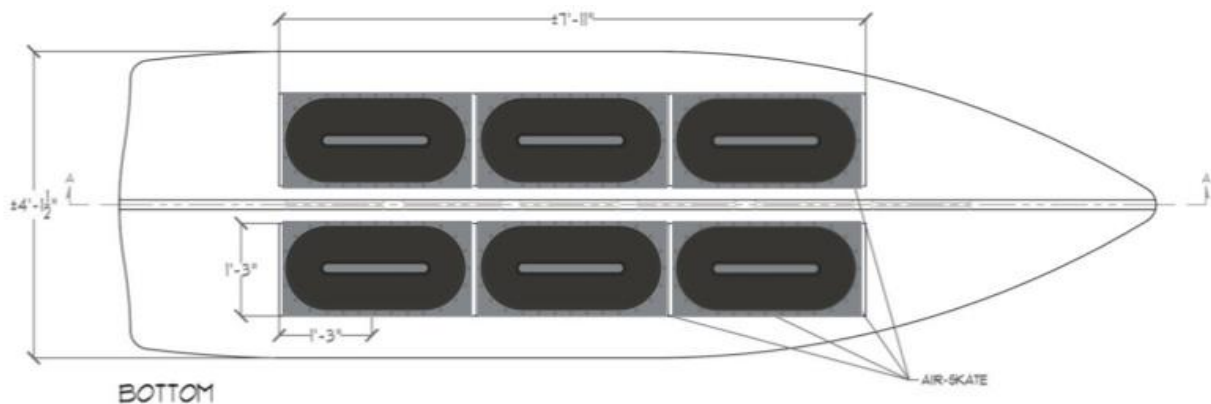


Figure 3E: Sketch of possible pod bottom view. Shown are the oval shaped skates for reference.

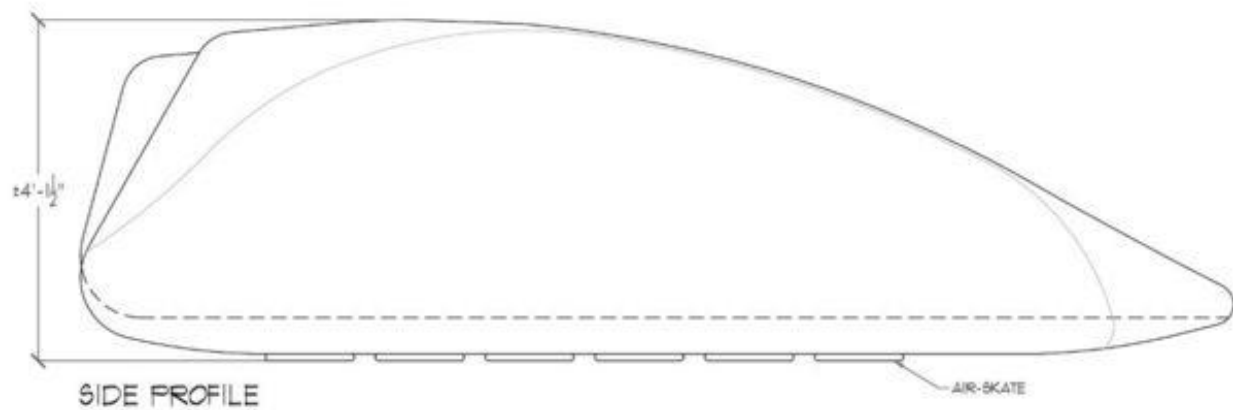


Figure 3F: Sketch of possible pod side profile

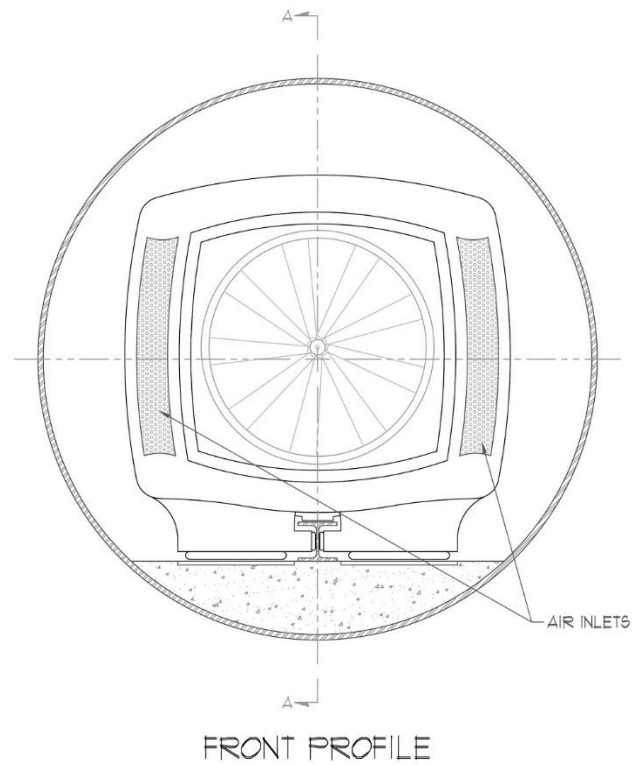


Figure 3G: Sketch of possible front pod profile in tube

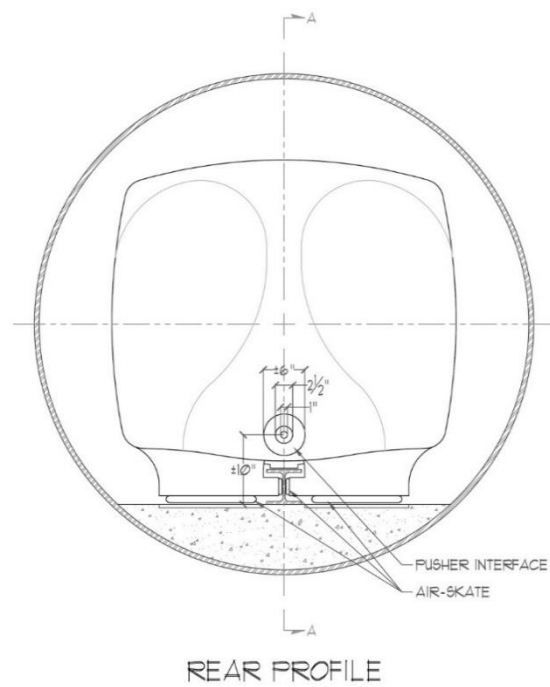


Figure 3H: Sketch of possible rear pod profile in tube

The following solid models, Figures 3I-3J, show the initial models for the air-skates when the plan was still to make an oblong, unidirectional skate.

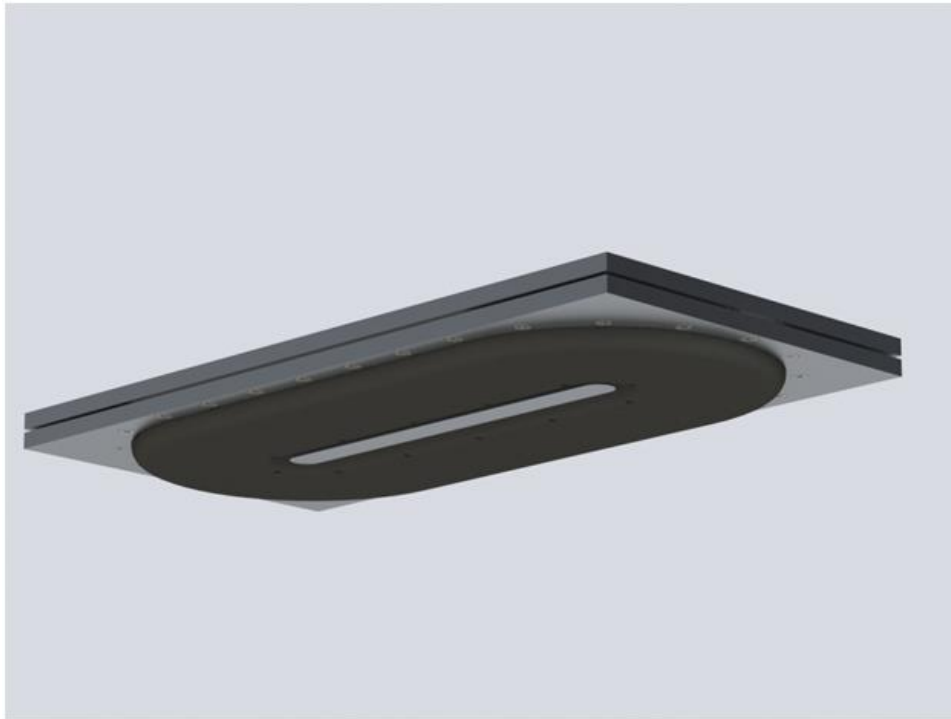


Figure 3I: Air-skate bottom: pliable skirt releases high pressure air from the inside; air slips out from under skirt supplying lift.



Figure 3J: Side view showing bolt depth and size, air inlet nozzle, as well as pliable membrane interior on the bottom. All sketches made in AutoCAD.

3.2 Concept Selection

While we were still aiming to compete at SpaceX's Hyperloop competition, we chose to compete in the non-wheeled class. This meant we needed a form of levitation with absolutely no wheeled support and we selected ideas for this based on the given sub track layout. Since we needed passive coils in the track to make Mag-Lev work with Halbach Arrays, we couldn't pursue a Mag-Lev idea. This allowed us to choose for certain to design levitation via air-bearings. As discussed above, we selected air-bearings based on how they interfaced with the track. The compliant air bearing would work best based on the fact that it could tolerate variations in the track, such as roughness and even small steps in the track while still being able to tolerate high loads. This is because it combines the high load capacities of a rigid air bearing with the clearance capabilities of a skirted plenum (a traditional hovercraft style bearing).

3.3 Quantitative Analysis

Flow Rate Analysis

Our team modeled the interaction of the air-skates with the aluminum surface in the form of a simple fluid dynamics problem. Some assumptions that we made were: incompressible flow, flow between two parallel plates, 50% error in our calculated skate and track interfacing area, and also a 50% efficiency for the compressed air system. Some of the desired criteria from this analysis were air flowrate, pressure gradients to maintain a specific levitation height between the skates and track surface, and volume of air to maintain levitation for the length and duration of the pod's trajectory. See below for air-skate analysis. Flowrate in cubic feet per minute was calculated in the following Eq. 1, where h is half the height of the air gap, P is the effective pressure, L is the circumference of the annular area, μ is the dynamic viscosity, and l is the height of the air gap.

$$\dot{Q} = \frac{2h^3 PL}{3\mu l} \quad (1)$$

The effective pressure mentioned above is calculated according to Eq. 2 where the applied weight to the skate, F , is divided by the annular area of the skirt defined by the outer and the inner radius.

$$P = \frac{F}{\pi(r_o^2 - r_i^2)} \quad (2)$$

From figure C1 in appendix C, initial calculations for a single air-skate are present. Here, we estimated an air gap of 0.04[in]. With a boundary layer of 0.04[in], the required flow rate to maintain this height is relatively high for our capabilities. In appendix C, Figures C2 and C3 show our initial attempt at modeling our air-skate traveling at a speed of 30 mph. As seen in figure C3, we assumed the velocity profile was linear for simplicity's sake, and also that the pressure profile within the air gap is constant. These assumptions tend to oversimplify our model, since the results here are not exactly matching up with our static case. This first round of Couette flow analysis formed the basis for the program we made in EES, as shown in figures C4 through C6

Initially, calculations were done for an air layer height of 0.040[in]. Results due to this height showed us that we'd need an incredible volume of air to support levitation. Thus, our team made the decision based on research of existing air bearings, to decrease the effective air height layer to 0.010[in]. Because height is a third degree term in the flowrate calculation, the impact is quite large on flowrate (see figure 3K below). This new height gave us a much more reasonable required volume of compressed air, as well as a realistic flowrate.

For slow movement in a non-evacuated environment, "smart" or active suspension will not be needed because once sufficient airflow is achieved for levitation, the height at which the air-skate hovers above the ground is controlled by a negative feedback loop, inherent of the fluid dynamic system. At the required airflow, if the air-skate gets too close to the ground the flowrate will decrease and pressure will increase, thus increasing lift on the skate, and increasing the height at which the skate hovers above the ground. Visa versa, when the skate is too high above the ground, flowrate increases, decreasing pressure, the skate loses lift and descends toward the ground.

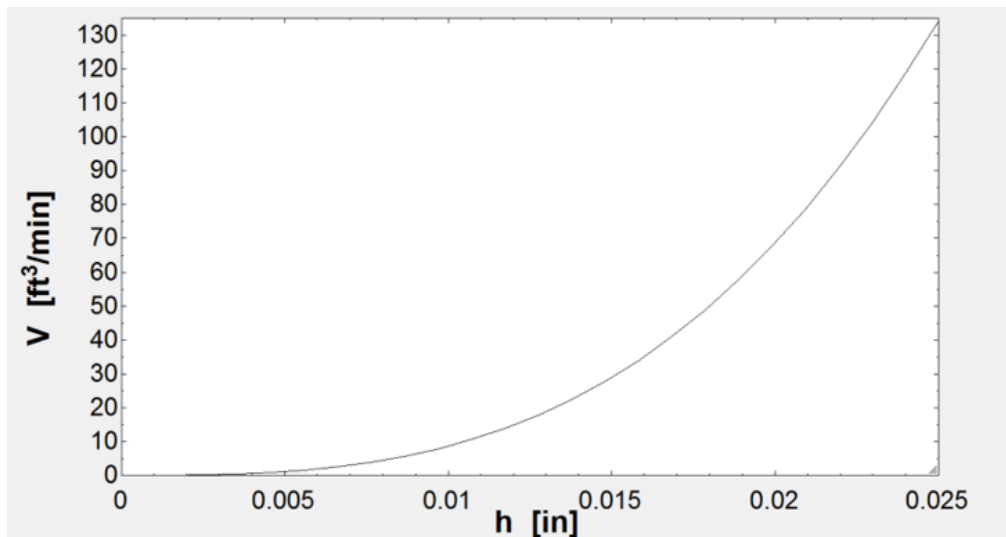


Figure 3K: EES plot showing required volumetric flow rate for a particular clearance height doe an annular diameter of 10 inches.

Plate Sizing Analysis

The effects of what the operating pressure has on plate deflection of the top plate from inside the air chamber of the air skirt is what is being analyzed here. More specifically, the entire top plate and the air hose line and pressure gauge connection locations were analyzed in terms of acceptable deflections and stresses (as seen in figure 3). Deflections should be no larger than 0.002[in]. The air bearing geometry in ABAQUS was simplified by creating a single part, with an extruded cut where the pressure is acting. Figure 5 shows the boundary conditions, figure 6 shows loading, and figures 3 and 4 show relevant dimensions. Material properties include those for aluminum, 6061-T6: a modulus of 10E6 psi and a Poisson's ratio of 0.33, a thickness of 0.375[in], and a radius of 5[in].

In order to calculate maximum bending stress and deflection of the plate, some simplifications were made. The plate was modeled as a circle without tapped holes to avoid complicated geometry.

Pressure load was estimated as an effective pressure as mentioned above in Eq. 2. For maximum bending stress, the following was used where t is the plate thickness, P is the effective pressure, and r is the outside radius.

$$\sigma_m = \frac{3Pr^2}{4t^2} \quad (3)$$

Maximum deflection was calculated using Eq. 4 below. Variables are identical to those in Eq. 3, but E is the modulus of the material.

$$\delta_m = \frac{0.174Pr^4}{Et^3} \quad (4)$$

For an example of the calculated values from Eq. 3 and 4, see appendix C, figure C7.

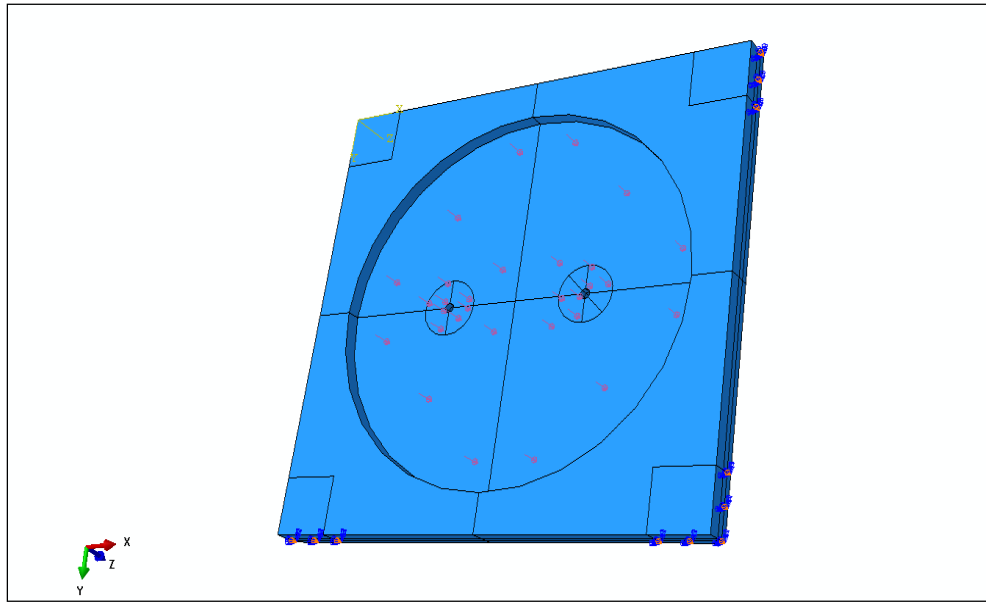


Figure 3L: Full model depicting applied pressure location along inner diameter on bottom surface of top plate.

Mesh Development & Analysis

The following includes our mesh convergence study based on bending stress (S11) and maximum deflection (U) by using standard quadratic hex element types without reduced integration. Various partitions were used to generate acceptable element shapes throughout the model. Circular partitions were made about the tapped holes. Vertical and horizontal partitions were also used within these circular partitions to isolate a desired element shape about the tapped holes.

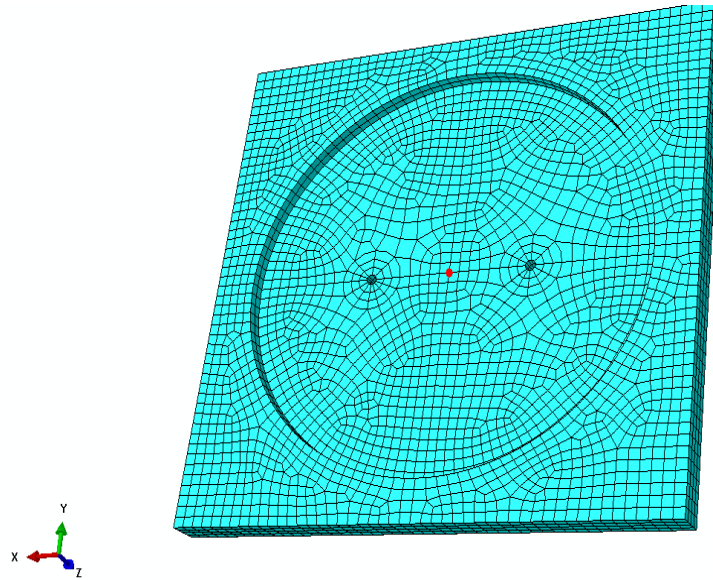


Figure 3M: Meshed part with convergence location indicated in center of part.

See figures C10 and C11 in appendix C for mesh convergence data. Various seed sizes were tested and the best fit for our model was 0.25[in] as seen in table 3A. Further quality control was performed on the mesh as seen in figures C12 and C13 in appendix C. Partitions about the threaded holes needed to be tuned in order to achieve an acceptable element shape, otherwise data about these locations would be skewed.

Table 3A: Mesh convergence data for full model. Highlighted is our chosen seed size based on element quality as seen in figure C10 and C11 in appendix C.

Number of Elements	Seed Size [in]	Stress, S11 [psi]	Max Deflection [in]	% Diff. S11	% Diff. U
218	2	397.616	0.001349	n/a	n/a
264	1.5	399.702	0.001371	-0.5	-1.6
580	1	412.858	0.001443	-3.3	-5.2
1738	0.5	423.686	0.001482	-2.6	-2.7
7350	0.25	431.448	0.001517	-1.8	-2.4
54267	0.125	433.08	0.001533	-0.4	-1.1

Table 3B: Element quality parameters of our full model compared to set limits for our convergence location with a seed size of 0.25 in. See figure C12 and C13 in appendix C.

	Limits	Model	%Difference
Number of elements	~	7350	~
Worst aspect ratio	5	4.33	-13%
Worst max angle	145	131.77	-9%
Worst min angle	35	43.56	24%

FEA Results

Results from our analysis were almost exact for the simplified model, but diverged for the full model. This is expected since the simple model is based on our hand calculations and the full model is not. However, the full model was expected to have these results because essentially more material is added and the boundary conditions changed. With that being said, results for the full model are within the 0.002[in] maximum deflection limit. As for the bending stress, this value is also well within the plastic deformation limit of the aluminum material. In the next iteration of our model, a more complex set of hand calculations would need to be performed for the full model. As of now, the results presented provide the senior project with verification to go forward with ordering parts for building the prototype.

Table 3C: Tabulated bending stress and maximum displacement for our hand calculations, initial model based on hand calculations, and the expanded, full model. See figures C14 through C17 in appendix C to see results mentioned here.

	Bending Stress [psi]	Max. Displacement [in]
Hand Calculations	443	0.00069
Simplified Model	437	0.00067
Full Model	636	0.00149

Table 3D: Differences in results for hand calculations, simplified model, and full model.

	Hand Calcs. vs Simplified	Hand Calcs. vs Full
% Diff S11	1.4	30
% Diff U	3.0	54

From the successful results produced from our FEA analysis, our group decided to steer away from aluminum to use steel instead. This provided us with cheaper, less thick, and equivalently weighted plates as a substitution.

3.4 Proof of Concept

Phase 1: The Preliminary Build of the Compliant Skate

Our first Proof of Concept was built with a compliant skirt made from an 8-inch diameter wheelbarrow inner tube. We bought 2'x4' board of Masonite for use as the rigid body of the skate. A 6.5[in] diameter disk was cut out of the Masonite board that would fit just below the center of the 6[in] inner diameter wheelbarrow tube. A second square foot piece was cut for the top board. We epoxied the disk to the tube so a small airtight chamber formed in the middle of the bottom side of the skate. Below the disk, we poked a circle of holes directed into this "chamber" so that air would be able to flow from the inner tube to the chamber pressurizing the bottom of the skate. The air supply system we built with: a quick-connect to attach to the wall supply, a needle valve that allowed us to regulate pressure, a tee-section where we attached a pressure gauge, a barb connection that allowed us to connect the air supply to a 1/4[in] air hose that then attached to the Schrader valve on the inner-tube. Once the air-supply system was set up, we ground off the hard, rigid lines from the inner tube, and got ready for testing. A summary of all parts and prices for this build can be seen in table 3A.

Table 3E: Bill of Materials for Compliant Skate using wheelbarrow tube & Masonite. All items purchased at Miner's Ace Hardware and are shown before tax. The total includes the addition of 8% sales tax.

Item	Description	Quantity	Cost (each)
Masonite	1/4" thick hardboard	1	\$5.99
Compliant Tube	400x6" wheelbarrow inner-tube	1	\$10.99
Epoxy	Glue for hardboard to inner-tube	1	\$4.99
Quick Connect	1/4" quick-connect air-supply plug	1	\$2.59
Needle Valve	Needle Valve to regulate flow	1	\$9.99
Thread Seal Tape	Thread Seal Tape to seal connections	1	\$1.59
Pipe Tee	1/4" tee to connect to pressure gauge	1	\$8.99
Pressure Gauge	Read downstream pressure	1	\$9.99
Barbed fitting	fixture to connect gauge to air-hose	1	\$1.95
Air Hose	5 [ft] of 1/4" air hose tubing	1	\$2.99
		Total	\$64.87

Phase 2: The Preliminary Testing of the Compliant Skate

During testing, we were able to successfully levitate the skate at just under 5[psi], while getting 250[lbf] of lift. We noticed that due to near no-load, the tube wasn't acting compliant at all, and thus touching the ground at some points causing a lot of friction. Since heavier loads would flatten

out the skate and make it more compliant, we went as far as to support our body weight on the skate, which worked successfully.

Phase 3: The Preliminary Results of the Rigid Skate

We learned two things while adjusting the pressure within the skate while sitting on said skate:

1. Lower pressure $\sim 5\text{-}10$ [psi]
 - a. PRO: Allowed for more compliance and a smoother ride over small bumps: had less kinetic friction.
 - b. CON: Was more sensitive to tilting, so if skate wasn't perfectly flat, it'd grip the ground and gain static friction.
2. Higher pressure $\sim 10\text{-}15$ [psi]
 - a. PRO: Less sensitive to touching ground when tilting, thus was less likely to be snagged by static friction.
 - b. CON: More kinetic friction due to bearing surface being less compliant and rubbing more on the ground.



Figure 3N: First Proof of Concept design using wheelbarrow inner tube and Masonite.

From the results of our compliant air-skate test rig, we decided to further our proof of concept by building two more test rigs. This time, however, they were to be rigid air bearings made from solid acrylic. This absence of compliant skirting enabled us to narrow in on the operating parameters and to better verify our analysis results. Instead of using a concrete surface, we tested these rigid skates on a micro flat surface with a high tolerance in flatness. When in operation, the rigid air-skates were able to smoothly traverse across the micro flat with only an initial nudge from the user. This verified for us that no frictional contact was being made. Upon inspection of the bottom of the rigid air-skates, no smudges or scratches were present to indicate contact with the surface. From here, we then made our measurements of the operating pressure from the pressure gauge,

and the air gap by use of a digital caliper. The results from our analysis can be seen in Figure 4C in appendix C. These numbers (pressure and air gap) were to be compared to with measured values from our test rigs. Our results for the air gap were no more than 15% off, and the operating pressure could only be estimated to be less than 2 [psi] due to the resolution of the pressure gauge. Although these results are for a rigid air-skate, the model is the same for a compliant air-skate. With these results, our group believes that the concept is verified in order to move forward with an actual prototype. Therefore, the compliant air-skate is the chosen prototype to advance to the high speed application scenario.

Our next designs were rigid, acrylic skates with different cavity sizes. The skate on the left with the 4[in] diameter cavity had a high pressure drop along the outside rim. The skate on the right with the 3/4[in] diameter was more stable than its larger cavity counterpart, and changes in pressure didn't affect its stability either. This skate operated at less than 2[psi], and had an air gap of 0.005[in]. This verified our initial calculations for static conditions and two flat plates.

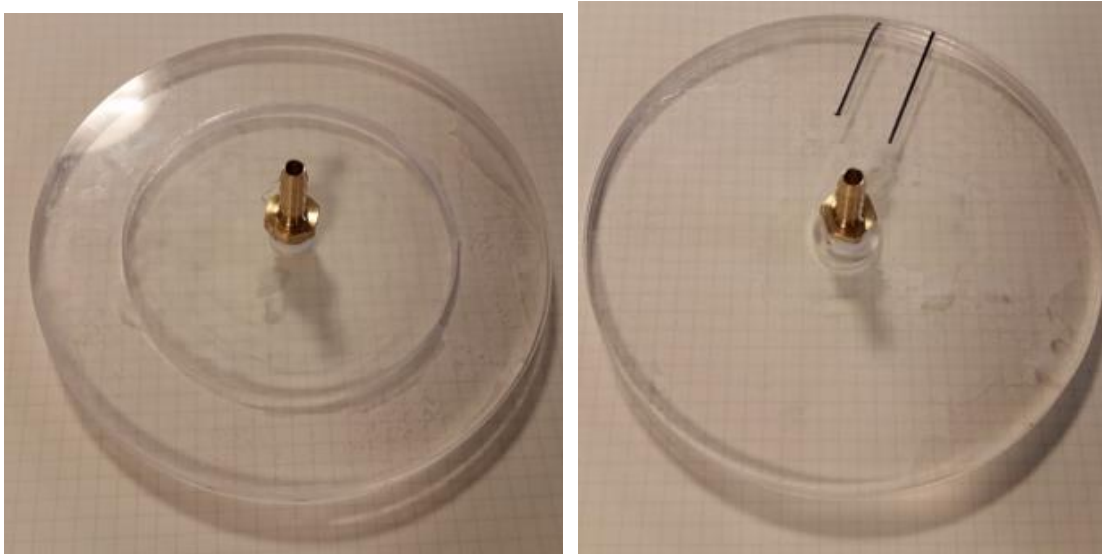


Figure 30: Acrylic skates with outside diameter of 6". Left to right: 4" and 3/4" diameter cavity.

Our proof of concept prototypes produced results that verified our initial analysis performed in our EES program. See figures C4 and C6 in appendix C. From our first prototype, the compliant inner tube air-skate, we learned that the operating pressure was roughly within the calculated value range (at most off by 15%). Estimations that were made for the analysis were annular area of the inner tube (effective contact area of tube and ground) and skate weight. In a controlled and safe manner where three assistants supported and balanced another user sitting on the skate, operation of the compliant air-skate was observed. While the user's center of gravity was maintained over the center of the air-skate, the user was able to smoothly glide over the ground with minimal applied load from an assistant. This indicated to us that the proof of concept test rig was successful in that it skimmed over the ground with minimal friction. Some problems with this test rig were that the inner tube had surface creases, lines, and ridges due to manufacturing and company logo. These

defects in surface smoothness as well as inconsistent stretching of the tube caused locations of frictional contact with the ground. Also, due to this surface smoothness issue, gaining an air gap measurement was near impossible. Even so, the test rig worked as anticipated based on analysis.

Chapter 4: Description of the Final Design

4.1 Design Description

The compliant air-skate we have designed will have a one square-foot foot print. Our concept of this air-skate consists of three main parts: body, skirt, and supply line. We plan to fabricate the body of the skate out of 12-gauge steel plate. The body itself will consist of three main parts: the upper plate, the bottom plate, and the skirt and support button. The top plate will be a 12[in] by 12[in] square with a centered 11[in] diameter ring of 12, 1/4-28 tapped holes. The top plate will have a 1/2" -13 tapped hole in the center as well as two more 1/4-18 NPSM tapped holes opposite each other spaced half-way between the center and the ring.

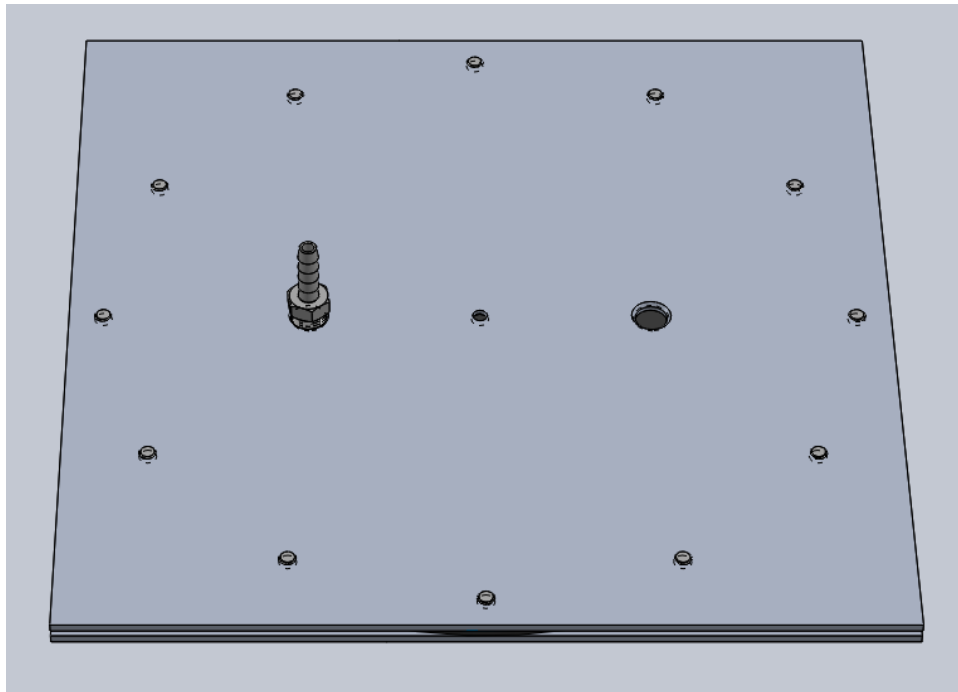


Figure 4A: Top canted view of solid model assembly showing air skate design

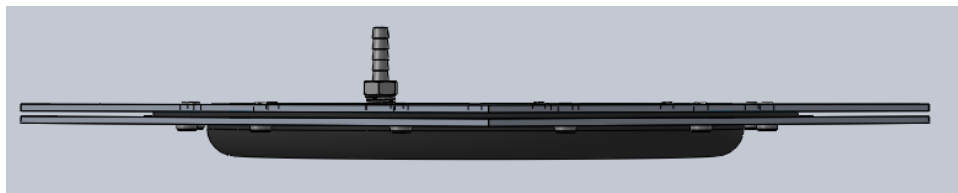


Figure 4B: Side view of air skate assembly

The bottom plate will again be a 12[in] by 12[in] square with a matching 11[in] ring of 12, 0.386[in] thru holes with an angled countersink. This plate however will have a 10[in] diameter

center hole cut out of it. The skirt support block will be a small circular piece with about a 2[in] diameter. This block will also have a matching 0.386 countersunk through hole cut into it.

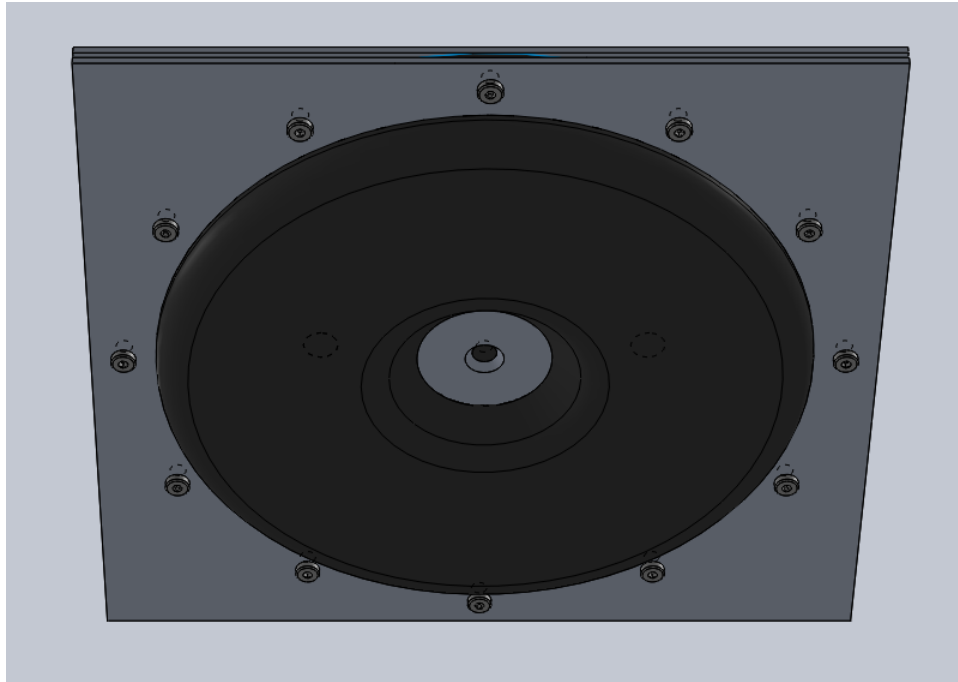


Figure 4C: Bottom canted view of solid model assembly

The skirt is made of a fiberglass silicon composite. Two layers of 6oz. Fiberglass suspended in silicon rubber offered the best combination of flexibility without stretching. This was compared to neoprene, rip stop nylon and flexible PVC vinyl. The body and the skirt will then be assembled together. The skirt will be sandwiched between the upper and lower plates and those plates would then be fastened together using 3/8-16 Torx head screws. The screws would run up through the bottom plate and skirt block, through the skirting material, and into the top plate where the screws would catch threads. The ballooned out portion of the skirt material and the top plate together should then form a donut shaped chamber. Other than the two NPSM holes in the upper plate and the eight additional holes in the skirt, the chamber should be airtight as the skirt material acts like a gasket sealing between the plates. A render of the skirt is shown in figure 4D below.

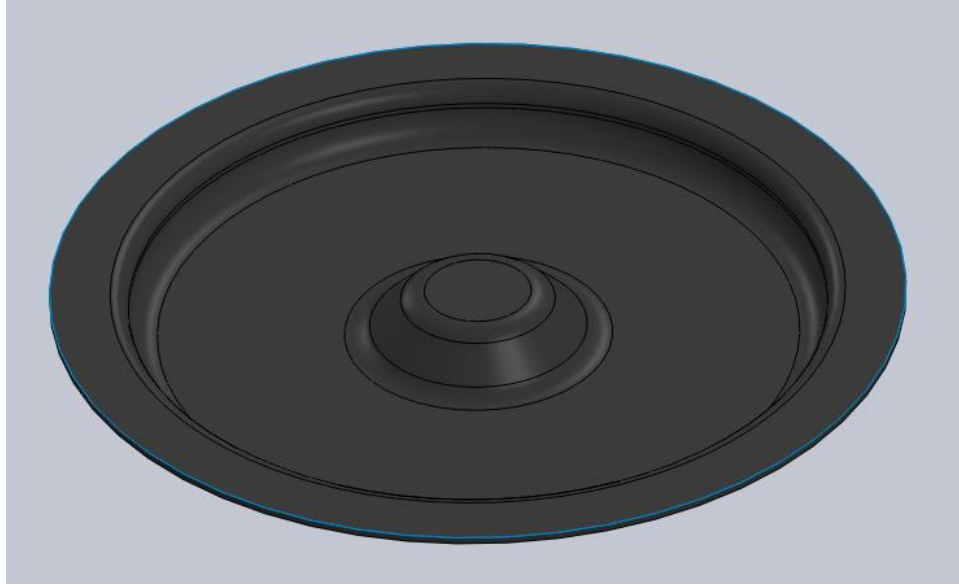


Figure 4D: Solid model of skirt

The supply line as seen in Figure 4A consists of all of the components required to supply, regulate, and measure airflow to the skate. This air supply manifold will consist of: a quick connect fitting to connect to wall supplied air, an inline flowmeter to measure the air flow, and a needle valve to control the air flow. This manifold will end in a barbed hose fitting which will connect to vinyl tubing. There will be a second barbed fitting sealed into one of the tapped NPSM holes on the top plate of the body to connect the other end of the tubing to. The second tapped NPSM hole will hold a pressure gauge in order to measure the pressure at the skate without needing to account for major/minor losses. Each of the male connectors going into the NPSM tapped holes will be wrapped in thread seal tape to ensure an airtight fitting.

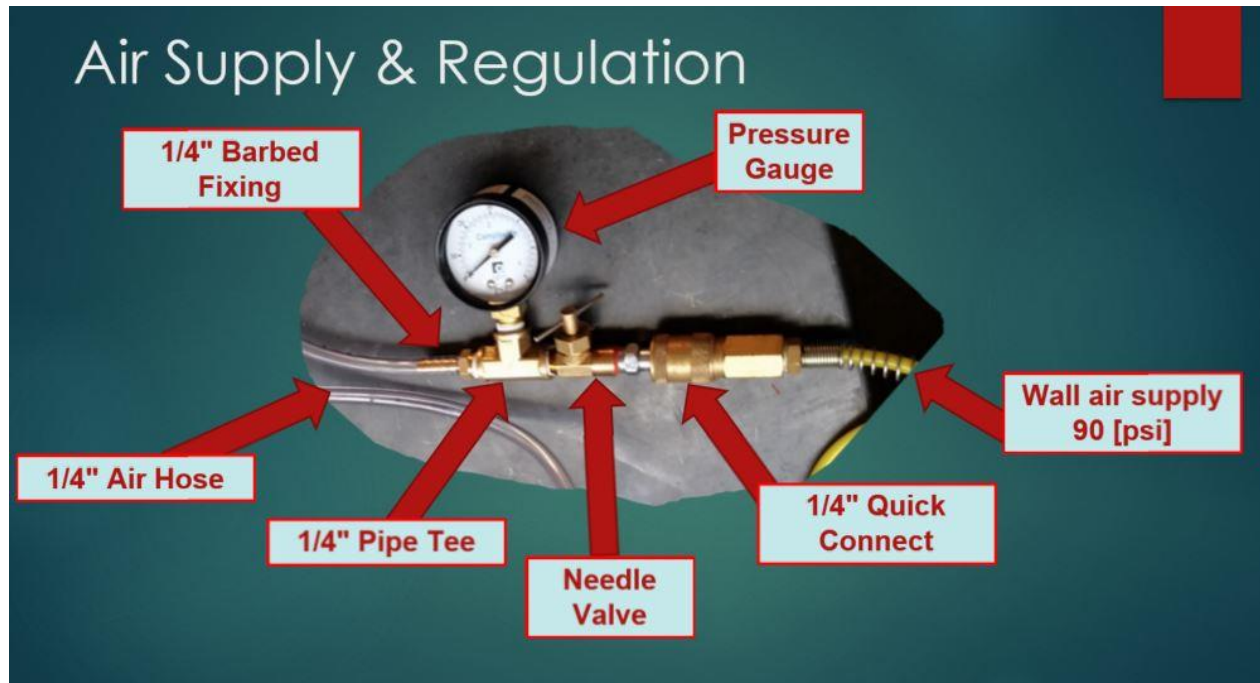


Figure 4E. Depiction of air supply manifold. Wall air enters the needle valve, which is opened enough to allow for the desired pressure in the air-skate. A pressure gauge then measures this pressure. Following down the air hose would be where the flowmeter is connected, which is then connected to the air-skate.

4.8 safety considerations

We will be using wall-supplied air at 90[psi], but past the needle valve, the maximum downstream pressure is 30[psi], and the air tubes handle 60[psi]. If wear from frictional contact of the skirt on ground causes rupture or blowout in the tube, it will cause a failure in lift, and will happen slowly due to the pre-made holes in the tube itself.

4.4 Supporting Information and Cost Analysis

Table 4A: Bill of Materials for prototype

Item	Description	Quantity	Cost (each)	Source
Steel Plate	12"x12"x1/8" plate stock	6	\$10.61	BNB Steel
Compliant Skirt	Silicone-Glass Fiber	3	\$0	Kevin Daily
Quick Connect	1/4" quick-connect to air-supply	1	\$2.59	Ace Hardware
Needle Valve	For flow regulation	1	\$9.99	Ace Hardware
Thread Seal Tape	Seal connections	1	\$1.59	Ace Hardware
Pipe Tee	1/4" "T" to connect pressure gauge	1	\$8.99	Ace Hardware
Pressure Gauge	Downstream pressure	1	\$16.05	McMaster

Barbed fixing	Fixture to connect tee to air-hose	1	\$1.95	Ace Hardware
Air Hose	5[ft] of ¼" air hose tubing	1	\$2.99	Ace Hardware
Flowmeter	In-Line flowmeter	1	\$65	McMaster
Screws	3/8" - 28 Cap Head	13	\$0.82	McMaster
<u>NET</u>	<u>Total Cost</u>	<u>19 items</u>	<u>\$241.01</u>	

Chapter 5: Product Realization

5.1 Manufacturing Processes

The majority of the manufacturing of the body of the skate was done on the mill and drill press. We started with stock steel plate squares 12[in]x12[in]x1/8[in] and mark out the bolt pattern. We then clamped the 2 plates together and match drilled the holes to the size needed for tapping the top plate so that holes were aligned. We then separated the plates and individually tapped the holes of the top plate and bored out/countersink the holes on the bottom plate. We then inserted the screws to check for alignment. We then left the screws in place to hold the plates together. The plates were then moved to the mill where we cut out the donut shape hole of the bottom plate. This was done using a rotary table with the spindle fixed in place. Once this was complete, the top plate was then returned to the drill press to drill the holes for the larger pipe threads to accept the air fitting. Those holes were then tapped and all edges were ground and sanded smooth thus completing the body of the skate. Each of the three frames took about 4 hours of fabrication.

Shown in the following figures are the team machining the various plates for the skates, as well as the mold being routed in the ShopBot. In figures 5A and 5B, the three top plates are shown clamped together. Centered on a rotary table, the mill cuts radially as the table is rotated. From these cut top plates, each one was stacked upon and aligned with its bottom plate. Once stacked and clamped, through holes were drilled for the radial screw pattern. Once the holes were drilled, the top plate was tapped for our 3/8"-28 Cap Head screws.



Figure 5A: Machining of the plates on mill



Figure 5B: Machining of plates on mill, showcasing the radial cutting pattern used.

The mold was made by routing out polyurethane foam using a ShopBot CNC router. Using 14[in]x14[in]x1.5[in] foam blocks, the ShopBot routed out the toolpath dictated by Solidworks' plugin, HSM Works. First, the toolpath was designed to plane off a 0.25[in] segment, from which the mold separating line was made. Then, the program routed out the rest of the material as seen in Figures 5C and 5D.

After the mold were routed, they were coated in a thin layer of polyurethane resin and then bondo. The molds were then wet sanded to a mirror polish to allow the silicone to separate from the mold. Even though these precautions were taken to allow the silicon to release, the molds still broke every cast. The foam was stiff enough to make releasing the silicon a challenge without breaking. The CNC routing requires a CNC machine to be available, as well as a shop tech available to run it; this shouldn't take more than an hour or two from start to finish, including set up. Then once the mold has been polished, a layer of silicone is applied, the fiberglass is laid over, and a second layer of silicone is applied. The top of the mold is firmly set on top, and the skirt is given overnight to solidify. Once the skirt is broken out of the mold, ¼" holes are punched out along the circumference where the bolts of the air skate frame will be holding it together.

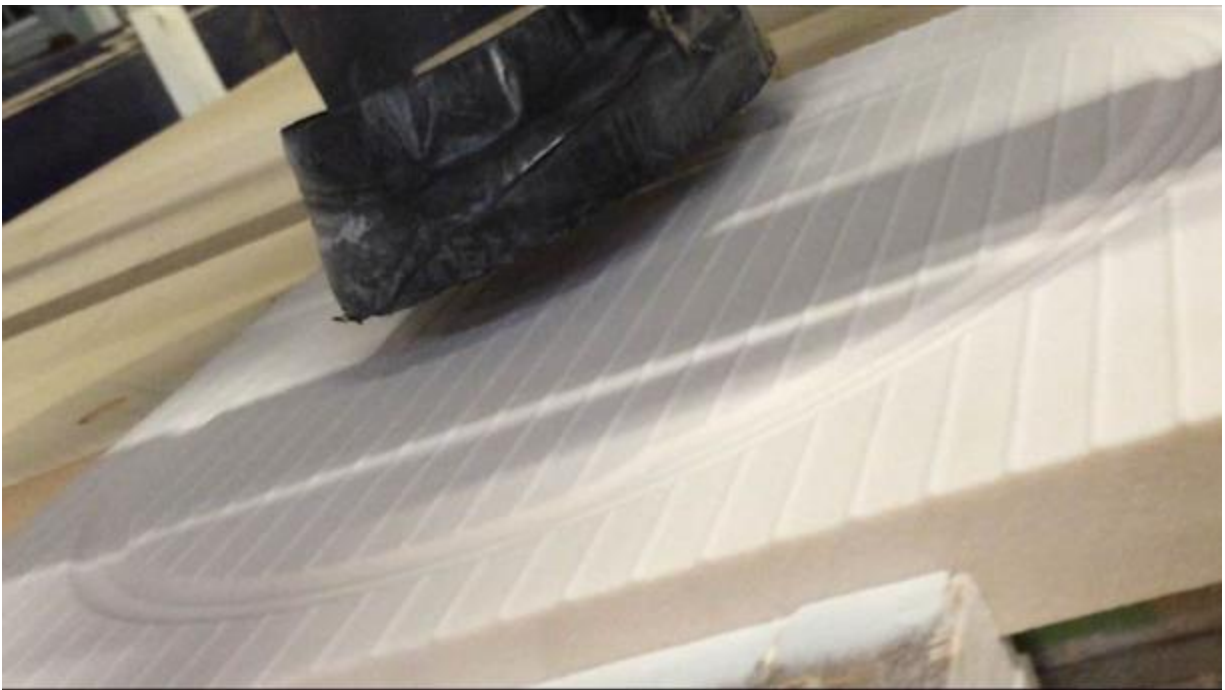


Figure 5C: Close up of ShopBot mold routing.



Figure 5D: Top and bottom half of finished skirt molds fresh from the ShopBot.

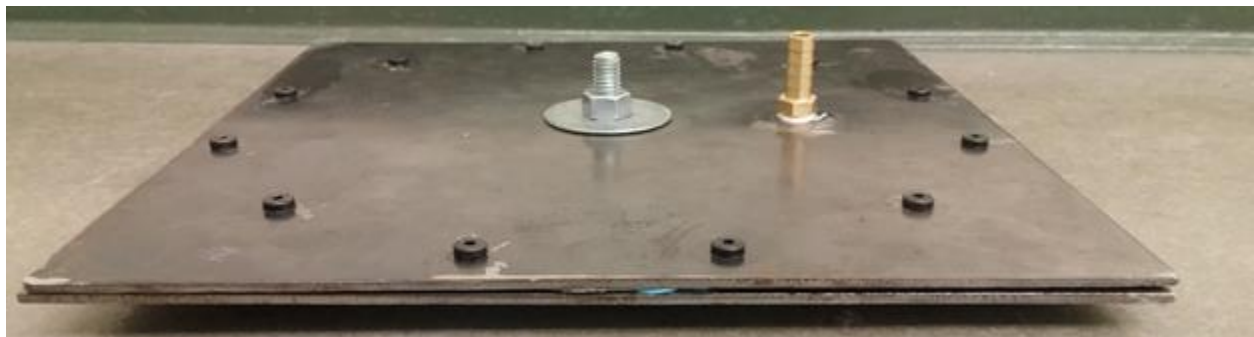


Figure 5E: Side view of a single finished air skate. From this view, the gasket of the skirt between the two plates screwed together can be seen.

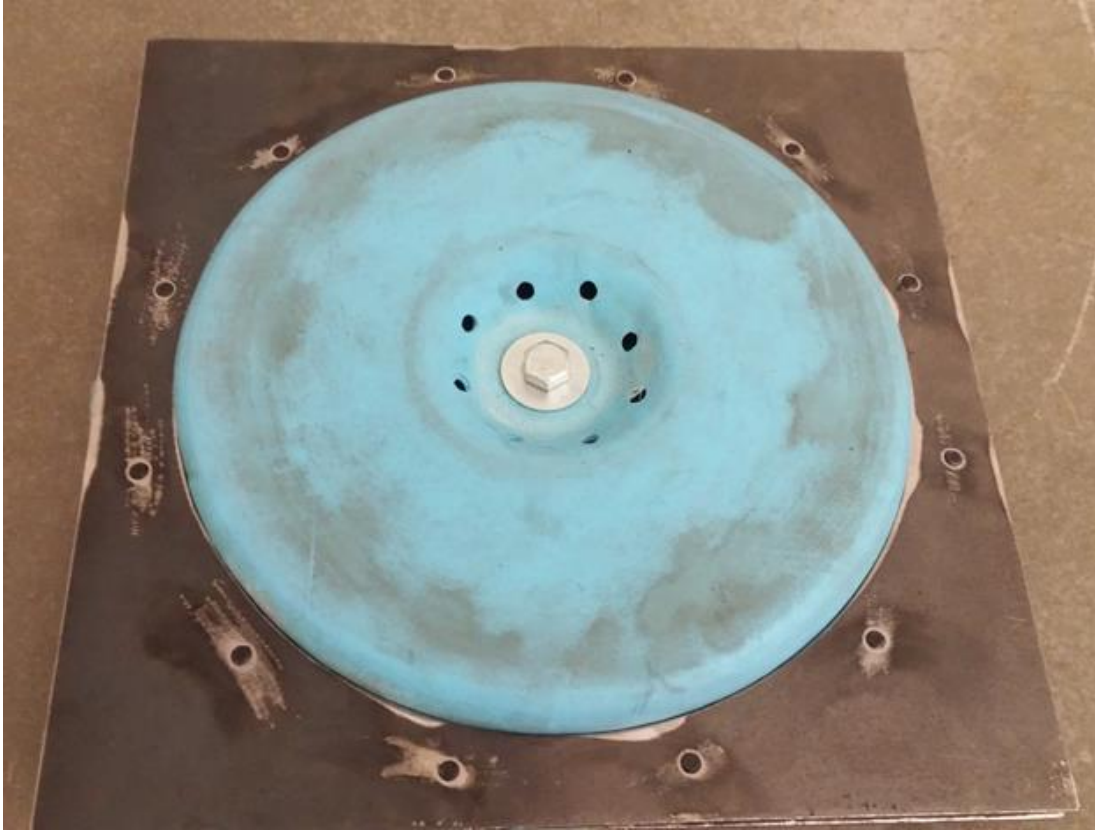


Figure 5F: Finished air skate. Shown here is the underside of the skate with the skirt visible. Scuff marks are visible due to riding over uneven ground.

5.2 Recommendations for future manufacturing of your design

We recommend CNC milling the steel plates for small to medium scale manufacturing. It is not likely a large enough demand of these skates would exist to warrant casting or high volume processes. The manufacture process for the silicon skirt would benefit greatly from a gelcoat and composite mold. Instead of routing a female mold, a male plug could be made in the same fashion. A hand layup composite mold could be pulled from this plug and be used to pull many silicon skirt castings without damage.

Chapter 6: DESIGN VERIFICATION PLAN

6.1 Test Descriptions with photos

The prototype compliant air bearing was tested for verification of calculated parameters by various methods. The primary requirements that needed to be verified were weight of skate, effective pressure, air gap height, and flow rate. 2 of the 4 parameter measurements were built into the system; flowrate was measured with an in-line flowmeter connected to the air hose and pressure was measured with a more precise pressure gauge connected directly to the body of the skate.

The weight of the skate was measured by simply placing the entire prototype on a zeroed scale. And finally, the air gap was measured with premeasured shims that were inserted under the skirt during operation. Prototype parameters were then placed into our EES program that calculated our theoretical model results. From these, comparisons could be made with our actual measurements.

Testing procedure took place as follows:

1. Place entire prototype on a scale to read weight
2. Connect prototype to air supply
3. Place prototype on a sufficiently flat surface (minimum flatness tolerance of 0.01 in)
4. Turn on air
5. Open needle valve until desired pressure is reached indicated on pressure gauge
6. Allow to reach steady state
7. Read values off flowmeter and pressure gauge
8. Use micrometer to measure air gap in multiple locations along outer circumference
9. Compare values from EES program to measured values

The required equipment for this procedure involved:

1. Weight scale
2. Assembled prototype
3. Air supply manifold
4. Wall air supply
5. Micro flat surface
6. Micrometer
7. Computer running EES program

The time frame involved to assemble, test, and post process our results was accomplished in a single afternoon. Due to Engineering IV at Cal Poly being overcrowded on the weekend, our aim was to accomplish testing during off hours where we would have sufficient space to work. The procedure of setting up the prototype and taking the required measurements took roughly 4 hours.



Figure 6A: testing air skate craft on linoleum surface.

6.2 Specification Verification checklist or DVPR

This final air-skate design should be able to perform above and beyond our specifications. For starters, our goal of holding up 250 pounds per square foot of skate should be no problem. The skate we have designed is in fact a square foot and will have about 71 square inches of lift area. Operating at around our specified 5[psi], we expect our aluminum skate to support upwards of 300[lbs]. Due to the fact that our initial proof of concept was also about a square foot but with a much smaller lift area and was capable of easily supporting around 200[lbs] while riddled with flaws, we feel this estimate to be accurate. The only specification we are still not entirely confident with is our ride height. From our analysis the skate should be able to ride comfortably at .01[in] with a reasonable air flow, but since we were not able to measure this in the inner tube proof of concept, we do not have real life data to back up this assumption. It might turn out that to achieve enough lift we will need additional air flow which would necessitate an additional parallel air supply line. This would give us a similar pressure while increasing our airflow thus increasing the skate's ride height.

Chapter 7: CONCLUSIONS

Our air skate setup exceeded our results. The triangular formation of three air skates was able to not only balance but also levitate roughly 400[lbs]. Each individual compliant skirt was able to dynamically adjust its lift abilities without the air needing to be regulated. If the air skate was under more load, the skirt would comply and create a bigger lift area, creating more lift for the

same pressure. It worked vice versa where if it wasn't under much load, the lift area would decrease and reduce lift. This made the skate dynamically stable as well as balanced. Our air-skate, in balanced levitation, was able to levitate a 42-gallon bucket of water. Note: 42 gallons of water weighs 336[lbs] and the plywood frame of the air skate combined with the metal skirt frames weighs just over 70[lbs]. The air supply required to levitate the 400lbs was 3[psi] at 3[ft³/min], which translates to a relatively low amount of power required to levitate such a load.

Furthermore, the skate was able to levitate two more water-weight bags, each weighing roughly 150[lbs]; at a slightly higher pressure of 4[psi] and similar flow rate of 3[ft³/min], the air skate was able to levitate roughly 700[lbs] while gliding across an extremely rough floor. When testing on linoleum, the air skate never snagged the ground or touched down since that surface was close to specification of 0.04[in] smoothness. However, during senior project while demoing on a rough concrete surface that had clearly visible surface defects, the air skate still managed to levitate and glide over the surface, however it was less balanced and scraped the floor more often due to the surface defects.

Appendix A: QFD, Decision Matrices etc. (As appropriate)

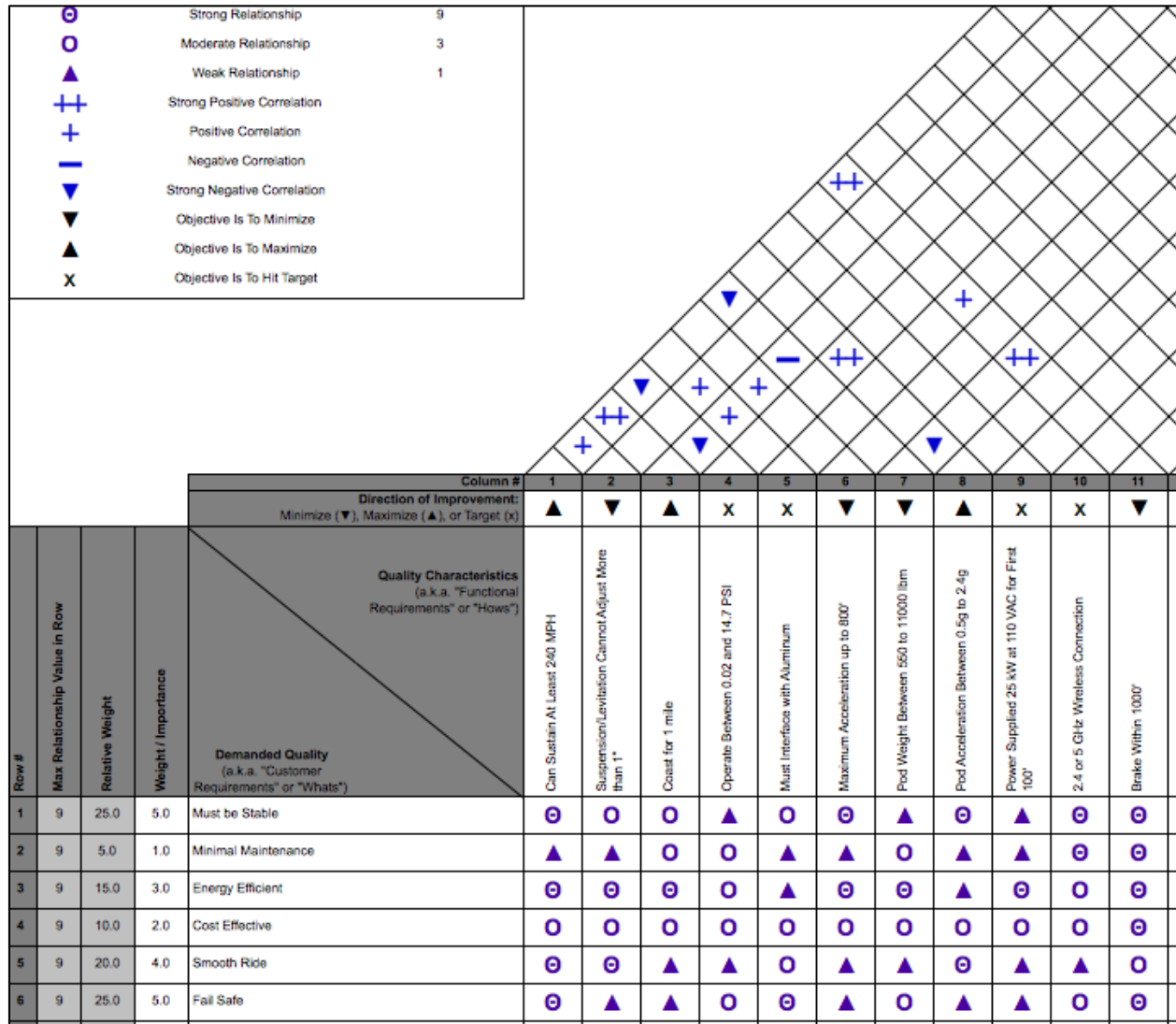
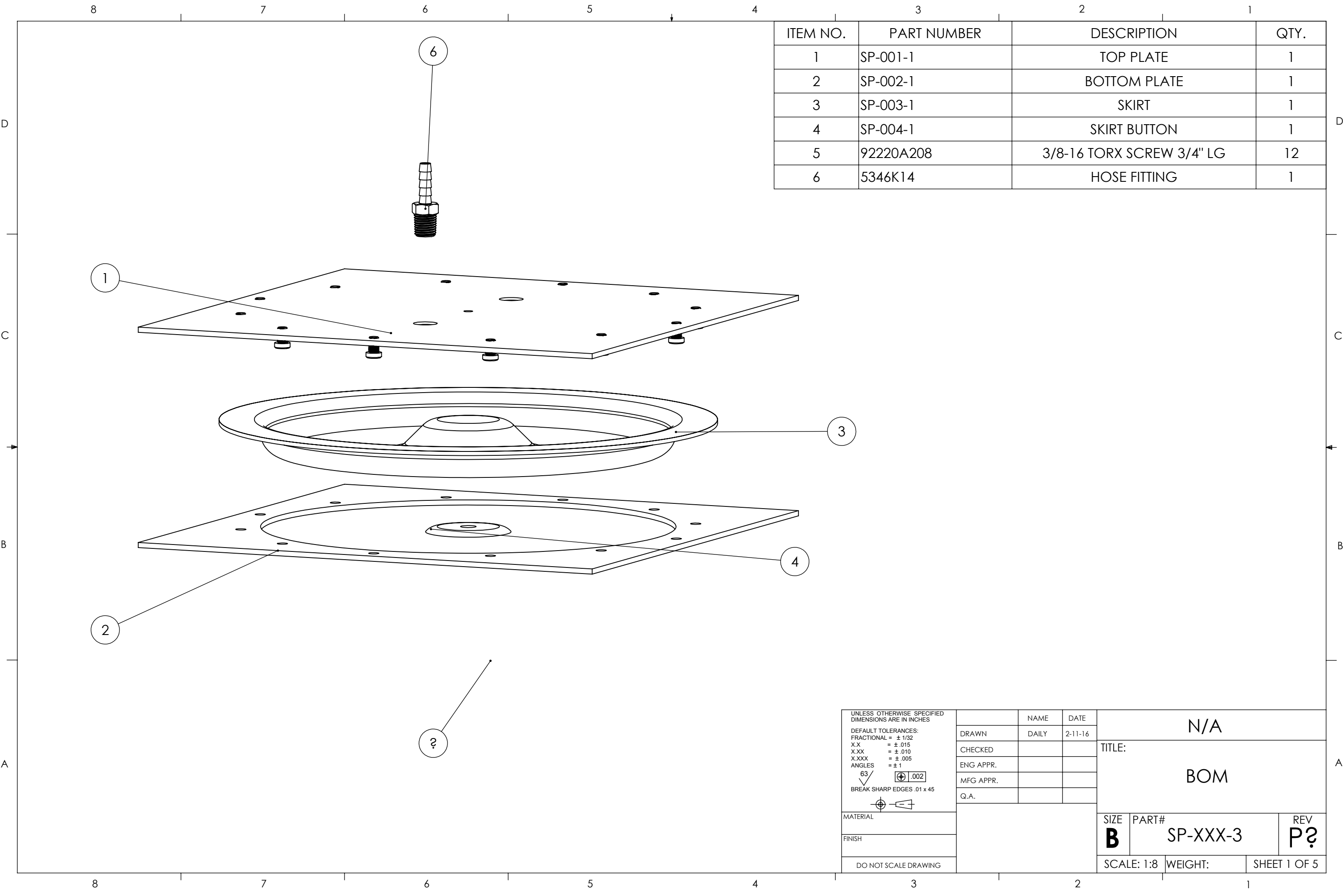


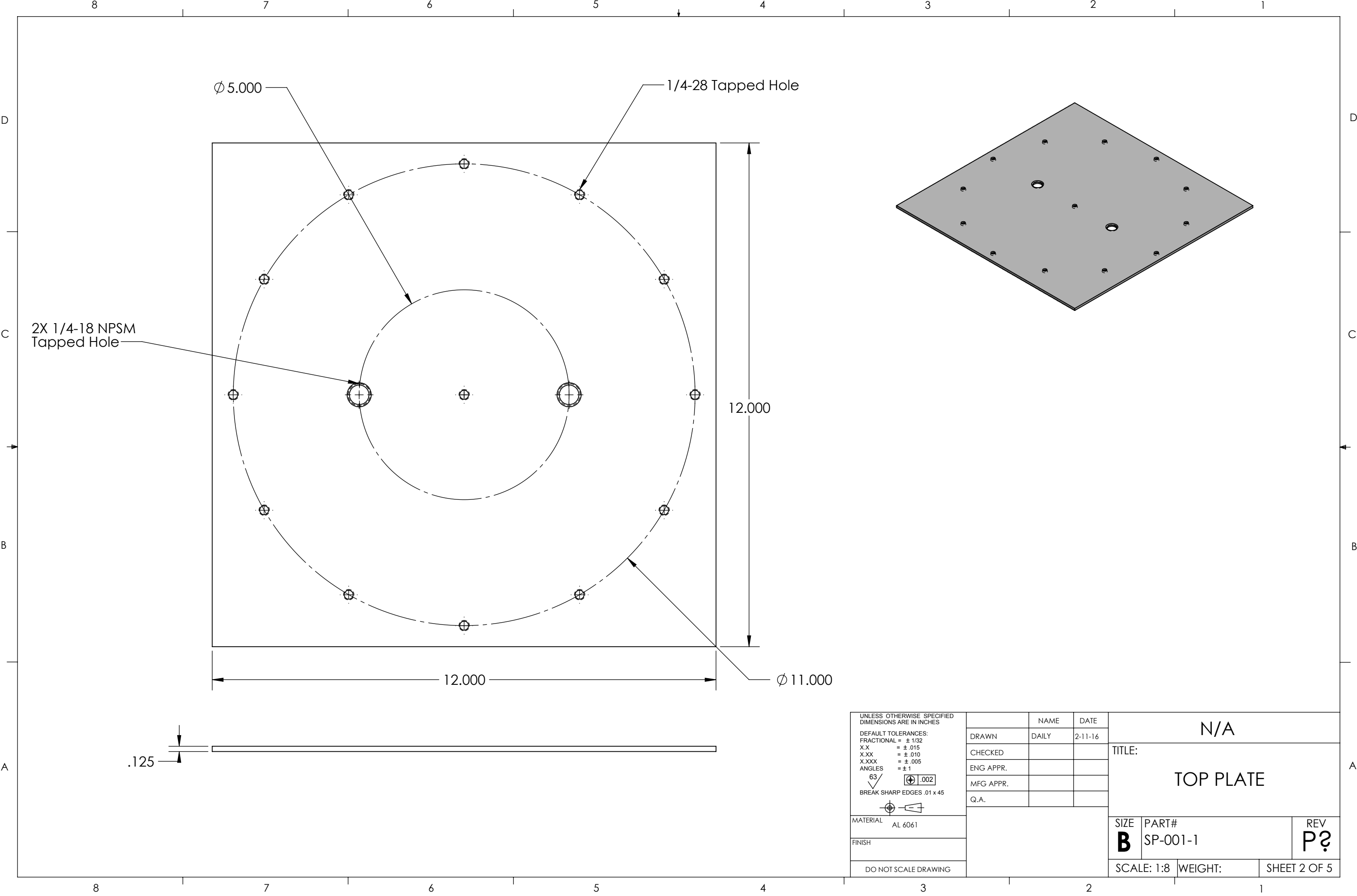
Figure A: Quality Function Development chart.

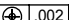

Appendix B: Final Drawings (Assemblies with Bill of Materials, detailed part drawings)

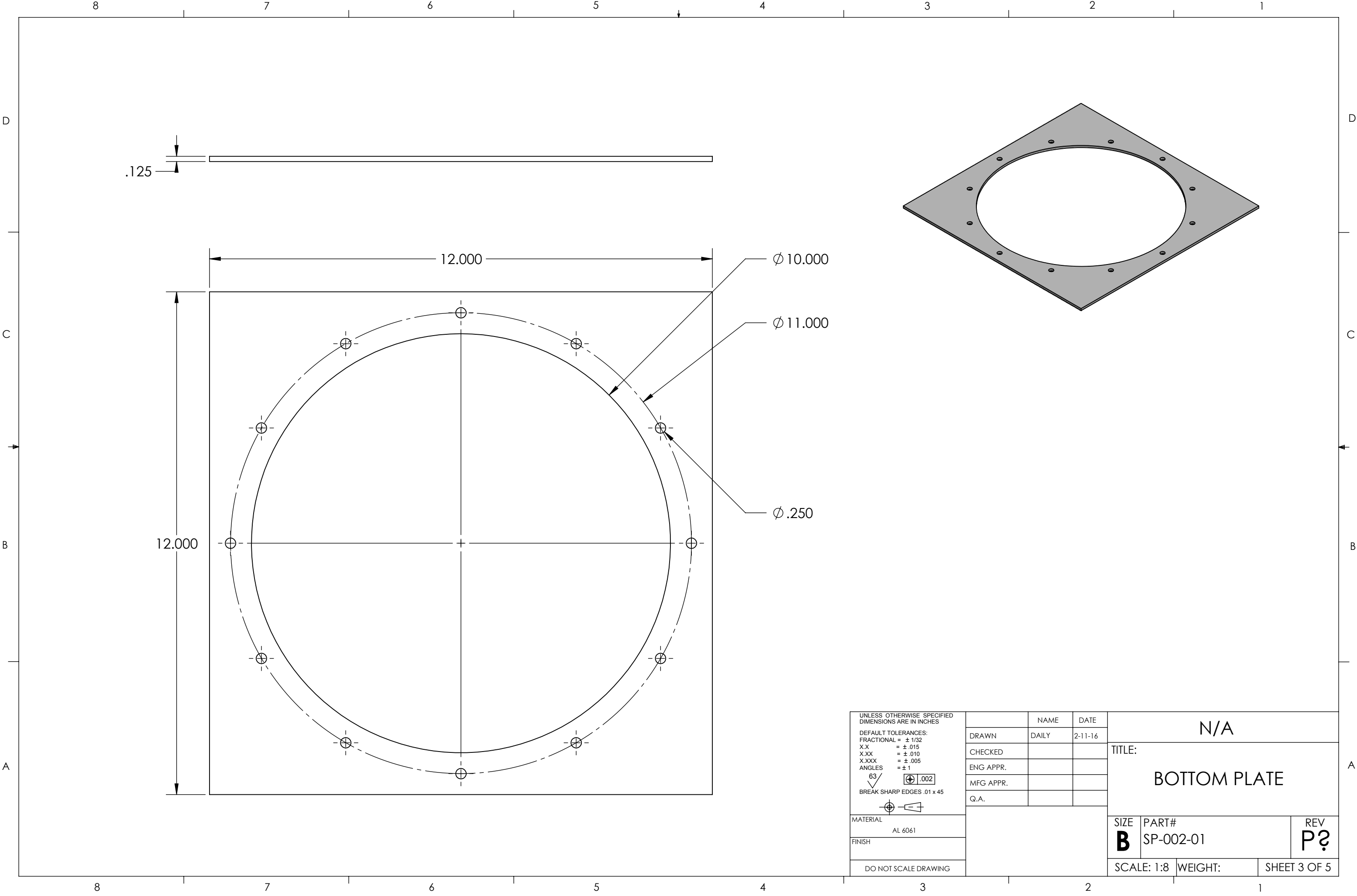



ITEM NO.	PART NUMBER	DESCRIPTION	QTY.
1	SP-001-1	TOP PLATE	1
2	SP-002-1	BOTTOM PLATE	1
3	SP-003-1	SKIRT	1
4	SP-004-1	SKIRT BUTTON	1
5	92220A208	3/8-16 TORX SCREW 3/4" LG	12
6	5346K14	HOSE FITTING	1

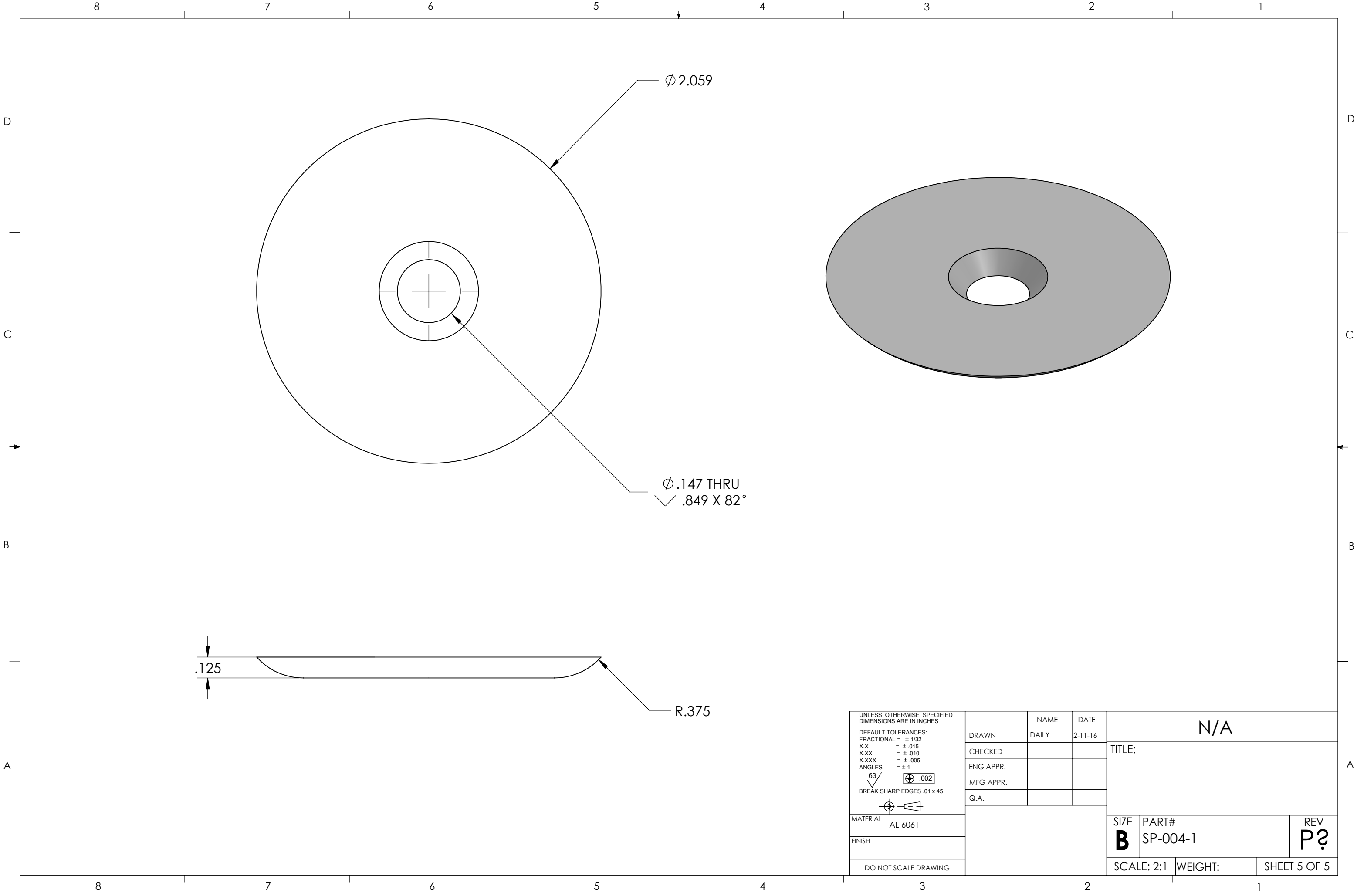
UNLESS OTHERWISE SPECIFIED DIMENSIONS ARE IN INCHES				NAME		DATE		N/A					
DEFAULT TOLERANCES: FRACTIONAL = ± 1/32 X.X = ± .015 X.XX = ± .010 X.XXX = ± .005 ANGLES = ± 1 <div>63/</div> <div><div><div></div><div></div><div></div></div><div>.002</div></div> <div>BREAK SHARP EDGES .01 x 45</div> <div><div><div></div><div></div><div></div></div><div></div></div>		DRAWN		DAILY		2-11-16							
		CHECKED						TITLE: BOM					
		ENG APPR.											
		MFG APPR.											
		Q.A.											
MATERIAL								SIZE		PART#		REV	
FINISH								B		SP-XXX-3		P?	
DO NOT SCALE DRAWING								SCALE: 1:8		WEIGHT:		SHEET 1 OF 5	



UNLESS OTHERWISE SPECIFIED DIMENSIONS ARE IN INCHES		NAME		DATE		N/A							
DEFAULT TOLERANCES: FRACTIONAL = ± 1/32		DRAWN		DAILY		2-11-16		TITLE: TOP PLATE					
X.X = ± .015		CHECKED											
X.XX = ± .010		ENG APPR.											
X.XXX = ± .005		MFG APPR.											
ANGLES = ± 1		Q.A.											
63/√ BREAK SHARP EDGES .01 x 45													
								SIZE		PART#		REV	
MATERIAL AL 6061								B		SP-001-1		P?	
FINISH													
DO NOT SCALE DRAWING								SCALE: 1:8		WEIGHT:		SHEET 2 OF 5	



UNLESS OTHERWISE SPECIFIED DIMENSIONS ARE IN INCHES DEFAULT TOLERANCES: FRACTIONAL = ± 1/32 X.X = ± .015 X.XX = ± .010 X.XXX = ± .005 ANGLES = ± 1 63/ BREAK SHARP EDGES .01 x 45  MATERIAL AL 6061 FINISH DO NOT SCALE DRAWING		NAME	DATE	N/A		
	DRAWN	DAILY	2-11-16			
	CHECKED			TITLE: BOTTOM PLATE		
	ENG APPR.					
	MFG APPR.					
	Q.A.					
			SIZE	PART#	REV	
			B	SP-002-01	P?	
			SCALE: 1:8	WEIGHT:	SHEET 3 OF 5	



Appendix C: Detailed Supporting Analysis

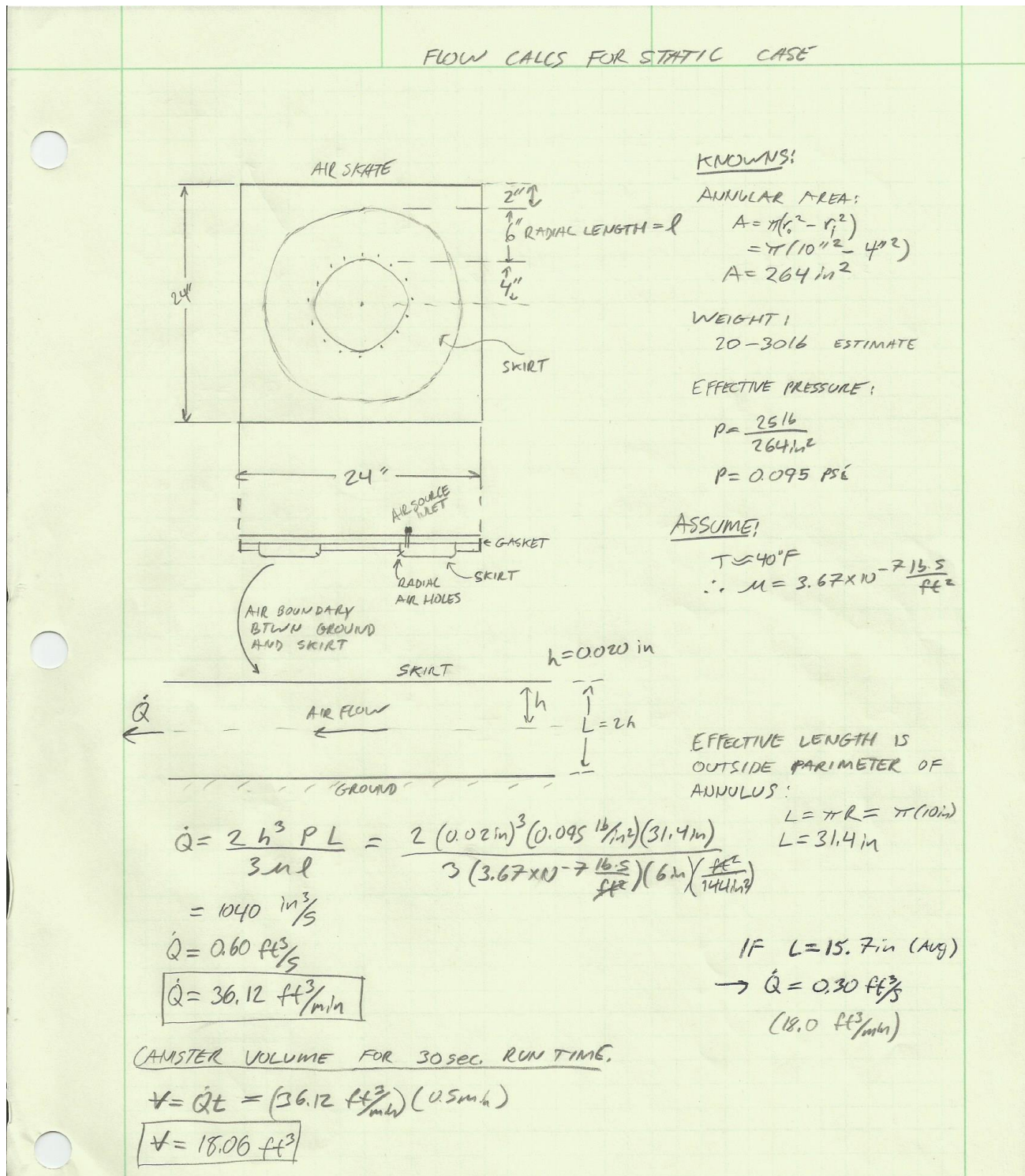


Figure C1: Initial calculation for a single air-skate. Depiction of the boundary layer between the skate membrane and the track surface. L is the total height between the surfaces, P is the acting pressure of the skate due to its weight.

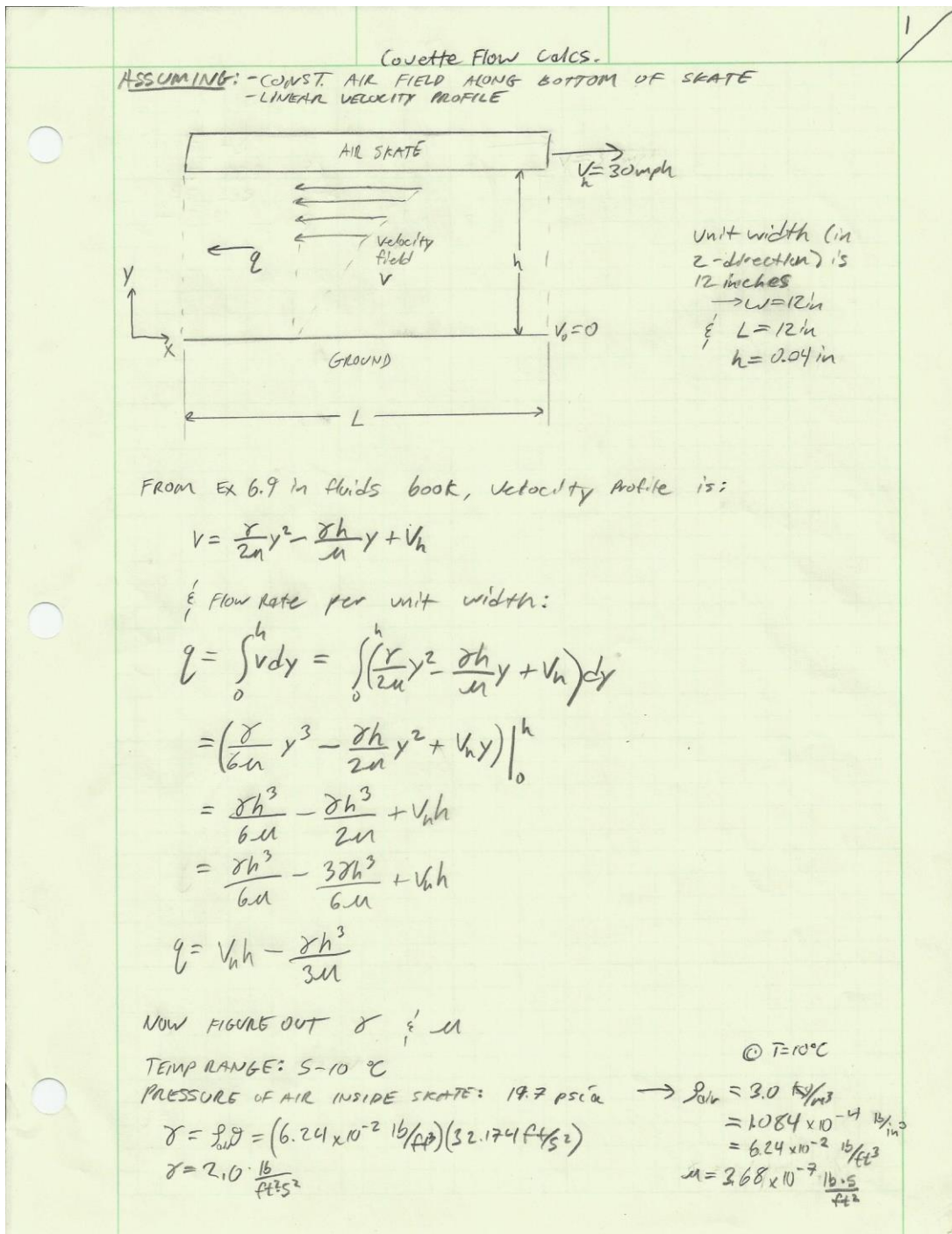


Figure C2: Calculations to model our air-skate traveling on a flat surface at a specific speed. Assumed here is constant pressure along length and height of air gap. This is an oversimplification that is accounted for in the EES program as seen below in figure C3.

3

Couette flow calcs

$$q = V_h h - \frac{\sigma h^3}{3\mu}$$

$$V_h = 30 \text{ mph} = 44 \frac{\text{ft}}{\text{s}}$$

$$h = 0.04 \text{ in} = 0.0033 \text{ ft}$$

$$\sigma = 2.0 \frac{\text{lb}}{\text{ft}^2 \cdot \text{s}^2}$$

$$\mu = 3.68 \times 10^{-7} \frac{\text{lb} \cdot \text{s}}{\text{ft}^2}$$

$$q = (44 \frac{\text{ft}}{\text{s}})(0.0033 \text{ ft}) - \frac{(2.0 \frac{\text{lb}}{\text{ft}^2 \cdot \text{s}^2})(0.0033 \text{ ft})^3}{3(3.68 \times 10^{-7} \frac{\text{lb} \cdot \text{s}}{\text{ft}^2})}$$

$$q = 0.065 \frac{\text{ft}^2}{\text{s}}$$

TIMES
EFFECTIVE
LENGTH

$$\dot{Q} = 0.17 \frac{\text{ft}^3}{\text{s}} \quad (10.2 \frac{\text{ft}^3}{\text{min}})$$

THIS IS A GOOD INDICATOR FOR WHAT THE REAR SECTION OF AIR SKATE IS EXPERIENCING B/C AIR FIELD IS NOT CONST. IN REALITY (AIR COMES FROM AIR SKATES, NOT FROM INFRONT OF AIR SKATE)

REYNOLDS # AT THESE CONDITIONS:

$$V = 1.52 \times 10^{-4} \frac{\text{ft}}{\text{s}}$$

$$Re = \frac{\rho V L}{\mu} = \frac{(6.24 \times 10^{-2} \frac{\text{lb}}{\text{ft}^3})(44 \frac{\text{ft}}{\text{s}})(1 \text{ ft})}{3.68 \times 10^{-7} \frac{\text{lb} \cdot \text{s}}{\text{ft}^2}}$$

$$= 7460870 \frac{\text{ft}}{\text{s}^2}$$

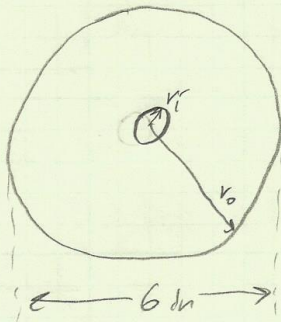
DIVIDE BY GRAVITY

$$= \frac{7460870 \frac{\text{ft}}{\text{s}^2}}{32.174 \frac{\text{ft}}{\text{s}^2}}$$

$$Re = 231891 \rightarrow \text{TURBULENT FLOW}$$

Figure C3: Results of the Couette flow analysis. Although reasonable for a 0.04-inch air gap, the flow rate we desire is much lower.

Rigid Bearing Head Cakes for static case



Experimental Results

Air gap w/ weight: ≈ 0.005 in

Weight: ≈ 50 lb

Pressure: Less than 2 psi (Limited by resolution of pressure gauge)

Physical properties of Rigid skate:

Effective pressure:

$$p = \frac{50 \text{ lb}}{27.5 \text{ in}^2} = 1.8 \text{ psi}$$

$$A = \pi (r_o^2 - r_i^2)$$

$$= \pi (3 \text{ in}^2 - 0.5 \text{ in}^2)$$

$$A = 27.5 \text{ in}^2$$

$$W = 50 \text{ lb}$$

$$\mu = 3.67 \times 10^{-7} \frac{\text{lb} \cdot \text{s}}{\text{ft}^2} (@ T \approx 40^\circ \text{F})$$

$$\dot{Q} = \frac{2 (0.0025 \text{ in})^3 (1.8 \text{ lb/in}^2) (3.93 \text{ in})}{3 (3.67 \times 10^{-7} \frac{\text{lb} \cdot \text{s}}{\text{ft}^2}) (2.5 \text{ in}) (\frac{\text{ft}^2}{144 \text{ in}^2})}$$

$$L = \pi R = \pi (1.25 \text{ in}) = 3.93 \text{ in}$$

$$\lambda = r_o - r_i = 2.5 \text{ in}$$

$$\dot{Q} = 11.57 \text{ in}^3/\text{s}$$

$$\dot{Q} = 0.382 \text{ cfm}$$

$$\dot{Q} = 0.764 \text{ cfm}$$

w/ an effective annulus length of 9.42 in

$$0.4 < \dot{Q} < 0.8 \text{ cfm}$$

Figure C4: Rigid air bearing test rig analysis. Calculated here are the effective pressure and flowrates based on weight of the skate, and annulus length (circumferential length at the center average radius and the outside radius).

Simplified Navier Stokes Equation for flow between two parallel flat plates

Assumes: Laminar, Viscous, Incompressible Fluid

Air is considered incompressible fluid as long as mach number is below .3

Air flow is not viscous, but there is no other simple solution available to solve for turbulent flow between two parallel plates.

$h = 0.005$ [in] flow field height from bottom plate

$\Delta P = 5$ [psi] desired operating pressure

$b = \frac{h}{2}$ flow height from centerline

$\mu_1 = \text{Visc}(\text{Air}, T = 40 \text{ [F]})$ [lb_m/ft-hr] Viscosity of air at temp

$\mu = \mu_1 \cdot \left[0.0000085336 \cdot \frac{\text{lb}_m \cdot \text{s}^2}{\text{ft}^2 \cdot \text{hr}} \right]$ convert units of viscosity

$l = 5$ [in] escape length

$Q = 2 \cdot b^3 \cdot \frac{\Delta P}{3 \cdot \mu \cdot l}$ flowrate is a function of air gap height, pressure differential and viscosity

$l_{\text{perimeter}} = \pi \cdot \frac{6}{12} \cdot 1$ [ft] Width of flowfield

$V = Q \cdot l_{\text{perimeter}} \cdot \frac{60 \text{ [sec]}}{1 \text{ [min]}}$ volumetric flow rate

Figure C5: EES code depicting flowrate and air gap height

	h [in]	V [ft ³ /min]
Run 1	0.0005	0.002685
Run 2	0.001521	0.07555
Run 3	0.002542	0.3526
Run 4	0.003563	0.9711
Run 5	0.004583	2.068
Run 6	0.005604	3.78
Run 7	0.006625	6.245
Run 8	0.007646	9.6
Run 9	0.008667	13.98
Run 10	0.009688	19.53
Run 11	0.01071	26.37
Run 12	0.01173	34.66
Run 13	0.01275	44.52
Run 14	0.01377	56.09
Run 15	0.01479	69.51
Run 16	0.01581	84.91
Run 17	0.01683	102.4
Run 18	0.01785	122.2
Run 19	0.01888	144.4
Run 20	0.0199	169.1
Run 21	0.02092	196.5
Run 22	0.02194	226.7
Run 23	0.02296	259.9
Run 24	0.02398	296.1
Run 25	0.025	335.6

Figure C6: Parametric study performed with EES that shows flowrate and air gap

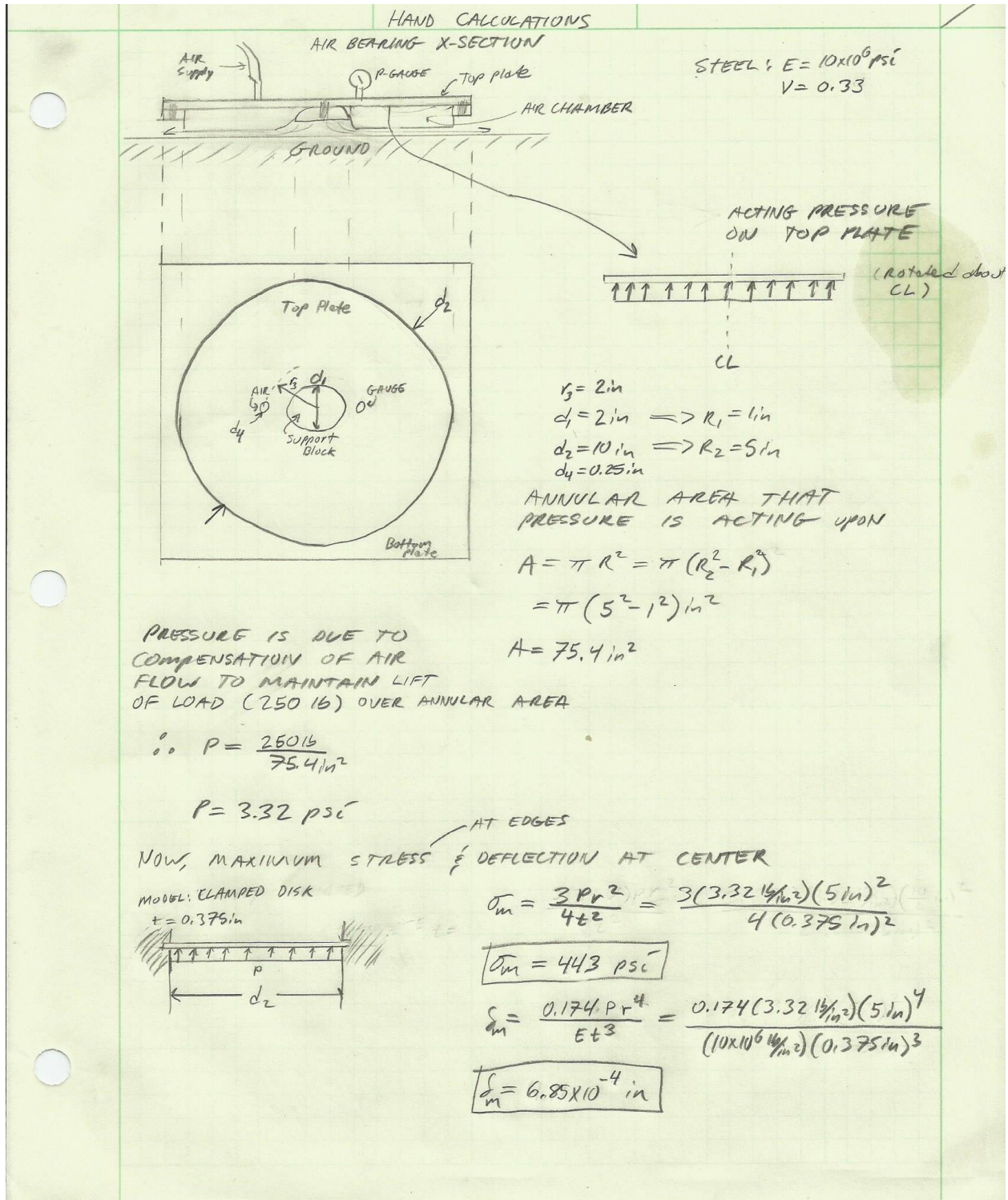


Figure C7: Results of maximum bending stress and deflection calculations.

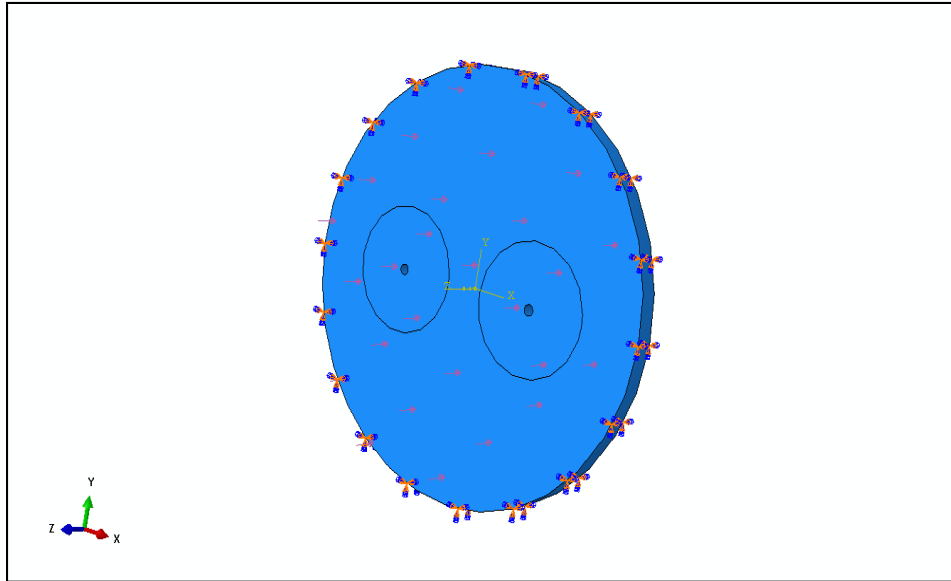


Figure C8: Initial model depicting boundary condition that simulates a fixed bolt pattern and also the pressure distribution.

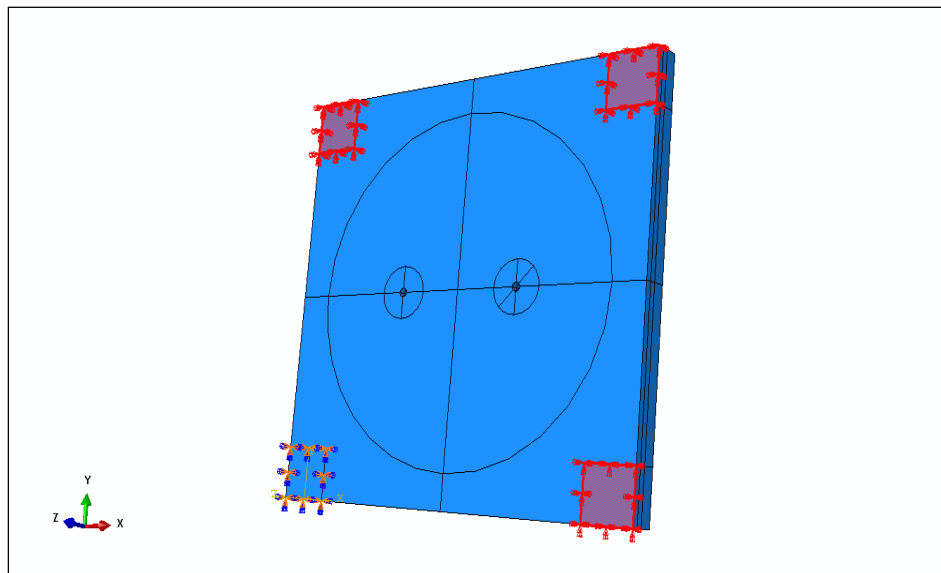


Figure C9: Full model depicting boundary conditions due to supports located along outer corners of top plate.

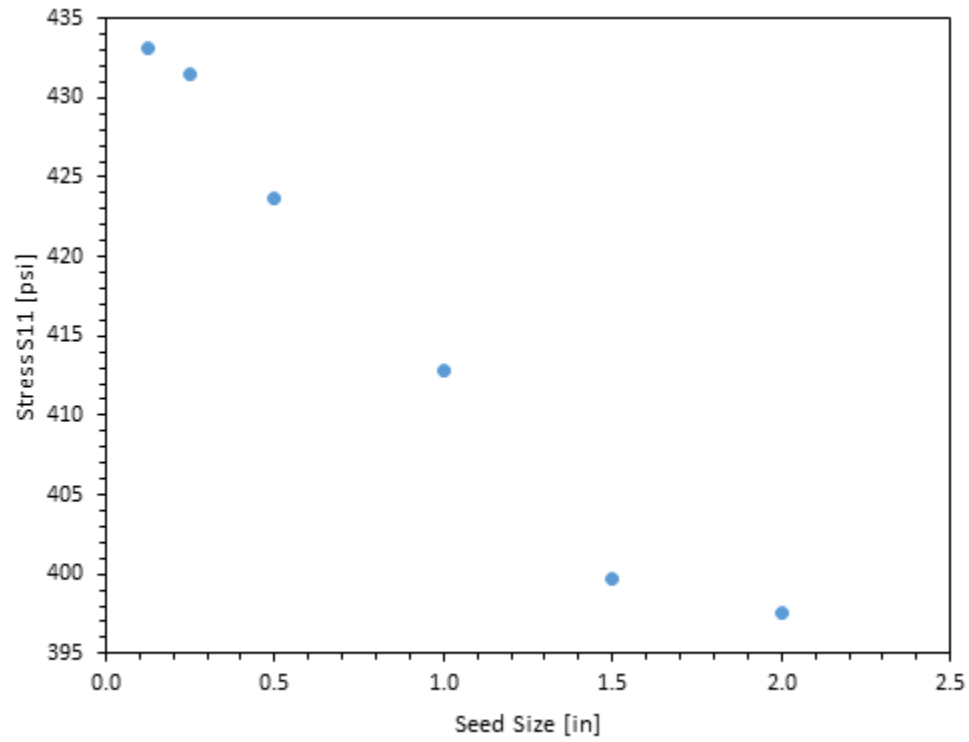


Figure C10: Convergence between seed size and stress.

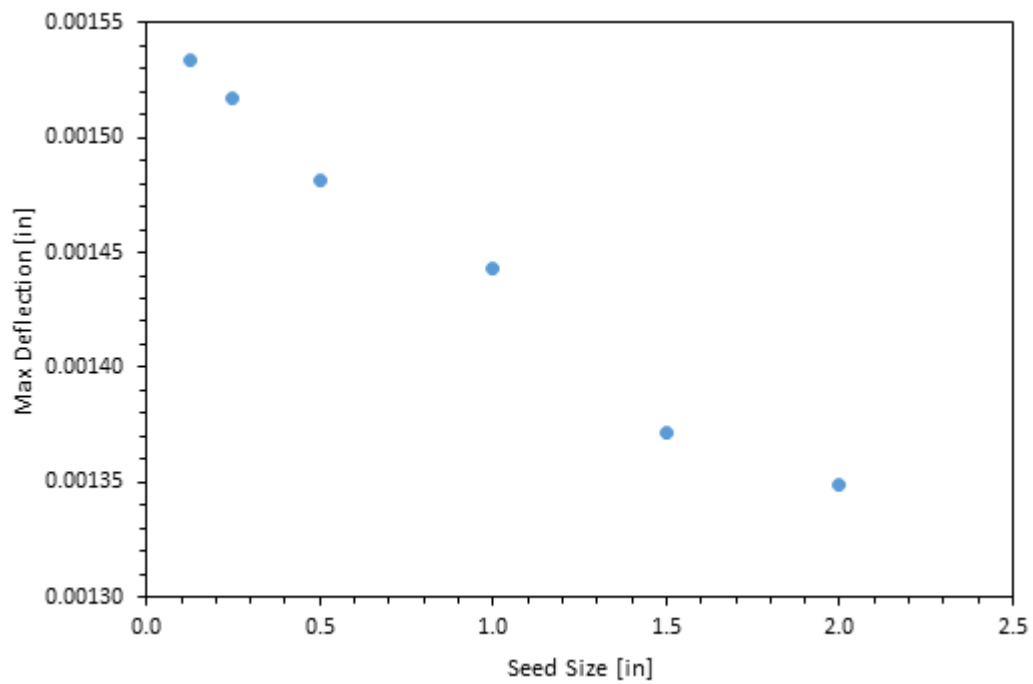


Figure C11: Convergence between seed size and displacement.

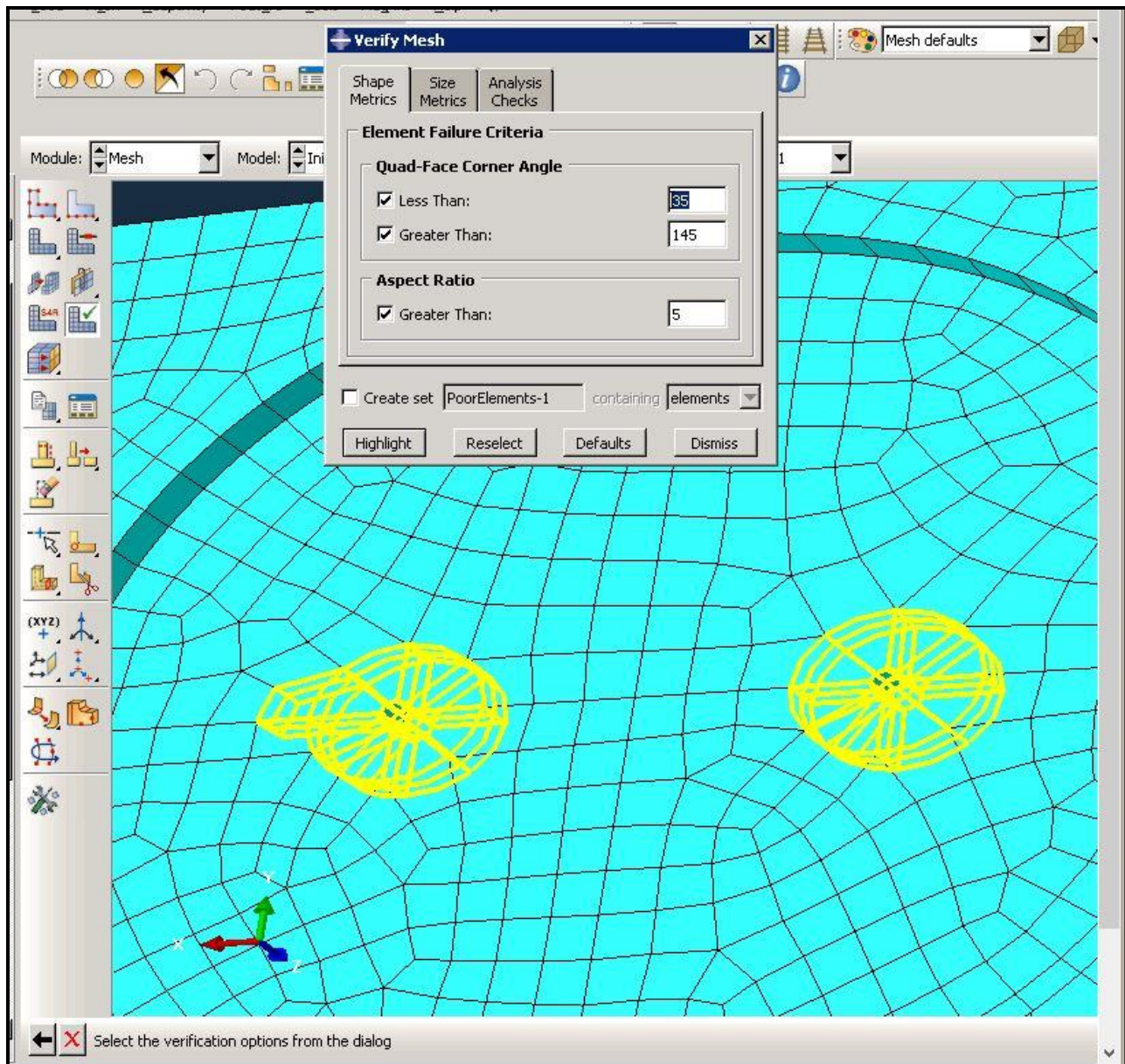


Figure C12: Element quality for a seed size of 0.5 in. These highlighted elements are out of tolerance and are unacceptable for us due to these locations developing stress concentrations. We need accurate deflection results for these locations.

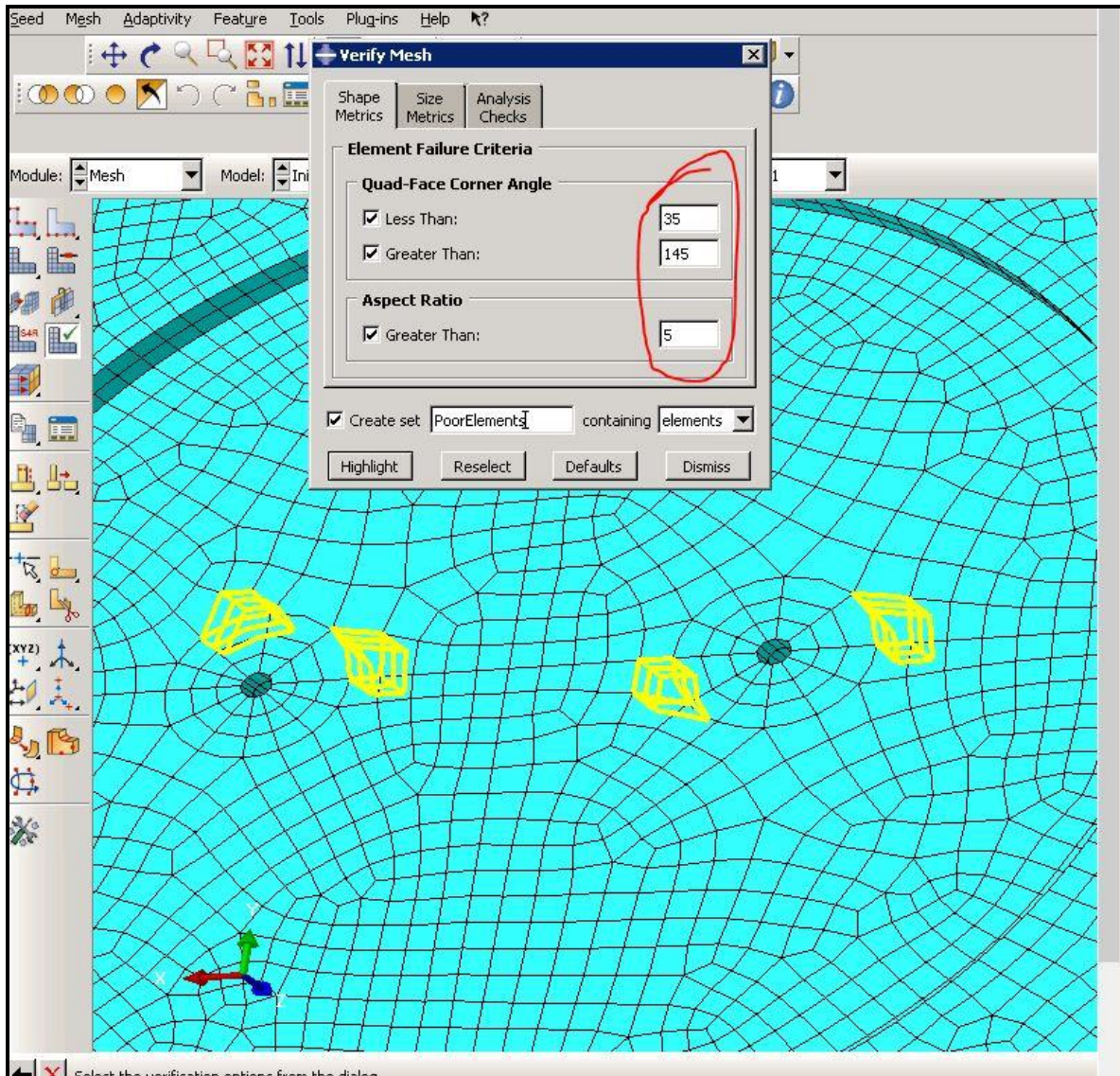


Figure C13: Element quality for a seed size of 0.25 in. These highlighted elements are out of tolerance but are acceptable since these locations are not vital for our results.

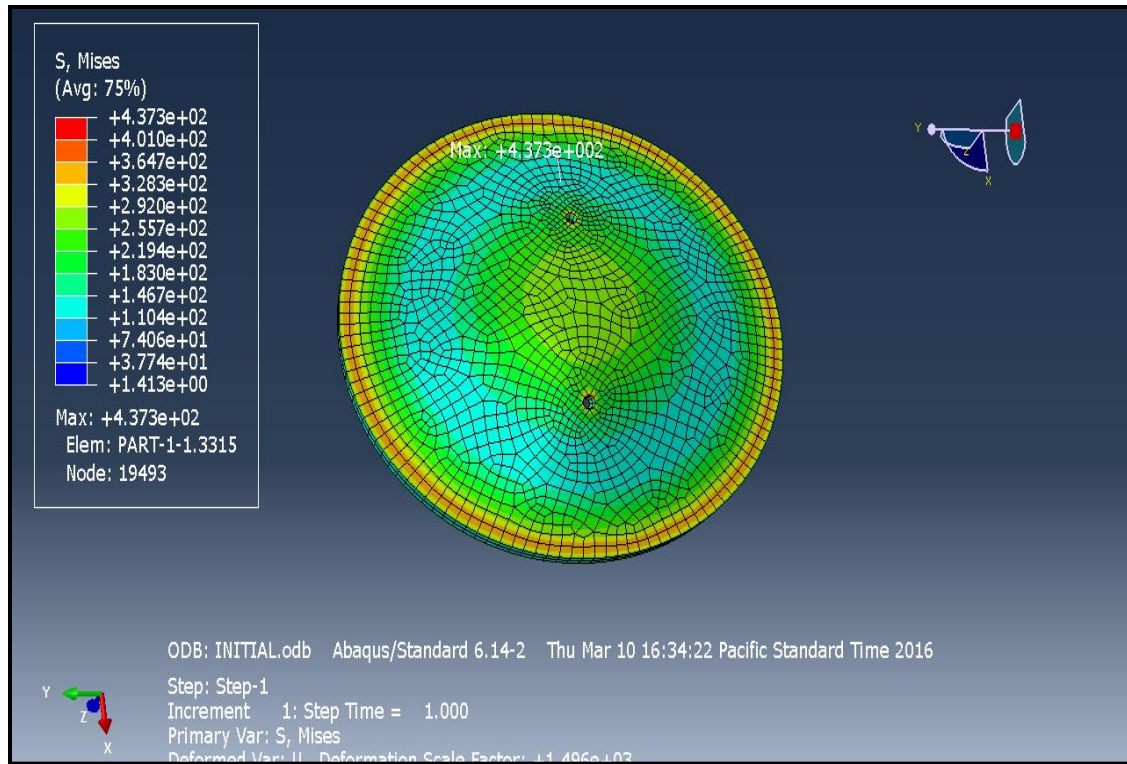


Figure C14: Initial model bending stress (psi).

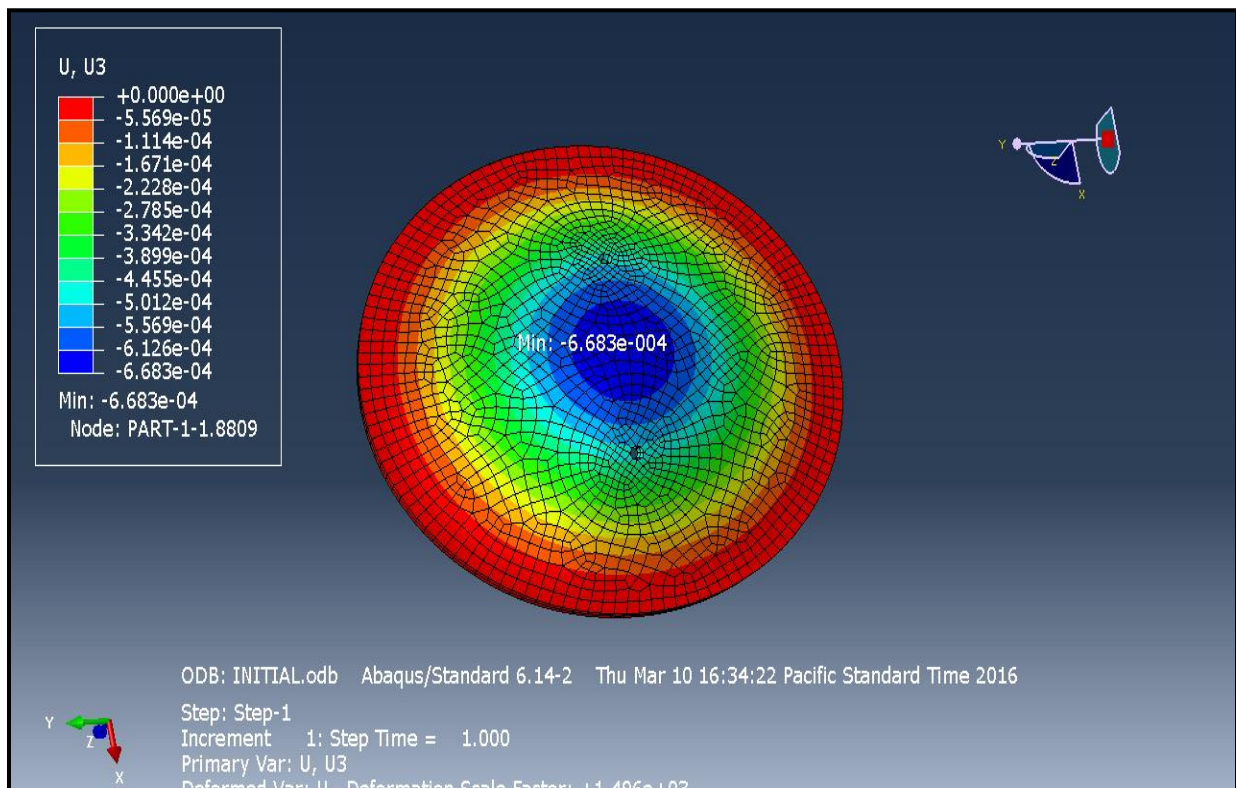


Figure C15: Initial model maximum displacement (inches).

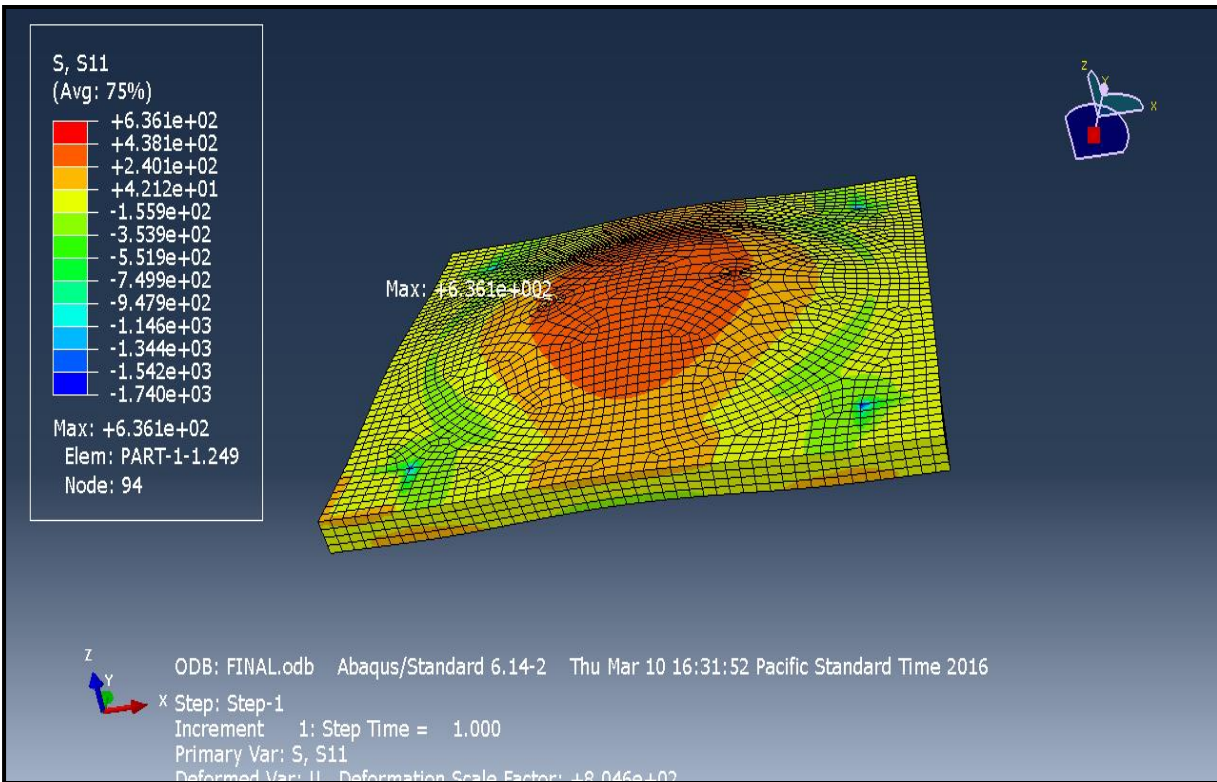


Figure C16: Full model bending stress (psi).

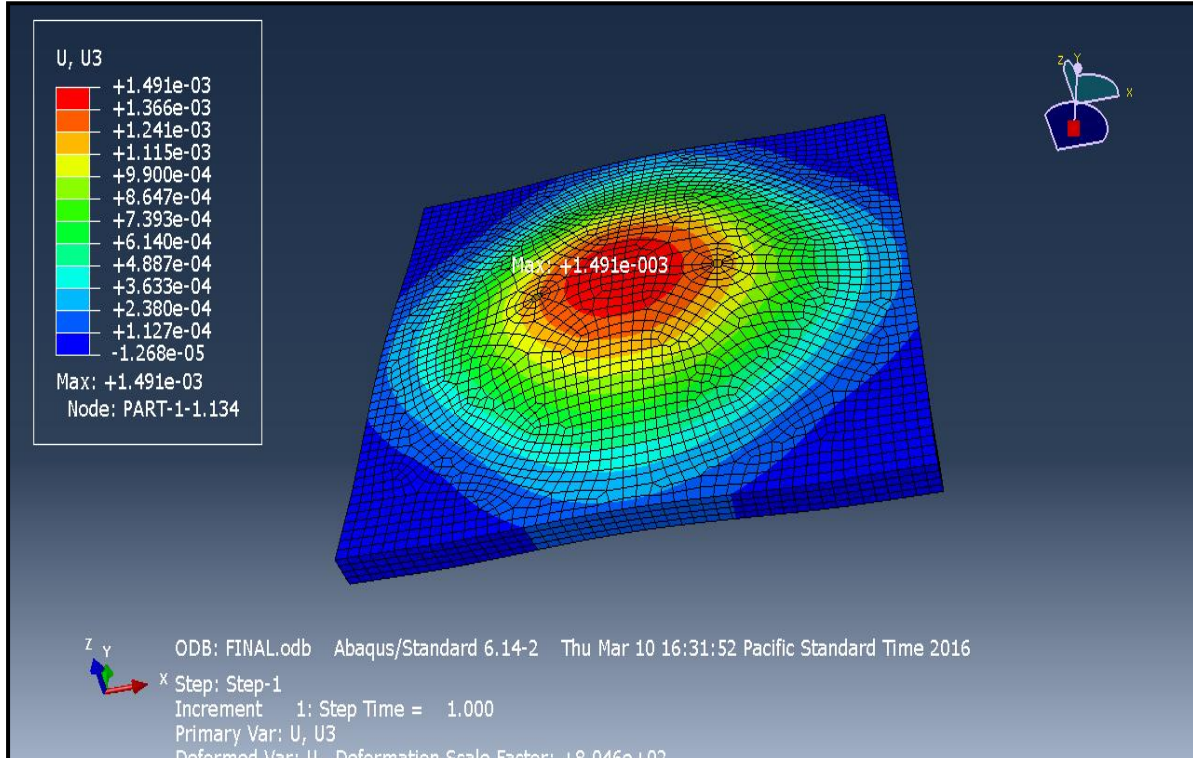


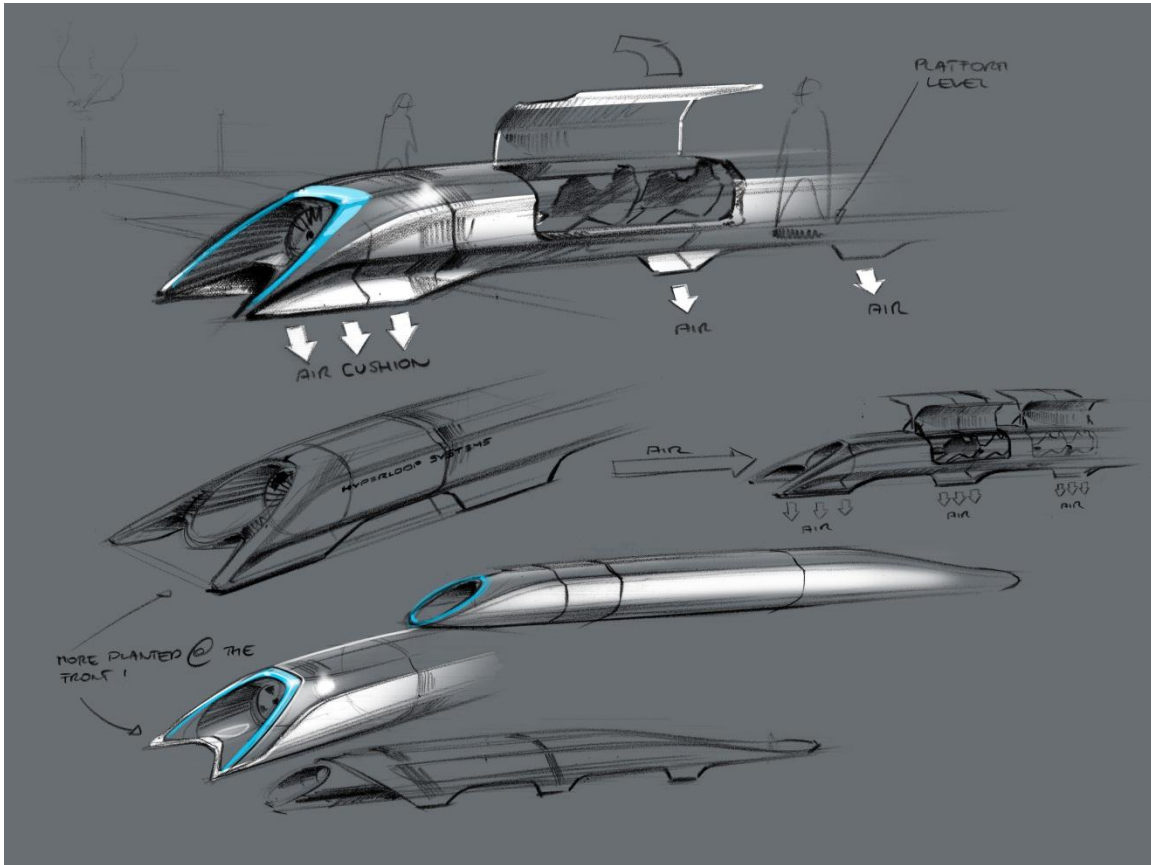
Figure C17: Full model maximum displacement (inches).

Appendix D: Operators Manual with Safety Guidelines

Operation of the air skate is relatively simple. To start, lock the frames together and ensure that all air hoses are properly attached (hosing covering as much of the barbed nipples as possible), and that there are no kinks in any lines. Next attach an air supply capable of supplying at least 5 psi at 9 ft³/min via the quick release fitting, the more constant the supply the better. Evenly load with the weight of choice, and slowly turn the needle valve until the skate pressure gage is reading 3-5 psi. The attached flowmeter should be reading around 3 ft³/min. If it is reading less, double check for hose kinks and then continue, if it is reading significantly more, the skate should be checked for leaks. Upon opening the needle valve, if there is a corner of the skate that isn't levitating or seems to be sticking, gently lift that side up so that the silicone skirt can inflate (larger loads will seal air inlet to skirt not allowing it inflate on its own); the skate should now be able to carry the load (also use this method to troubleshoot low flow rate readings). Note: under certain weights and shapes, and especially with an inconsistent air supply, the air skate could reach a resonant frequency, in which case one should immediately decrease the flowrate to the air skates.

Appendix E: Elon Musk's Hyperloop White Paper

Hyperloop Alpha



Intro

The first several pages will attempt to describe the design in everyday language, keeping numbers to a minimum and avoiding formulas and jargon. I apologize in advance for my loose use of language and imperfect analogies.

The second section is for those with a technical background. There are no doubt errors of various kinds and superior optimizations for elements of the system. Feedback would be most welcome - please send to hyperloop@spacex.com or hyperloop@teslamotors.com. I would like to thank my excellent compadres at both companies for their help in putting this together.

Background

When the California “high speed” rail was approved, I was quite disappointed, as I know many others were too. How could it be that the home of Silicon Valley and JPL - doing incredible things like indexing all the world’s knowledge and putting rovers on Mars - would build a bullet train that is both one of the most expensive per mile and one of the slowest in the world? Note, I am

hedging my statement slightly by saying “one of”. The head of the California high speed rail project called me to complain that it wasn’t the very slowest bullet train nor the very most expensive per mile.

The underlying motive for a statewide mass transit system is a good one. It would be great to have an alternative to flying or driving, but obviously only if it is actually *better* than flying or driving. The train in question would be both slower, more expensive to operate (if unsubsidized) and less safe by two orders of magnitude than flying, so why would anyone use it?

If we are to make a massive investment in a new transportation system, then the return should by rights be equally massive. Compared to the alternatives, it should ideally be:

- Safer
- Faster
- Lower cost
- More convenient
- Immune to weather
- Sustainably self-powering
- Resistant to Earthquakes
- Not disruptive to those along the route

Is there truly a new mode of transport - a fifth mode after planes, trains, cars and boats - that meets those criteria and is practical to implement? Many ideas for a system with most of those properties have been proposed and should be acknowledged, reaching as far back as Robert Goddard’s to proposals in recent decades by the Rand Corporation and ET3.

Unfortunately, none of these have panned out. As things stand today, there is not even a short distance demonstration system operating in test pilot mode anywhere in the world, let alone something that is robust enough for public transit. They all possess, it would seem, one or more fatal flaws that prevent them from coming to fruition.

Constraining the Problem

The Hyperloop (or something similar) is, in my opinion, the right solution for the specific case of high traffic city pairs that are less than about 1500 km or 900 miles apart. Around that inflection point, I suspect that supersonic air travel ends up being faster and cheaper. With a high enough altitude and the right geometry, the sonic boom noise on the ground would be no louder than current airliners, so that isn’t a showstopper. Also, a quiet supersonic plane immediately solves *every* long distance city pair without the need for a vast new worldwide infrastructure.

However, for a sub several hundred mile journey, having a supersonic plane is rather pointless, as you would spend almost all your time slowly ascending and descending and very little time at cruise speed. In order to go fast, you need to be at high altitude where the air density drops exponentially, as air at sea level becomes as thick as molasses (not literally, but you get the picture) as you approach sonic velocity.

So What is Hyperloop Anyway?

Short of figuring out real teleportation, which would of course be awesome (someone please do this), the only option for super fast travel is to build a tube over or under the ground that contains a special environment. This is where things get tricky.

At one extreme of the potential solutions is some enlarged version of the old pneumatic tubes used to send mail and packages within and between buildings. You could, in principle, use very powerful fans to push air at high speed through a tube and propel people-sized pods all the way from LA to San Francisco. However, the friction of a 350 mile long column of air moving at anywhere near sonic velocity against the inside of the tube is so stupendously high that this is impossible for all practical purposes.

Another extreme is the approach, advocated by Rand and ET3, of drawing a hard or near hard vacuum in the tube and then using an electromagnetic suspension. The problem with this approach is that it is incredibly hard to maintain a near vacuum in a room, let alone 700 miles (round trip) of large tube with dozens of station gateways and thousands of pods entering and exiting every day. All it takes is one leaky seal or a small crack somewhere in the hundreds of miles of tube and the whole system stops working.

However, a low pressure (vs. almost no pressure) system set to a level where standard commercial pumps could easily overcome an air leak and the transport pods could handle variable air density would be inherently robust. Unfortunately, this means that there is a non-trivial amount of air in the tube and leads us straight into another problem.

Overcoming the Kantrowitz Limit

Whenever you have a capsule or pod (I am using the words interchangeably) moving at high speed through a tube containing air, there is a minimum tube to pod area ratio below which you will choke the flow. What this means is that if the walls of the tube and the capsule are too close together, the capsule will behave like a syringe and eventually be forced to push the entire column of air in the system. Not good.

Nature's top speed law for a given tube to pod area ratio is known as the Kantrowitz limit. This is highly problematic, as it forces you to either go slowly

or have a super huge diameter tube. Interestingly, there are usually two solutions to the Kantrowitz limit - one where you go slowly and one where you go really, really fast.

The latter solution sounds mighty appealing at first, until you realize that going several thousand miles per hour means that you can't tolerate even wide turns without painful g loads. For a journey from San Francisco to LA, you will also experience a rather intense speed up and slow down. And, when you get right down to it, going through transonic buffet in a tube is just fundamentally a dodgy prospect.

Both for trip comfort and safety, it would be best to travel at high subsonic speeds for a 350 mile journey. For much longer journeys, such as LA to NY, it would be worth exploring super high speeds and this is probably technically feasible, but, as mentioned above, I believe the economics would probably favor a supersonic plane.

The approach that I believe would overcome the Kantrowitz limit is to mount an electric compressor fan on the nose of the pod that actively transfers high pressure air from the front to the rear of the vessel. This is like having a pump in the head of the syringe actively relieving pressure.

It would also simultaneously solve another problem, which is how to create a low friction suspension system when traveling at over 700 mph. Wheels don't work very well at that sort of speed, but a cushion of air does. Air bearings, which use the same basic principle as an air hockey table, have been demonstrated to work at speeds of Mach 1.1 with very low friction. In this case, however, it is the pod that is producing the air cushion, rather than the tube, as it is important to make the tube as low cost and simple as possible.

That then begs the next question of whether a battery can store enough energy to power a fan for the length of the journey with room to spare. Based on our calculations, this is no problem, so long as the energy used to accelerate the pod is not drawn from the battery pack.

This is where the external linear electric motor comes in, which is simply a round induction motor (like the one in the Tesla Model S) rolled flat. This would accelerate the pod to high subsonic velocity and provide a periodic reboost roughly every 70 miles. The linear electric motor is needed for as little as ~1% of the tube length, so is not particularly costly.

Making the Economics Work

The pods and linear motors are relatively minor expenses compared to the tube itself - several hundred million dollars at most, compared with several billion dollars for the tube. Even several billion is a low number when compared with several tens of billion proposed for the track of the California rail project.

The key advantages of a tube vs. a railway track are that it can be built above the ground on pylons and it can be built in prefabricated sections that are dropped in place and joined with an orbital seam welder. By building it on pylons, you can almost entirely avoid the need to buy land by following alongside the mostly very straight California Interstate 5 highway, with only minor deviations when the highway makes a sharp turn.

Even when the Hyperloop path deviates from the highway, it will cause minimal disruption to farmland roughly comparable to a tree or telephone pole, which farmers deal with all the time. A ground based high speed rail system by comparison needs up to a 100 ft wide swath of dedicated land to build up foundations for both directions, forcing people to travel for several miles just to get to the other side of their property. It is also noisy, with nothing to contain the sound, and needs unsightly protective fencing to prevent animals, people or vehicles from getting on to the track. Risk of derailment is also not to be taken lightly, as demonstrated by several recent fatal train accidents.

Earthquakes and Expansion Joints

A ground based high speed rail system is susceptible to Earthquakes and needs frequent expansion joints to deal with thermal expansion/contraction and subtle, large scale land movement.

By building a system on pylons, where the tube is not rigidly fixed at any point, you can dramatically mitigate Earthquake risk and avoid the need for expansion joints. Tucked away inside each pylon, you could place two adjustable lateral (XY) dampers and one vertical (Z) damper.

These would absorb the small length changes between pylons due to thermal changes, as well as long form subtle height changes. As land slowly settles to a new position over time, the damper neutral position can be adjusted accordingly. A telescoping tube, similar to the boxy ones used to access airplanes at airports would be needed at the end stations to address the cumulative length change of the tube.

Can it Really be Self-Powering?

For the full explanation, please see the technical section, but the short answer is that by placing solar panels on top of the tube, the Hyperloop can generate far in excess of the energy needed to operate. This takes into account storing enough energy in battery packs to operate at night and for periods of extended cloudy weather. The energy could also be stored in the form of compressed air that then runs an electric fan in reverse to generate energy, as demonstrated by LightSail.

Hyperloop Preliminary Design Study

Technical Section

1. Abstract

Existing conventional modes of transportation of people consists of four unique types: rail, road, water, and air. These modes of transport tend to be either relatively slow (e.g., road and water), expensive (e.g., air), or a combination of relatively slow and expensive (i.e., rail). Hyperloop is a new mode of transport that seeks to change this paradigm by being both fast and inexpensive for people and goods. Hyperloop is also unique in that it is an open design concept, similar to Linux. Feedback is desired from the community that can help advance the Hyperloop design and bring it from concept to reality.

Hyperloop consists of a low pressure tube with capsules that are transported at both low and high speeds throughout the length of the tube. The capsules are supported on a cushion of air, featuring pressurized air and aerodynamic lift. The capsules are accelerated via a magnetic linear accelerator affixed at various stations on the low pressure tube with rotors contained in each capsule. Passengers may enter and exit Hyperloop at stations located either at the ends of the tube, or branches along the tube length.

In this study, the initial route, preliminary design, and logistics of the Hyperloop transportation system have been derived. The system consists of capsules that travel between Los Angeles, California and San Francisco, California. The total one-way trip time is 35 minutes from county line to county line. The capsules leave on average every 2 minutes from each terminal carrying 28 people each (as often as every 30 seconds during rush hour and less frequently at night). This gives a total of 7.4 million people per tube that can be transported each year on Hyperloop. The total cost of Hyperloop is under \$6 billion USD for two one-way tubes and 40 capsules. Amortizing this capital cost over 20 years and adding daily operational costs gives a total of \$20 USD plus operating costs per one-way ticket on the passenger Hyperloop.

Useful feedback is welcomed on aspects of the Hyperloop design. E-mail feedback to hyperloop@spacex.com or hyperloop@teslamotors.com.

2. Table of Contents

1. Abstract.....	6
2. Table of Contents	6
3. Background	8
4. Hyperloop Transportation System.....	9
4.1. Capsule.....	11

4.1.1. Geometry	13
4.1.2. Interior	15
4.1.3. Compressor	17
4.1.4. Suspension	20
4.1.5. Onboard Power	22
4.1.6. Propulsion	22
4.1.7. Cost	23
4.2. Tube	24
4.2.1. Geometry	25
4.2.2. Tube Construction	27
4.2.3. Pylons and Tunnels	28
4.2.4. Station Construction	32
4.2.5. Cost	33
4.3. Propulsion	33
4.3.1. Capsule Components (Rotor)	36
4.3.2. Tube Components (Stator)	37
4.3.3. Energy Storage Components	38
4.3.4. Cost	38
4.3.5. Propulsion for Passenger Plus Vehicle System	39
4.4. Route	39
4.4.1. Route Optimization	41
4.4.1.1. Los Angeles/Grapevine - South	44
4.4.1.2. Los Angeles/Grapevine - North	45
4.4.1.2. Center Section of I-5	47
4.4.1.3. I-580/San Francisco Bay	49
4.4.3. Station Locations	51
4.5. Safety and Reliability	53
4.5.1. Onboard Passenger Emergency	53
4.5.2. Power Outage	54
4.5.2. Capsule Depressurization	54
4.5.3. Capsule Stranded in Tube	55
4.5.4. Structural Integrity of the Tube in Jeopardy	55
4.5.5. Earthquakes	55
4.5.6. Human Related Incidents	55
4.5.7. Reliability	56

4.6. Cost.....	56
5. Conclusions	57
6. Future Work	58

3. Background

The corridor between San Francisco, California and Los Angeles, California is one of the most often traveled corridors in the American West. The current practical modes of transport for passengers between these two major population centers include:

1. Road (inexpensive, slow, usually not environmentally sound)
2. Air (expensive, fast, not environmentally sound)
3. Rail (expensive, slow, often environmentally sound)

A new mode of transport is needed that has benefits of the current modes without the negative aspects of each. This new high speed transportation system has the following requirements:

1. Ready when the passenger is ready to travel (road)
2. Inexpensive (road)
3. Fast (air)
4. Environmentally friendly (rail/road via electric cars)

The current contender for a new transportation system between southern and northern California is the “California High Speed Rail.” The parameters outlining this system include:

1. Currently \$68.4 billion USD proposed cost
2. Average speed of 164 mph (264 kph) between San Francisco and Los Angeles
3. Travel time of 2 hours and 38 minutes between San Francisco and Los Angeles
 - a. Compare with 1 hour and 15 minutes by air
 - b. Compare with 5 hours and 30 minutes by car
4. Average one-way ticket price of \$105 one-way ([reference](#))
 - a. Compare with \$158 round trip by air for September 2013
 - b. Compare with \$115 round trip by road (\$4/gallon with 30 mpg vehicle)

A new high speed mode of transport is desired between Los Angeles and San Francisco; however, the proposed California High Speed Rail does not reduce current trip times or reduce costs relative to existing modes of transport. This preliminary design study proposes a new mode of high speed transport that reduces both the travel time and travel cost between Los Angeles and San Francisco. Options are also included to increase the transportation system to other major population centers across California. It is also worth noting the

energy cost of this system is less than any currently existing mode of transport (Figure 1). The only system that comes close to matching the low energy requirements of Hyperloop is the fully electric Tesla Model S.

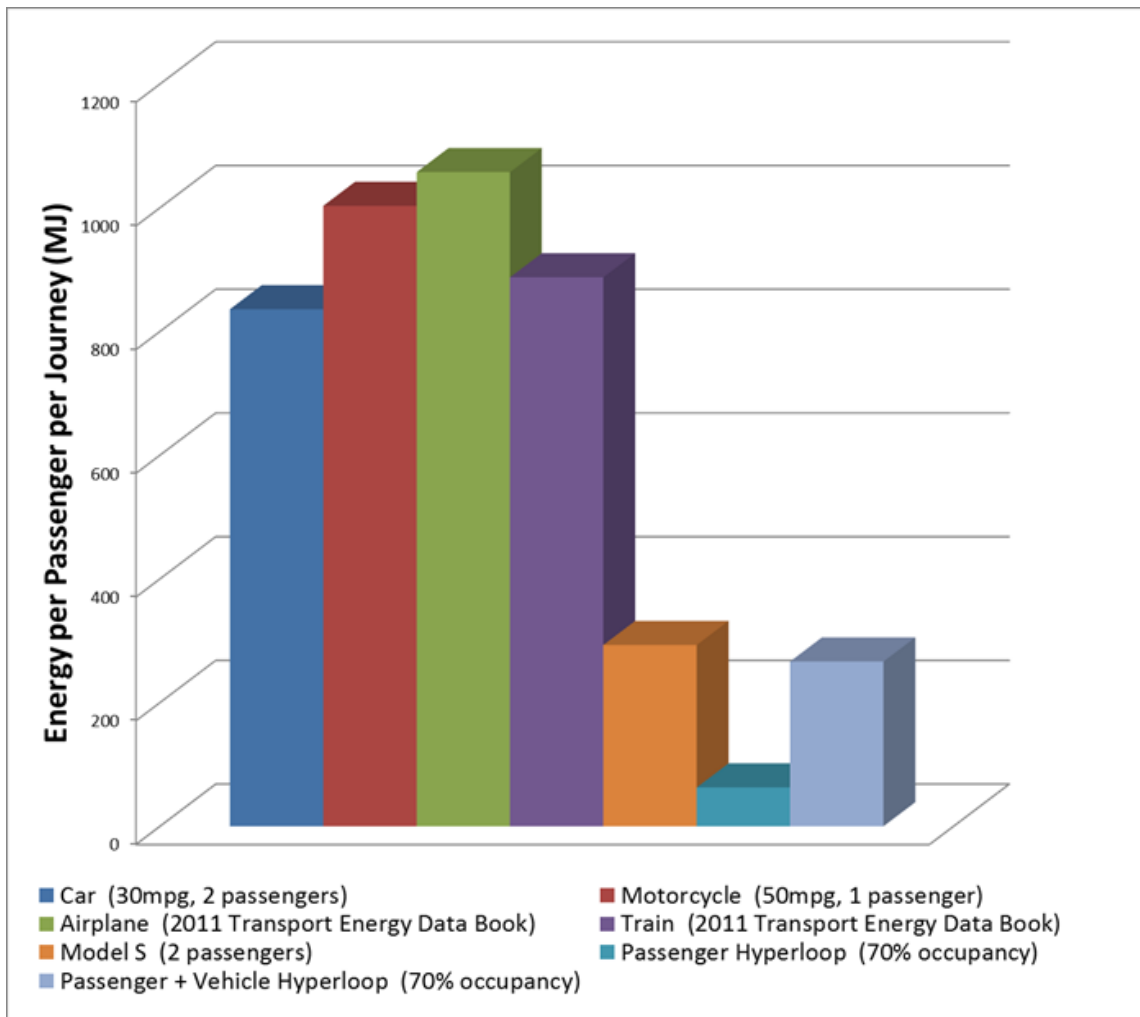


Figure 1. Energy cost per passenger for a journey between Los Angeles and San Francisco for various modes of transport.

4. Hyperloop Transportation System

Hyperloop (Figure 2 and Figure 3) is a proposed transportation system for traveling between Los Angeles, California, and San Francisco, California in 35 minutes. The Hyperloop consists of several distinct components, including:

1. Capsule:
 - a. Sealed capsules carrying 28 passengers each that travel along the interior of the tube depart on average every 2 minutes from Los Angeles or San Francisco (up to every 30 seconds during peak usage hours).

- b. A larger system has also been sized that allows transport of 3 full size automobiles with passengers to travel in the capsule.
 - c. The capsules are separated within the tube by approximately 23 miles (37 km) on average during operation.
 - d. The capsules are supported via air bearings that operate using a compressed air reservoir and aerodynamic lift.
- 2. Tube:
 - a. The tube is made of steel. Two tubes will be welded together in a side-by-side configuration to allow the capsules to travel both directions.
 - b. Pylons are placed every 100 ft (30 m) to support the tube.
 - c. Solar arrays will cover the top of the tubes in order to provide power to the system.
- 3. Propulsion:
 - a. Linear accelerators are constructed along the length of the tube at various locations to accelerate the capsules.
 - b. Rotors are located on the capsules to transfer momentum to the capsules via the linear accelerators.
- 4. Route:
 - a. There will be a station at Los Angeles and San Francisco. Several stations along the way will be possible with splits in the tube.
 - b. The majority of the route will follow I-5 and the tube will be constructed in the median.

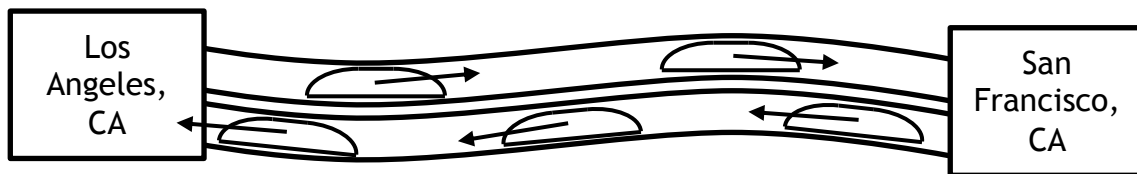


Figure 2. Hyperloop conceptual diagram.



Figure 3. Hyperloop tube stretching from Los Angeles to San Francisco.

In addition to these aspects of the Hyperloop, safety and cost will also be addressed in this study.

The Hyperloop is sized to allow expansion as the network becomes increasingly popular. The capacity would be on average 840 passengers per hour which is more than sufficient to transport all of the 6 million passengers traveling between Los Angeles and San Francisco areas per year. In addition, this accounts for 70% of those travelers to use the Hyperloop during rush hour. The lower cost of traveling on Hyperloop is likely to result in increased demand, in which case the time between capsule departures could be significantly shortened.

4.1. Capsule

Two versions of the Hyperloop capsules are being considered: a passenger only version and a passenger plus vehicle version.

Hyperloop Passenger Capsule

Assuming an average departure time of 2 minutes between capsules, a minimum of 28 passengers per capsule are required to meet 840 passengers per hour. It is possible to further increase the Hyperloop capacity by reducing the time between departures. The current baseline requires up to 40 capsules in activity during rush hour, 6 of which are at the terminals for loading and unloading of the passengers in approximately 5 minutes.

Hyperloop Passenger Plus Vehicle Capsule

The passenger plus vehicle version of the Hyperloop will depart as often as the passenger only version, but will accommodate 3 vehicles in addition to the passengers. All subsystems discussed in the following sections are featured on both capsules.

For travel at high speeds, the greatest power requirement is normally to overcome air resistance. Aerodynamic drag increases with the square of speed, and thus the power requirement increases with the cube of speed. For example, to travel twice as fast a vehicle must overcome four times the aerodynamic resistance, and input eight times the power.

Just as aircraft climb to high altitudes to travel through less dense air, Hyperloop encloses the capsules in a reduced pressure tube. The pressure of air in Hyperloop is about 1/6 the pressure of the atmosphere on Mars. This is an operating pressure of 100 Pascals, which reduces the drag force of the air by 1,000 times relative to sea level conditions and would be equivalent to flying above 150,000 feet altitude. A hard vacuum is avoided as vacuums are expensive and difficult to maintain compared with low pressure solutions. Despite the low pressure, aerodynamic challenges must still be addressed. These include managing the formation of shock waves when the speed of the capsule approaches the speed of sound, and the air resistance increases sharply. Close to the cities where more turns must be navigated, capsules travel at a lower speed. This reduces the accelerations felt by the passengers, and also reduces power requirements for the capsule. The capsules travel at 760 mph (1,220 kph, Mach 0.99 at 68 °F or 20 °C).

The proposed capsule geometry houses several distinct systems to reside within the outer mold line (Figure 4).

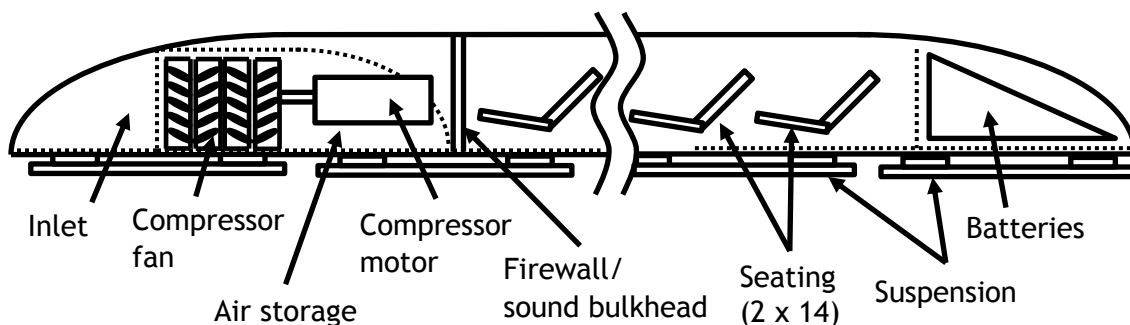


Figure 4. Hyperloop passenger capsule subsystem notional locations (not to scale).

4.1.1. Geometry

In order to optimize the capsule speed and performance, the frontal area has been minimized for size while maintaining passenger comfort (Figure 5 and Figure 6).

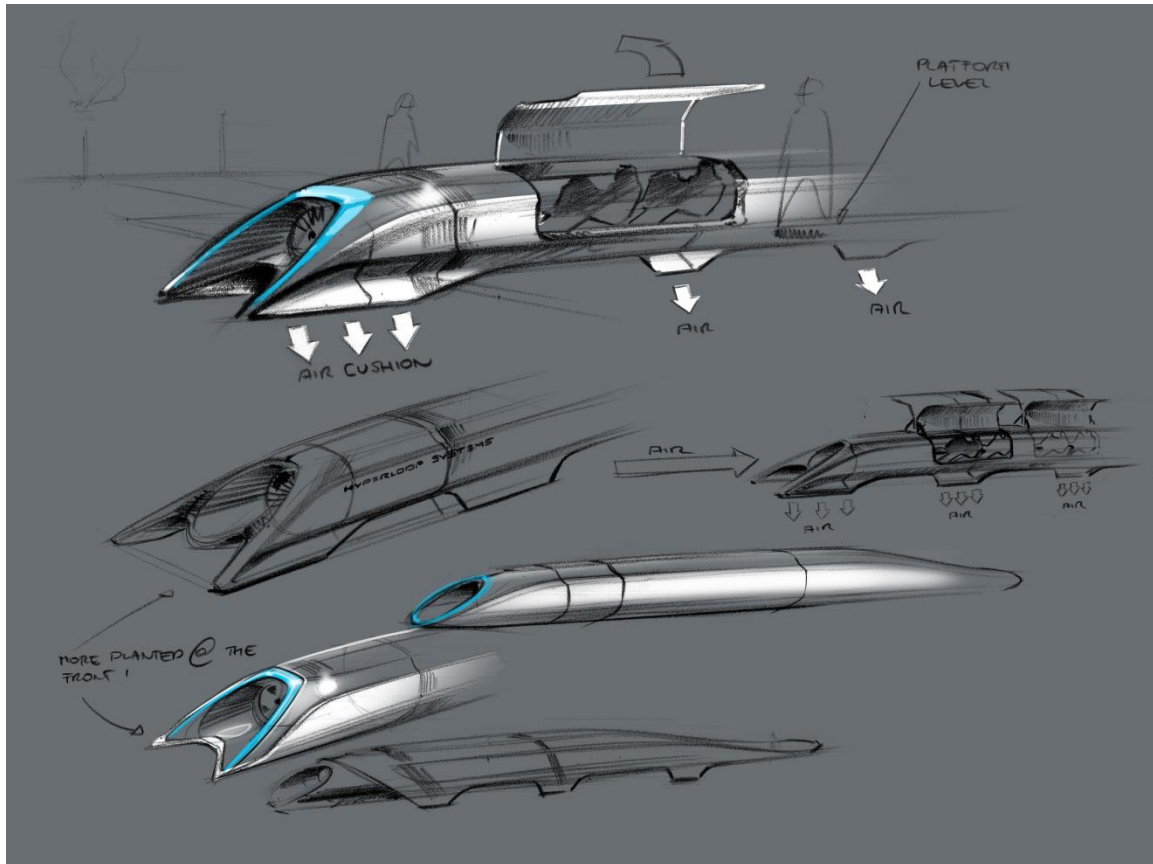


Figure 5. Hyperloop passenger transport capsule conceptual design sketch.

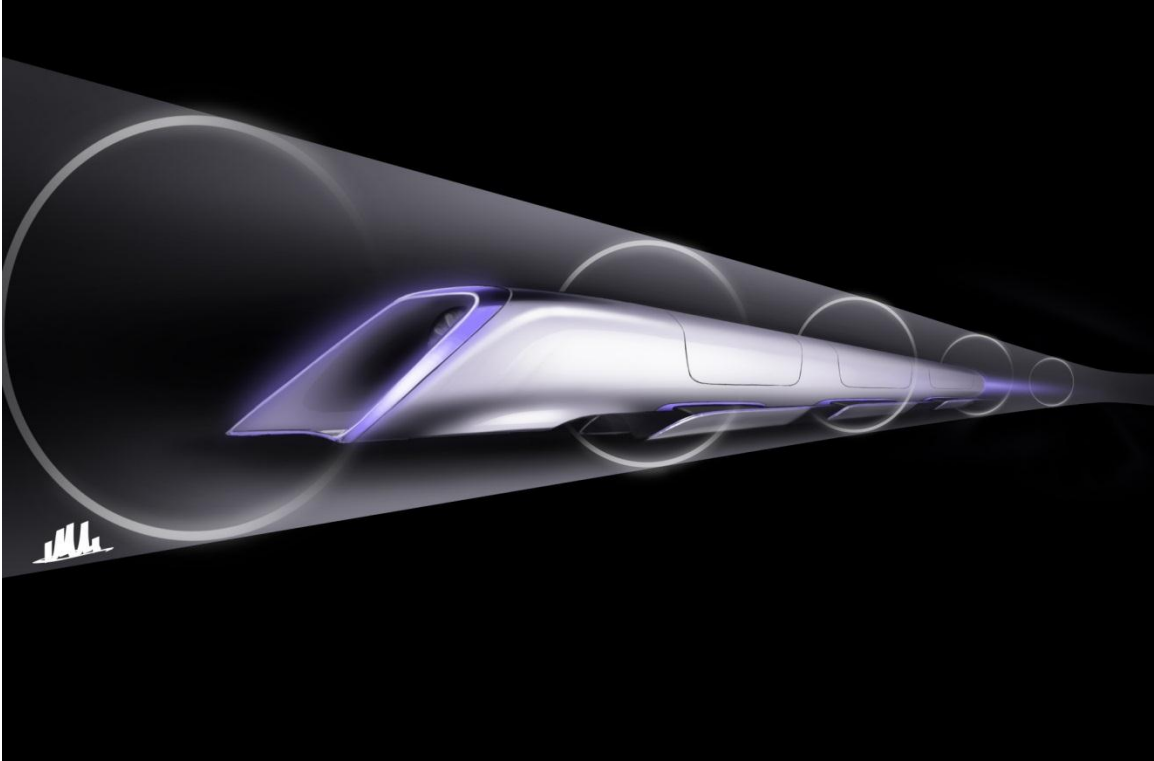


Figure 6. Hyperloop passenger transport capsule conceptual design rendering.

The vehicle is streamlined to reduce drag and features a compressor at the leading face to ingest oncoming air for levitation and to a lesser extent propulsion. Aerodynamic simulations have demonstrated the validity of this ‘compressor within a tube’ concept (Figure 7).

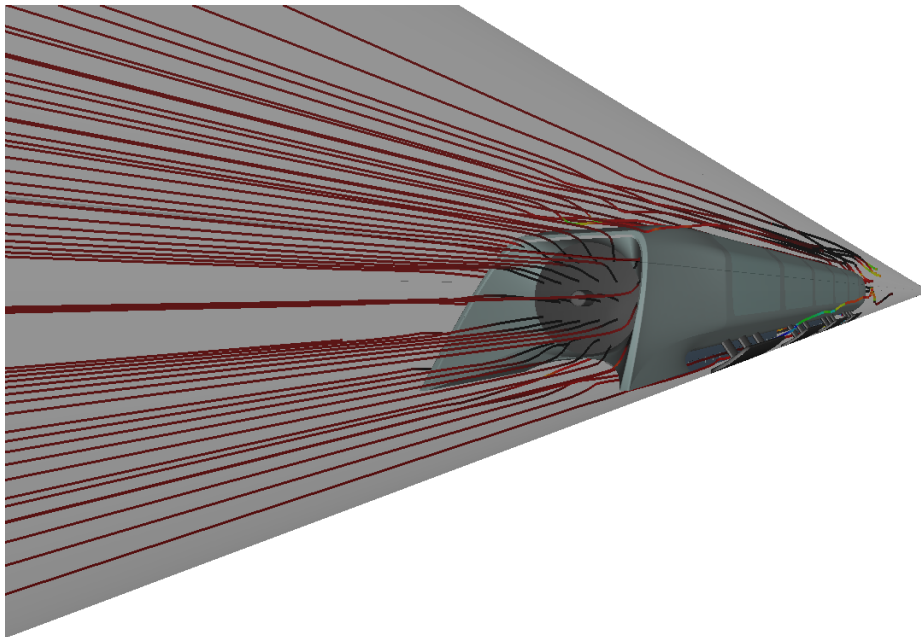


Figure 7. Streamlines for capsule traveling at high subsonic velocities inside Hyperloop.

Hyperloop Passenger Capsule

The maximum width is 4.43 ft (1.35 m) and maximum height is 3.61 ft (1.10 m). With rounded corners, this is equivalent to a 15 ft² (1.4 m²) frontal area, not including any propulsion or suspension components.

The aerodynamic power requirements at 700 mph (1,130 kph) is around only 134 hp (100 kW) with a drag force of only 72 lb_f (320 N), or about the same force as the weight of one oversized checked bag at the airport. The doors on each side will open in a gullwing (or possibly sliding) manner to allow easy access during loading and unloading. The luggage compartment will be at the front or rear of the capsule.

The overall structure weight is expected to be near 6,800 lb (3,100 kg) including the luggage compartments and door mechanism. The overall cost of the structure including manufacturing is targeted to be no more than \$245,000.

Hyperloop Passenger Plus Vehicle Capsule

The passenger plus vehicle version of the Hyperloop capsule has an increased frontal area of 43 ft² (4.0 m²), not including any propulsion or suspension components. This accounts for enough width to fit a vehicle as large as the Tesla Model X.

The aerodynamic power requirement at 700 mph (1,130 kph) is around only 382 hp (285 kW) with a drag force of 205 lb_f (910 N). The doors on each side will open in a gullwing (or possibly sliding) manner to accommodate loading of vehicles, passengers, or freight.

The overall structure weight is expected to be near 7,700 lb (3,500 kg) including the luggage compartments and door mechanism. The overall cost of the structure including manufacturing is targeted to be no more than \$275,000.

4.1.2. Interior

The interior of the capsule is specifically designed with passenger safety and comfort in mind. The seats conform well to the body to maintain comfort during the high speed accelerations experienced during travel. Beautiful landscape will be displayed in the cabin and each passenger will have access their own personal entertainment system.

Hyperloop Passenger Capsule

The Hyperloop passenger capsule (Figure 8 and Figure 9) overall interior weight is expected to be near 5,500 lb (2,500 kg) including the seats, restraint systems, interior and door panels, luggage compartments, and entertainment

displays. The overall cost of the interior components is targeted to be no more than \$255,000.

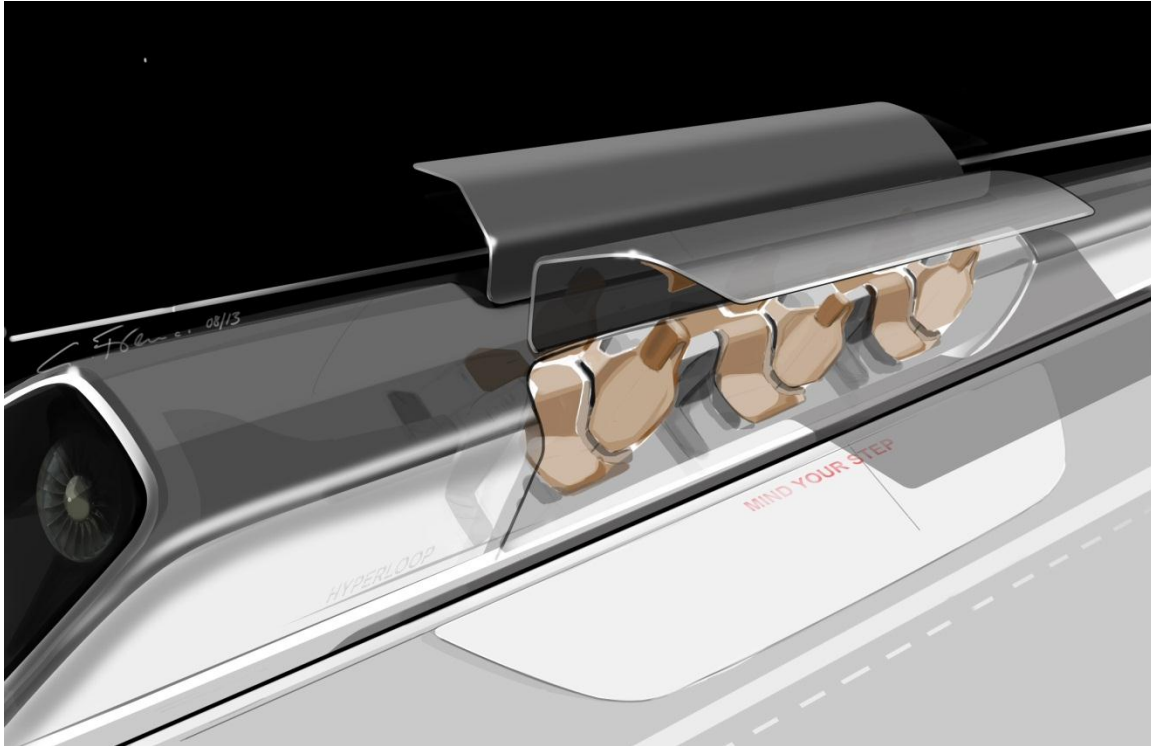


Figure 8. Hyperloop passenger capsule version with doors open at the station.

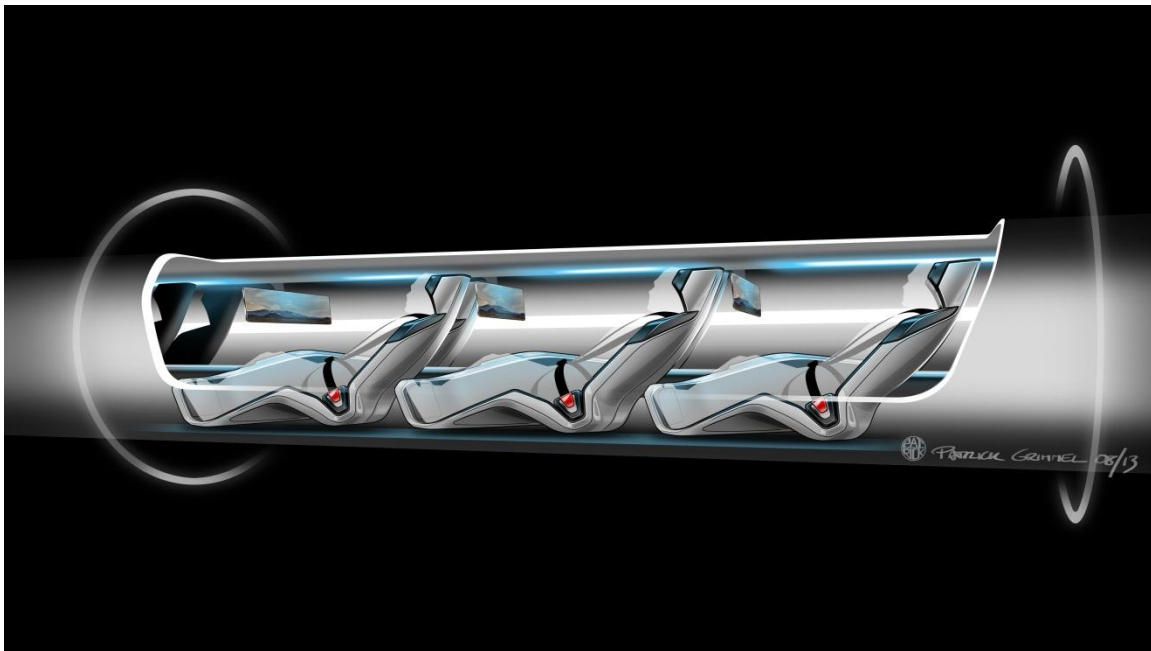


Figure 9. Hyperloop passenger capsule version cutaway with passengers onboard.

Hyperloop Passenger Plus Vehicle Capsule

The Hyperloop passenger plus vehicle capsule overall interior weight is expected to be near 6,000 lb (2,700 kg) including the seats, restraint systems, interior and door panels, luggage compartments, and entertainment displays. The overall cost of the interior components is targeted to be no more than \$185,000. Note this cost is lower than the passenger only capsule interior as vehicles do not require the same level of comfort as passengers.

4.1.3. Compressor

One important feature of the capsule is the onboard compressor, which serves two purposes. This system allows the capsule to traverse the relatively narrow tube without choking flow that travels between the capsule and the tube walls (resulting in a build-up of air mass in front of the capsule and increasing the drag) by compressing air that is bypassed through the capsule. It also supplies air to air bearings that support the weight of the capsule throughout the journey.

The air processing occurs as follows (Figure 10 and Figure 11) (note mass counting is tracked in Section 4.1.4):

Hyperloop Passenger Capsule

1. Tube air is compressed with a compression ratio of 20:1 via an axial compressor.
2. Up to 60% of this air is bypassed:
 - a. The air travels via a narrow tube near bottom of the capsule to the tail.
 - b. A nozzle at the tail expands the flow generating thrust to mitigate some of the small amounts of aerodynamic and bearing drag.
3. Up to 0.44 lb/s (0.2 kg/s) of air is cooled and compressed an additional 5.2:1 for the passenger version with additional cooling afterward.
 - a. This air is stored in onboard composite overwrap pressure vessels.
 - b. The stored air is eventually consumed by the air bearings to maintain distance between the capsule and tube walls.
4. An onboard water tank is used for cooling of the air.
 - a. Water is pumped at 0.30 lb/s (0.14 kg/s) through two intercoolers (639 lb or 290 kg total mass of coolant).
 - b. The steam is stored onboard until reaching the station.
 - c. Water and steam tanks are changed automatically at each stop.
5. The compressor is powered by a 436 hp (325 kW) onboard electric motor:
 - a. The motor has an estimated mass of 372 lb (169 kg), which includes power electronics.

- b. An estimated 3,400 lb (1,500 kg) of batteries provides 45 minutes of onboard compressor power, which is more than sufficient for the travel time with added reserve backup power.
- c. Onboard batteries are changed at each stop and charged at the stations.

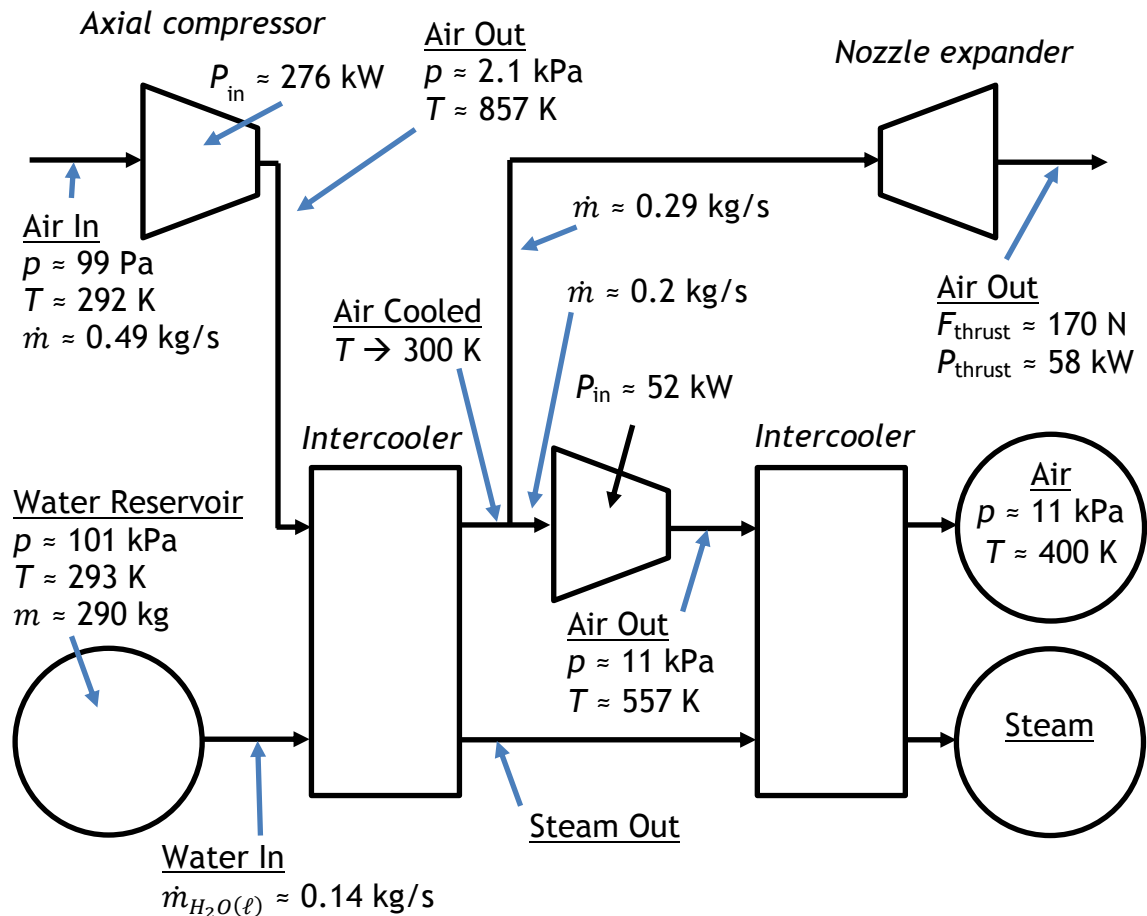


Figure 10. Compressor schematic for passenger capsule.

Hyperloop Passenger Plus Vehicle Capsule

1. Tube air is compressed with a compression ratio of 20:1 via an axial compressor.
2. Up to 85% of this air is bypassed:
 - a. The air travels via a narrow tube near bottom of the capsule to the tail.
 - b. A nozzle at the tail expands the flow generating thrust to mitigate some of the small amounts of aerodynamic and bearing drag.
3. Up to 0.44 lb/s (0.2 kg/s) of air is cooled and compressed an additional 6.2:1 for the passenger plus vehicle version with additional cooling afterward.

- a. This air is stored in onboard composite overwrap pressure vessels.
 - b. The stored air is eventually consumed by the air bearings to maintain distance between the capsule and tube walls.
4. An onboard water tank is used for cooling of the air.
 - a. Water is pumped at 0.86 lb/s (0.39 kg/s) through two intercoolers (1,800 lb or 818 kg total mass of coolant).
 - b. The steam is stored onboard until reaching the station.
 - c. Water and steam tanks are changed automatically at each stop.
5. The compressor is powered by a 1,160 hp (865 kW) onboard electric motor:
 - a. The motor has an estimated mass of 606 lb (275 kg), which includes power electronics.
 - b. An estimated 8,900 lb (4,000 kg) of batteries provides 45 minutes of onboard compressor power, which is more than sufficient for the travel time with added reserve backup power.
 - c. Onboard batteries are changed at each stop and charged at the stations.

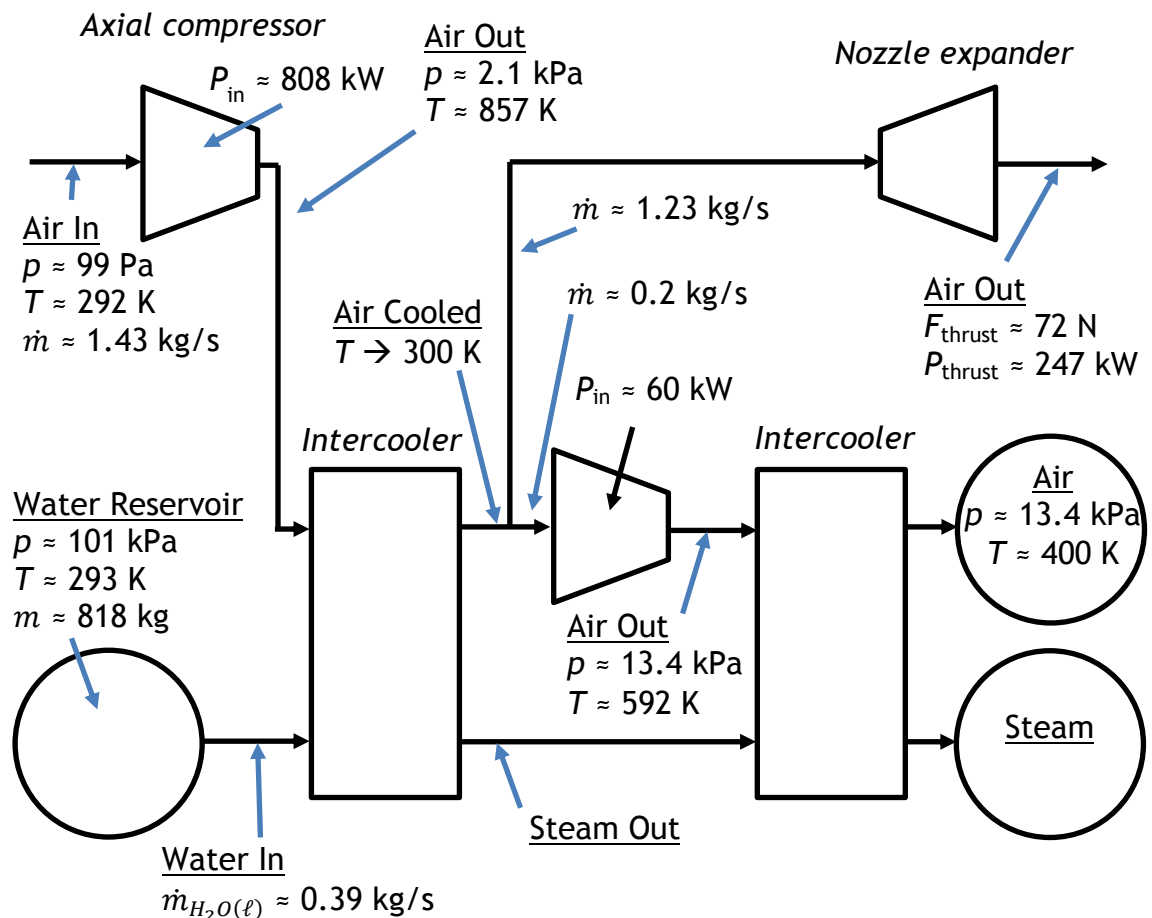


Figure 11. Compressor schematic for passenger plus vehicle capsule.

4.1.4. Suspension

Suspending the capsule within the tube presents a substantial technical challenge due to transonic cruising velocities. Conventional wheel and axle systems become impractical at high speed due frictional losses and dynamic instability. A viable technical solution is magnetic levitation; however the cost associated with material and construction is prohibitive. An alternative to these conventional options is an air bearing suspension. Air bearings offer stability and extremely low drag at a feasible cost by exploiting the ambient atmosphere in the tube.

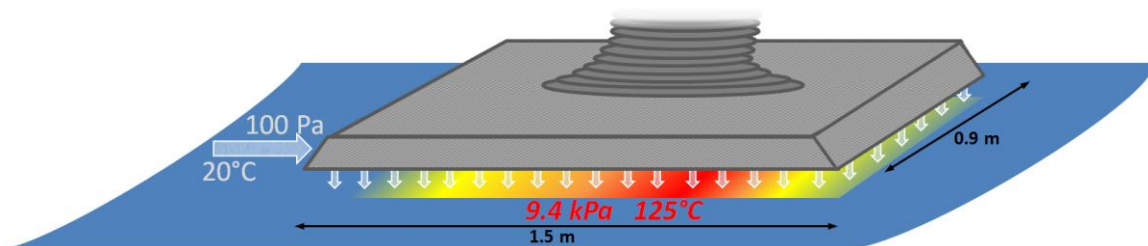


Figure 12: Schematic of air bearing skis that support the capsule.

Externally pressurized and aerodynamic air bearings are well suited for the Hyperloop due to exceptionally high stiffness, which is required to maintain stability at high speeds. When the gap height between a ski and the tube wall is reduced, the flow field in the gap exhibits a highly non-linear reaction resulting in large restoring pressures. The increased pressure pushes the ski away from the wall, allowing it to return to its nominal ride height. While a stiff air bearing suspension is superb for reliability and safety, it could create considerable discomfort for passengers onboard. To account for this, each ski is integrated into an independent mechanical suspension, ensuring a smooth ride for passengers. The capsule may also include traditional deployable wheels similar to aircraft landing gear for ease of movement at speeds under 100 mph (160 kph) and as a component of the overall safety system.

Hyperloop Passenger Capsule

Hyperloop capsules will float above the tube's surface on an array of 28 air bearing skis that are geometrically conformed to the tube walls. The skis, each 4.9 ft (1.5 meters) in length and 3.0 ft (0.9 meters) in width, support the weight of the capsule by floating on a pressurized cushion of air 0.020 to 0.050 in. (0.5 to 1.3 mm) off the ground. Peak pressures beneath the skis need only reach 1.4 psi (9.4 kPa) to support the passenger capsule (9% of sea level atmospheric pressure). The skis depend on two mechanisms to pressurize the thin air film: external pressurization and aerodynamics.

The aerodynamic method of generating pressure under the air bearings becomes appreciable at moderate to high capsule speeds. As the capsule

accelerates up to cruising speed, the front tip of each ski is elevated relative to the back tip such that the ski rests at a slight angle of 0.05° . Viscous forces trap a thin film of air in the converging gap between the ski and the tube wall. The air beneath the ski becomes pressurized which alters the flow field to satisfy fundamental laws of mass, momentum, and energy conservation. The resultant elevated pressure beneath the ski relative to the ambient atmosphere provides a net lifting force that is sufficient to support a portion of the capsule's weight.

However, the pressure field generated by aerodynamics is not sufficient to support the entire weight of the vehicle. At lower speeds, very little lift can be generated by aerodynamic mechanisms. As the capsule speed increases and compressibility effects become important, the pressure rise in the air bearing (assuming isothermal flow) will reach a limiting value which depends on the geometry of the air bearing. Thus additional sources of lift will be required.

Lift is supplemented by injecting highly pressurized air into the gap. By applying an externally supplied pressure, a favorable pressure distribution is established beneath the bearing and sufficient lift is generated to support the capsule. This system is known as an external pressure (EP) bearing and it is effective when the capsule is stationary or moving at very high speeds. At nominal weight and g-loading, a capsule on the Hyperloop will require air injection beneath the ski at a rate of 0.44 lb/s (0.2 kg/s) at 1.4 psi (9.4 kPa) for the passenger capsule. The air is introduced via a network of grooves in the bearing's bottom surface and is sourced directly from the high pressure air reservoir onboard the capsule.

The aerodynamically and externally pressurized film beneath the skis will generate a drag force on the capsule. The drag may be computed by recognizing that fluid velocity in the flow field is driven by both the motion of the tube wall relative to the ski and by a pressure gradient, which is typically referred to as a Couette-Poiseuille flow. Such flows are well understood, and the resultant drag can be computed analytically (as done in this alpha study) and improved and/or validated by computational methods. The predicted total drag generated by the 28 air bearings at a capsule speed of 760 mph (1,220 kph) is 31 lb_f (140 N), resulting in a 64 hp (48 kW) power loss.

The passenger capsule air bearing system weight is expected to be about 6,200 lb (2,800 kg) including the compressors, air tank, plumbing, suspension, and bearing surfaces. The overall cost of the air bearing components is targeted to be no more than \$475,000.

Hyperloop Passenger Plus Vehicle Capsule

The passenger plus vehicle version of the Hyperloop capsule places more aggressive lifting requirements on the air bearings, but the expanded diameter of the tube provides a greater surface area for lift generation. For this version,

an extra 12 in. (30 cm) of width would be added to each bearing. The nominal air supply pressure would increase to 1.6 psi (11.2 kPa), but the flow rate required would remain 0.44 lb/s (0.2 kg/s) thanks to the increased area under the skis. Drag on the skis at 42 lb_f (187 N), results in a power loss of 85 hp (63 kW).

The passenger plus vehicle capsule air bearing system weight is expected to be about 8,400 lb (3,800 kg) including the compressors, air tank, plumbing, suspension, and bearing surfaces. The overall cost of the air bearing components is targeted to be no more than \$565,000.

4.1.5. Onboard Power

The passenger capsule power system includes an estimated 5,500 lb (2,500 kg) of batteries to power the capsule systems in addition to the compressor motor (using 3,400 lb or 1,500 kg of the batteries) and coolant. The battery, motor, and electronic components cost is estimated to be near \$150,000 per capsule in addition to the cost of the suspension system.

The passenger plus vehicle capsule power system includes an estimated 12,100 lb (5,500 kg) of batteries to power capsule systems in addition to the compressor motor (using 8,900 lb or 4,000 kg of the batteries) and coolant. The battery, motor and electronic components cost is estimated to be near \$200,000 per capsule in addition to the cost of the suspension system.

4.1.6. Propulsion

In order to propel the vehicle at the required travel speed, an advanced linear motor system is being developed to accelerate the capsule above 760 mph (1,220 kph) at a maximum of 1g for comfort. The moving motor element (rotor) will be located on the vehicle for weight savings and power requirements while the tube will incorporate the stationary motor element (stator) which powers the vehicle. More details can be found in the section 4.3.

Hyperloop Passenger Capsule

The overall propulsion system weight attached to the capsule is expected to be near 2,900 lb (1,300 kg) including the support and emergency braking system. The overall cost of the system is targeted to be no more than \$125,000. This brings the total capsule weight near 33,000 lb (15,000 kg) including passenger and luggage weight.

Hyperloop Passenger Plus Vehicle Capsule

The overall propulsion system weight attached to the capsule is expected to be near 3,500 lb (1,600 kg) including the support and emergency braking system. The overall cost of the system is targeted to be no more than \$150,000. This

brings the total capsule weight near 57,000 lb (26,000) kg including passenger, luggage, and vehicle weight.

4.1.7. Cost

The overall cost of the Hyperloop passenger capsule version (Table 1) is expected to be under \$1.35 million USD including manufacturing and assembly cost. With 40 capsules required for the expected demand, the total cost of capsules for the Hyperloop system should be no more than \$54 million USD or approximately 1% of the total budget.

Although the overall cost of the project would be higher, we have also detailed the expected cost of a larger capsule (Table 2) which could carry not only passengers but cargo and cars/SUVs as well. The frontal area of the capsule would have to be increased to 43 ft² (4 m²) and the tube diameter would be increased to 10 ft 10 in. (3.3 m).

Table 1. Crew capsule weight and cost breakdown

Vehicle Component	Cost (\$)	Weight (kg)
Capsule Structure & Doors:	\$ 245,000	3100
Interior & Seats:	\$ 255,000	2500
Propulsion System:	\$ 75,000	700
Suspension & Air Bearings:	\$ 200,000	1000
Batteries, Motor & Coolant:	\$ 150,000	2500
Air Compressor:	\$ 275,000	1800
Emergency Braking:	\$ 50,000	600
General Assembly:	\$ 100,000	N/A
Passengers & Luggage:	N/A	2800
Total/Capsule:	\$ 1,350,000	15000
Total for Hyperloop:	\$ 54,000,000	

Vehicle Component	Cost (\$)	Weight (kg)
Capsule Structure & Doors:	\$ 275,000	3500
Interior & Seats:	\$ 185,000	2700
Propulsion System:	\$ 80,000	800
Suspension & Air Bearings:	\$ 265,000	1300
Batteries, Motor & Coolant:	\$ 200,000	5500
Air Compressor:	\$ 300,000	2500
Emergency Braking:	\$ 70,000	800
General Assembly:	\$ 150,000	N/A
Passengers & Luggage:	N/A	1400
Car & Cargo:	N/A	7500
Total/Capsule:	\$ 1,525,000	26000
Total for Hyperloop:	\$ 61,000,000	

4.2. Tube

The main Hyperloop route consists of a partially evacuated cylindrical tube that connects the Los Angeles and San Francisco stations in a closed loop system (Figure 2). The tube is specifically sized for optimal air flow around the capsule improving performance and energy consumption at the expected travel speed. The expected pressure inside the tube will be maintained around 0.015 psi (100 Pa, 0.75 torr), which is about 1/6 the pressure on Mars or 1/1000 the pressure on Earth. This low pressure minimizes the drag force on the capsule while maintaining the relative ease of pumping out the air from the tube. The efficiency of industrial vacuum pumps decreases exponentially as the pressure is reduced (Figure 13), so further benefits from reducing tube pressure would be offset by increased pumping complexity.

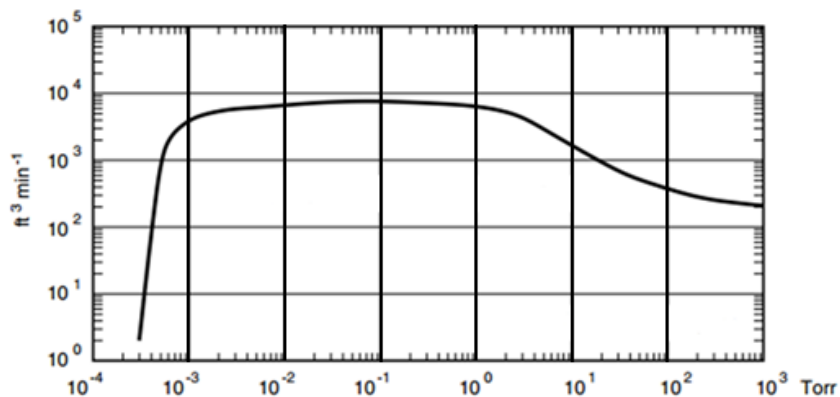


Figure 13. Typical vacuum pump speed for functional pressure range.

In order to minimize cost of the Hyperloop tube, it will be elevated on pillars which greatly reduce the footprint required on the ground and the size of the construction area required. Thanks to the small pillar footprint and by

maintaining the route as close as possible to currently operated highways, the amount of land required for the Hyperloop is minimized. More details are available for the route in section 4.4.

The Hyperloop travel journey will feel very smooth since the capsule will be guided directly on the inner surface of the tube via the use of air bearings and suspension; this also prevents the need for costly tracks. The capsule will bank off the walls and include a control system for smooth returns to nominal capsule location from banking as well. Some specific sections of the tube will incorporate the stationary motor element (stator) which will locally guide and accelerate (or decelerate) the capsule. More details are available for the propulsion system in section 4.3. Between linear motor stations, the capsule will glide with little drag via air bearings.

4.2.1. Geometry

The geometry of the tube depends on the choice of either the passenger version of Hyperloop or the passenger plus vehicles version of Hyperloop.

In either case, if the speed of the air passing through the gaps accelerates to supersonic velocities, then shock waves form. These waves limit how much air can actually get out of the way of the capsule, building up a column of air in front of its nose and increasing drag until the air pressure builds up significantly in front of the capsule. With the increased drag and additional mass of air to push, the power requirements for the capsule increase significantly. It is therefore very important to avoid shock wave formation around the capsule by careful selection of the capsule/tube area ratio. This ensures sufficient mass air flow around and through the capsule at all operating speeds. Any air that cannot pass around the annulus between the capsule and tube is bypassed using the onboard compressor in each capsule.

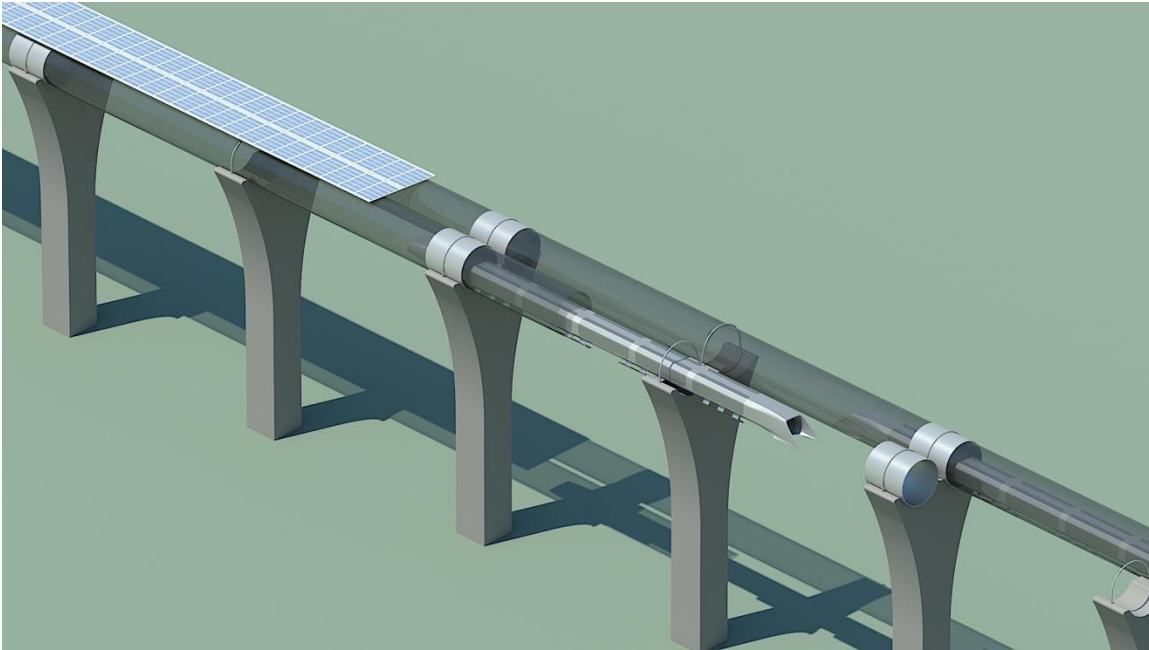


Figure 14. Hyperloop capsule in tube cutaway with attached solar arrays.

Passenger Hyperloop Tube

The inner diameter of the tube is optimized to be 7 ft 4 in. (2.23 m) which is small enough to keep material cost low while large enough to provide some alleviation of choked air flow around the capsule. The tube cross-sectional area is 42.2 ft² (3.91 m²) giving a capsule/tube area ratio of 36% or a diameter ratio of 60%. It is critical to the aerodynamics of the capsule to keep this ratio as large as possible, even though the pressure in the tube is extremely low. As the capsule moves through the tube, it must displace its own volume of air, in a loosely similar way to a boat in water. The displacement of the air is constricted by the walls of the tube, which makes it accelerate to squeeze through the gaps. Any flow not displaced must be ingested by the onboard compressor of each capsule, which increases power requirements.

The closed loop tube will be mounted side-by-side on elevated pillars as seen in Figure 5. The surface above the tubes will be lined with solar panels to provide the required system energy. This represents a possible area of 14 ft (4.25 m) wide for more than 350 miles (563 km) of tube length. With an expected solar panel energy production of 0.015 hp/ft² (120 W/m²), we can expect the system to produce a maximum of 382,000 hp (285 MW) at peak solar activity. This would actually be more energy than needed for the Hyperloop system and the detailed power requirements will be described in section 4.3.

Passenger Plus Vehicle Hyperloop Tube

The inner diameter of the tube is optimized to be 10 ft 10 in. (3.30 m), larger than the passenger version to accommodate the larger capsule. The tube cross-sectional area is 92.1 ft² (8.55 m²) giving a capsule/tube area ratio of 47% or a diameter ratio of 68%.

The closed passenger plus vehicle Hyperloop tube will be mounted side-by-side in the same manner as the passenger version as seen in Figure 5. The surface above the tubes will be lined with solar panels to provide the required system energy. This represents a possible area of 22 ft (6.6 m) wide for more than 350 miles (563 km) of tube length. With an expected solar panel energy production of 0.015 hp/ft² (120W/m²), we can expect the system to produce a maximum of 598,000 hp (446 MW) at peak solar activity. This would actually be more energy than needed for the passenger plus vehicle Hyperloop system and the specific power requirements will be detailed in section 4.3.

Station Connections

The stations are isolated from the main tube as much as possible in order to limit air leaks into the system. In addition, isolated branches and stations off the main tubes could be built to access some towns along the way between Los Angeles and San Francisco. Vacuum pumps will run continuously at various locations along the length of the tube to maintain the required pressure despite any possible leaks through the joints and stations. The expected cost of all required vacuum pumps is expected to be no more than \$10 million USD.

4.2.2. Tube Construction

In order to keep cost to a minimum, a uniform thickness steel tube reinforced with stringers was selected as the material of choice for the inner diameter tube. Tube sections would be pre-fabricated and installed between pillar supports spaced 100 ft (30 m) on average, varying slightly depending on location. This relatively short span allows keeping tube material cost and deflection to a minimum.

The steel construction allows simple welding processes to join different tube sections together. A specifically designed cleaning and boring machine will make it possible to surface finish the inside of the tube and welded joints for a better gliding surface. In addition, safety emergency exits and pressurization ports will be added in key locations along the length of the tube.

Passenger Hyperloop Tube

A tube wall thickness between 0.8 and 0.9 in. (20 to 23 mm) is necessary to provide sufficient strength for the load cases considered in this study. These cases included, but were not limited to, pressure differential, bending and

buckling between pillars, loading due to the capsule weight and acceleration, as well as seismic considerations.

The cost of the tube is expected to be less than \$650 million USD, including pre-fabricated tube sections with stringer reinforcements and emergency exits. The support pillars and joints which will be detailed in section 4.2.3.

Passenger Plus Vehicle Hyperloop Tube

The tube wall thickness for the larger tube would be between 0.9 and 1.0 in (23 to 25 mm). Tube cost calculations were also made for the larger diameter tube which would allow usage of the cargo and vehicle capsule in addition to the passenger capsule. In this case, the cost of the tube is expected to be less than \$1.2 billion USD. Since the spacing between pillars would not change and the pillars are more expensive than the tube, the overall cost increase is kept to a minimum.

4.2.3. Pylons and Tunnels

The tube will be supported by pillars which constrain the tube in the vertical direction but allow longitudinal slip for thermal expansion as well as dampened lateral slip to reduce the risk posed by earthquakes. In addition, the pillar to tube connection nominal position will be adjustable vertically and laterally to ensure proper alignment despite possible ground settling. These minimally constrained pillars to tube joints will also allow a smoother ride. Specially designed slip joints at stations will be able to take any tube length variance due to thermal expansion. This is an ideal location for the thermal expansion joints as the speed is much lower nearby the stations. It thus allows the tube to be smooth and welded along the high speed gliding middle section.

The spacing of the Hyperloop pillars retaining the tube is critical to achieve the design objective of the tube structure. The average spacing is 100 ft (30 m), which means there will be roughly 25,000 pillars supporting both Hyperloop tubes and overhead solar panels. The pillars will be 20 ft (6 m) tall whenever possible but may vary in height in hilly areas or where obstacles are in the way. Also, in some key areas, the spacing will have to vary in order to pass over roads or other obstacles. Small spacing between each support reduces the deflection of the tube keeping the capsule steadier and the journey more enjoyable. In addition, reduced spacing has increased resistance to seismic loading as well as the lateral acceleration of the capsule.

Due to the sheer quantity of pillars required, reinforced concrete was selected as the construction material due to its very low cost per volume. In some short areas, tunneling may be required to avoid going over mountains and to keep the route as straight as possible. The cost for the pillar construction and tube joints is anticipated to be no more than \$2.55 billion USD for the passenger version tube and \$3.15 billion USD for the passenger plus vehicle version tube.

The expected cost for the tunneling is expected to be no more than \$600 million USD for the smaller diameter tube and near \$700 million USD for the larger diameter tube.

Structural simulations (Figure 15 through Figure 20) have demonstrated the capability of the Hyperloop to withstand atmospheric pressure, tube weight, earthquakes, winds, etc. Dampers will be incorporated between the pylons and tubes to isolate movements in the ground from the tubes.

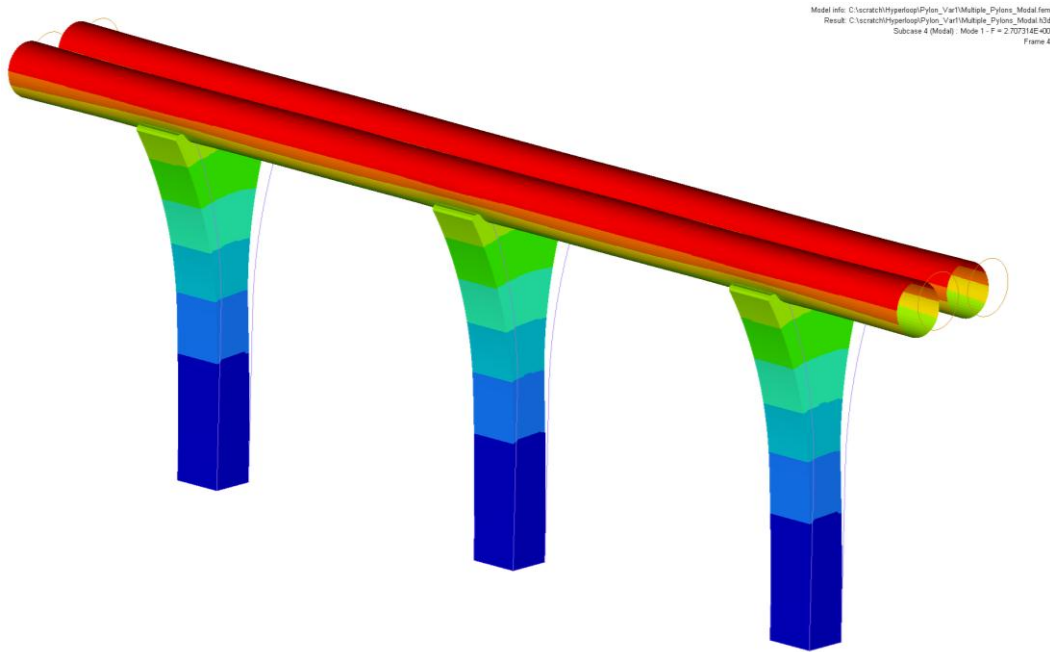


Figure 15. First mode shape of Hyperloop at 2.71Hz (magnified x1500).

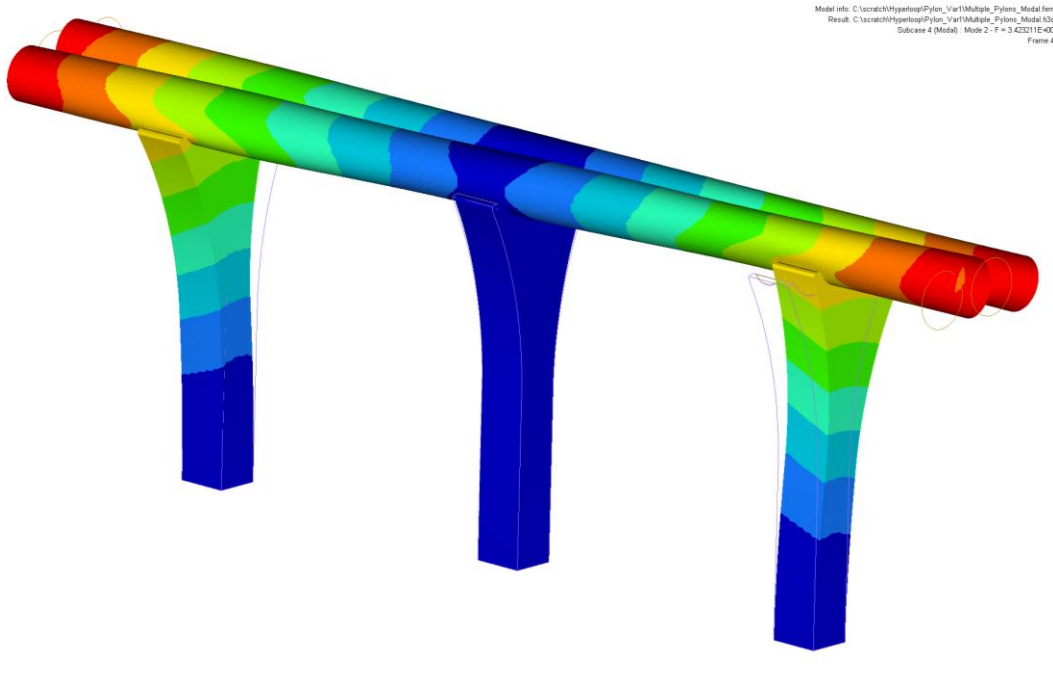


Figure 16. Second mode shape of Hyperloop at 3.42Hz (magnified x1500).

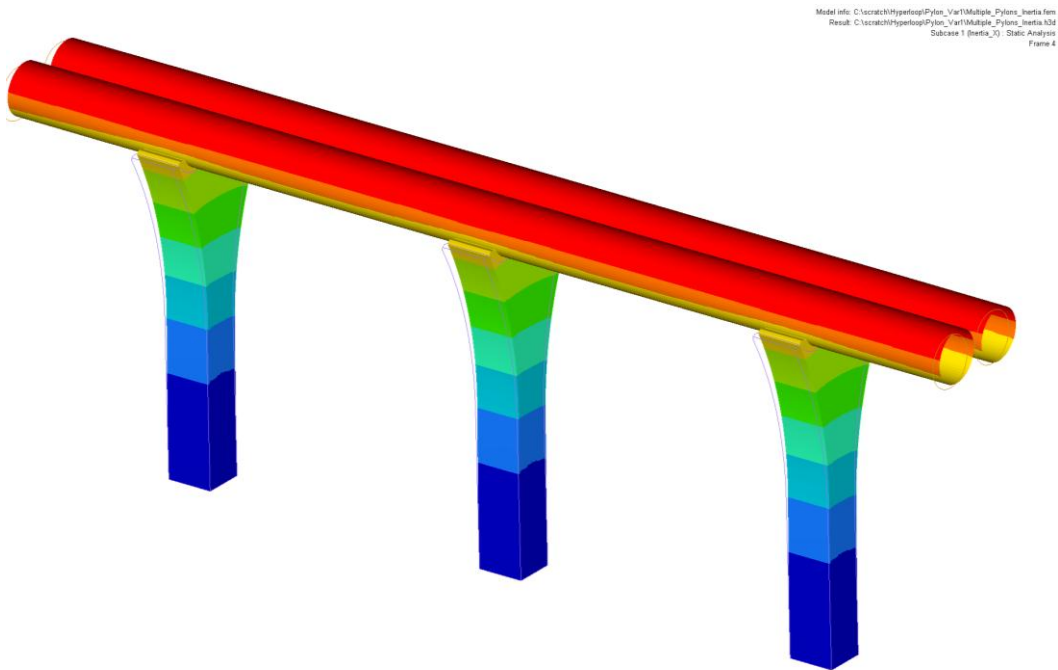


Figure 17. Deformation at 1g Inertia in X (in.) (magnified x10).

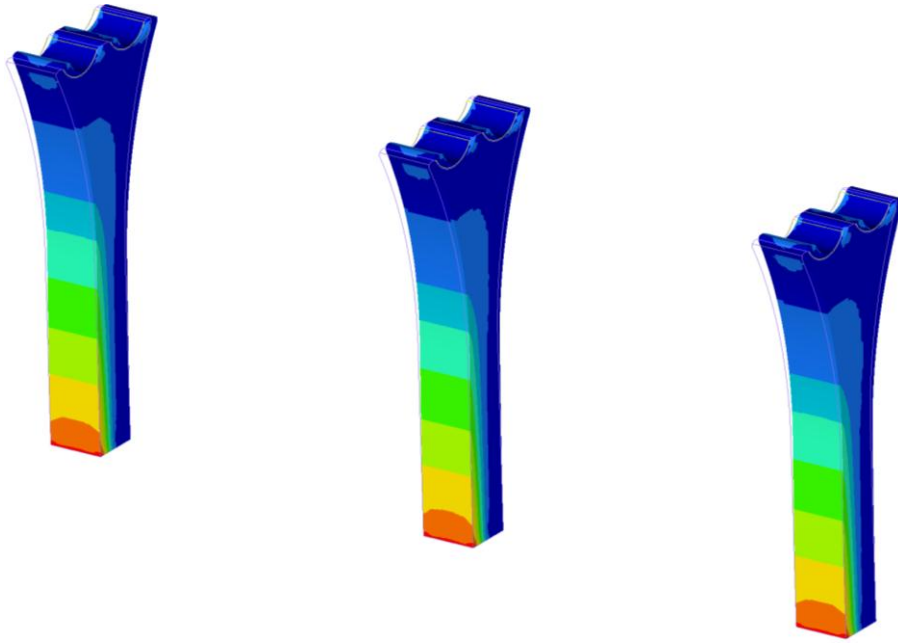


Figure 18. Maximum principal stress at 1g Inertia in X (psi) (magnified x10).

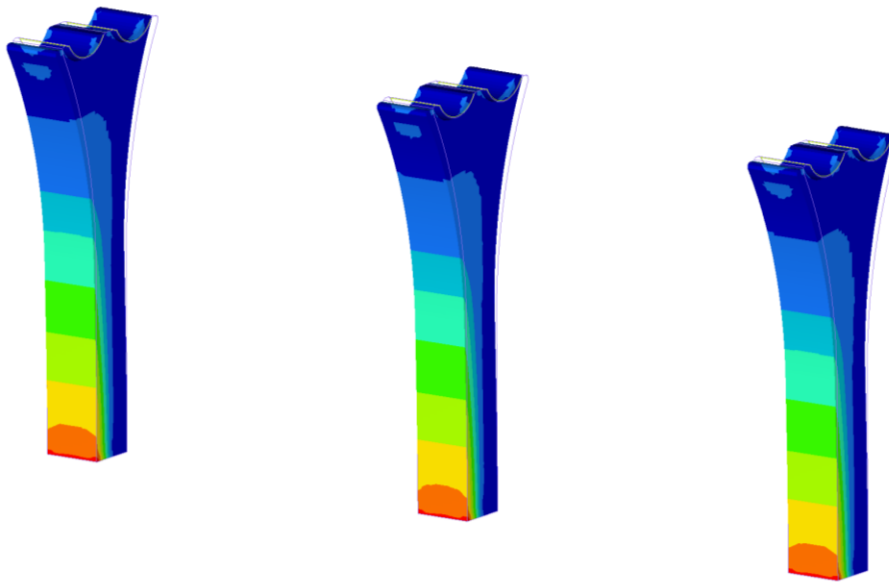


Figure 19. Minimum principal stress at 1g Inertia in X (psi) (magnified x10).

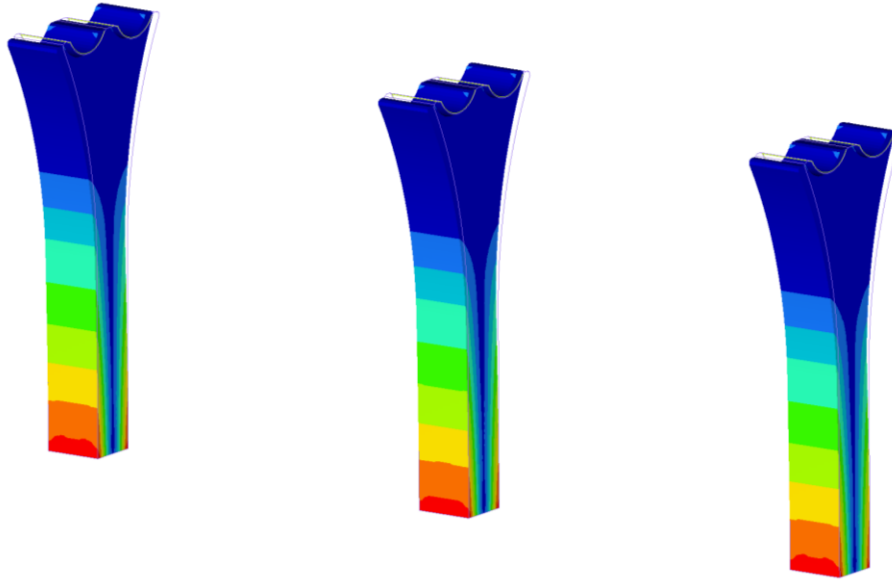


Figure 20. Maximum shear stress at 1g Inertia in X (psi) (magnified x10).

4.2.4. Station Construction

Hyperloop stations are intended to be minimalist but practical with a boarding process and layout much simpler than airports.

Due to the short travel time and frequent departures, it is envisaged that there will be a continual flow of passengers through each Hyperloop station, in contrast to the pulsed situation at airports which leads to lines and delays. Safety and security are paramount, and so security checks will still be made in a similar fashion as TSA does for the airport. The process could be greatly streamlined to reduce wait time and maintain a more continuous passenger flow.

All ticketing and baggage tracking for the Hyperloop will be handled electronically, negating the need for printing boarding passes and luggage labels. Since Hyperloop travel time is very short, the main usage is more for commuting than for vacations. There would be a luggage limit of 2 bags per person, for no more than 110 lb (50 kg) in total. Luggage would be stowed in a separate compartment at the rear of the capsule, in a way comparable to the overhead bins on passenger aircraft. This luggage compartment can be removed from the capsule, so that the process of stowing and retrieving luggage can be undertaken separately from embarking or disembarking the capsule's passenger cabin. In addition, Hyperloop staff will take care of loading and unloading passenger luggage in order to maximize efficiency.

The transit area at a Hyperloop terminal would be a large open area with two large airlocks signifying the entry and exit points for the capsules. An arriving capsule would enter the incoming airlock, where the pressure is equalized with

the station, before being released into the transit area. The doors of the capsule would open allowing the passengers to disembark. The luggage pod would be quickly unloaded by the Hyperloop staff or separated from the capsule so that baggage retrieval would not interfere with the capsule turnaround.

Once vacated, the capsule would be rotated on a turntable, and aligned for re-entry into the Hyperloop tube. The departing passengers, and their pre-loaded luggage pod, would then enter the capsule. A Hyperloop attendant would next perform a safety check of the seat belt of each passenger before the capsule is cleared for departure. At this point the capsule would then be moved forward into the exit airlock, where the pressure is lowered to the operating level of the Hyperloop, and then sent on its way. Note that loading and unloading would occur in parallel with up to three capsules at a given station at any time. The expected cost for each station is around \$125 million for a total of \$250 million USD initially.

4.2.5. Cost

The overall cost of the tube, pillars, vacuum pumps and stations is thus expected to be around \$4.06 billion USD for the passenger version of the Hyperloop. This does not include the cost of the propulsion linear motors or solar panels. The tube represents approximately 70% of the total budget.

The larger 10 ft 10 in. (3.3 m) tube would allow the cargo and vehicle capsules to fit at a total cost including the tube, pillars, vacuum pumps, and stations around \$5.31 billion USD. This minimal cost increase would allow a much more versatile Hyperloop system.

4.3. Propulsion

The propulsion system has the following basic requirements:

1. Accelerate the capsule from 0 to 300 mph (480 kph) for relatively low speed travel in urban areas.
2. Maintain the capsule at 300 mph (480 kph) as necessary, including during ascents over the mountains surrounding Los Angeles and San Francisco.
3. To accelerate the capsule from 300 to 760 mph (480 to 1,220 kph) at 1G at the beginning of the long coasting section along the I-5 corridor.
4. To decelerate the capsule back to 300 mph (480 kph) at the end of the I-5 corridor.

The Hyperloop as a whole is projected to consume an average of 28,000 hp (21 MW). This includes the power needed to make up for propulsion motor efficiency (including elevation changes), aerodynamic drag, charging the batteries to power on-board compressors, and vacuum pumps to keep the tube evacuated. A solar array covering the entire Hyperloop is large enough to

provide an annual average of 76,000 hp (57 MW), significantly more than the Hyperloop requires.

Since the peak powers of accelerating and decelerating capsules are up to 3 times the average power, the power architecture includes a battery array at each accelerator. These arrays provide storage of excess power during non-peak periods that can be used during periods of peak usage. Power from the grid is needed only when solar power is not available.

This section details a large linear accelerator, capable of the 300 to 760 mph (480 to 1,220 kph) acceleration at 1G. Smaller accelerators appropriate for urban areas and ascending mountain ranges can be scaled down from this system.

The Hyperloop uses a linear induction motor to accelerate and decelerate the capsule. This provides several important benefits over a permanent magnet motor:

- Lower material cost - the rotor can be a simple aluminum shape, and does not require rare-earth elements.
- Lighter capsule.
- Smaller capsule dimensions.

The lateral forces exerted by the stator on the rotor though low at 0.9 lb_f/ft (13 N/m) are inherently stabilizing. This simplifies the problem of keeping the rotor aligned in the air gap.

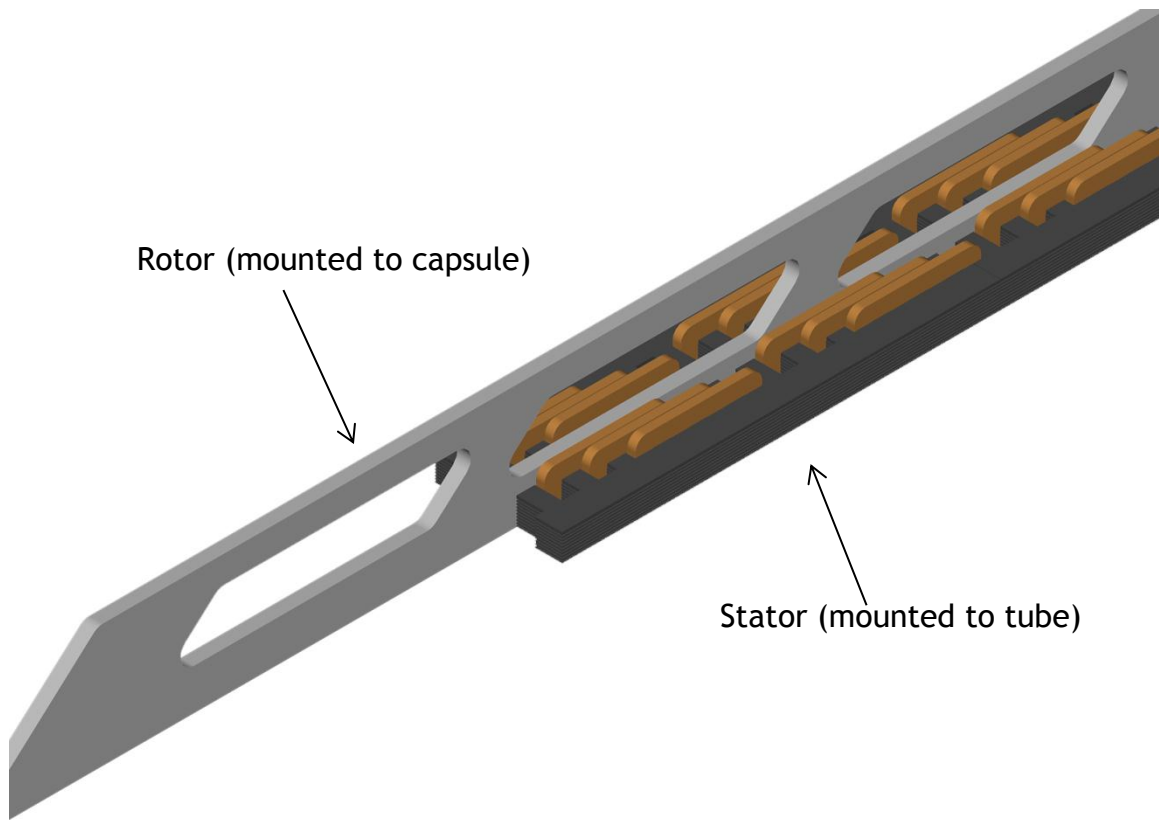


Figure 21. Rotor and stator 3D diagram

Each accelerator has two 70 MVA inverters, one to accelerate the outgoing capsule, and one to capture the energy from the incoming capsule. Inverters in the 10+ MVA power range are not unusual in mining, drives for large cargo ships, and railway traction. Moreover, 100+ MVA drives are commercially available. Relatively inexpensive semiconductor switches allow the central inverters to energize only the section of track occupied by a capsule, improving the power factor seen by the inverters.

The inverters are physically located at the highest speed end of the track to minimize conductor cost.

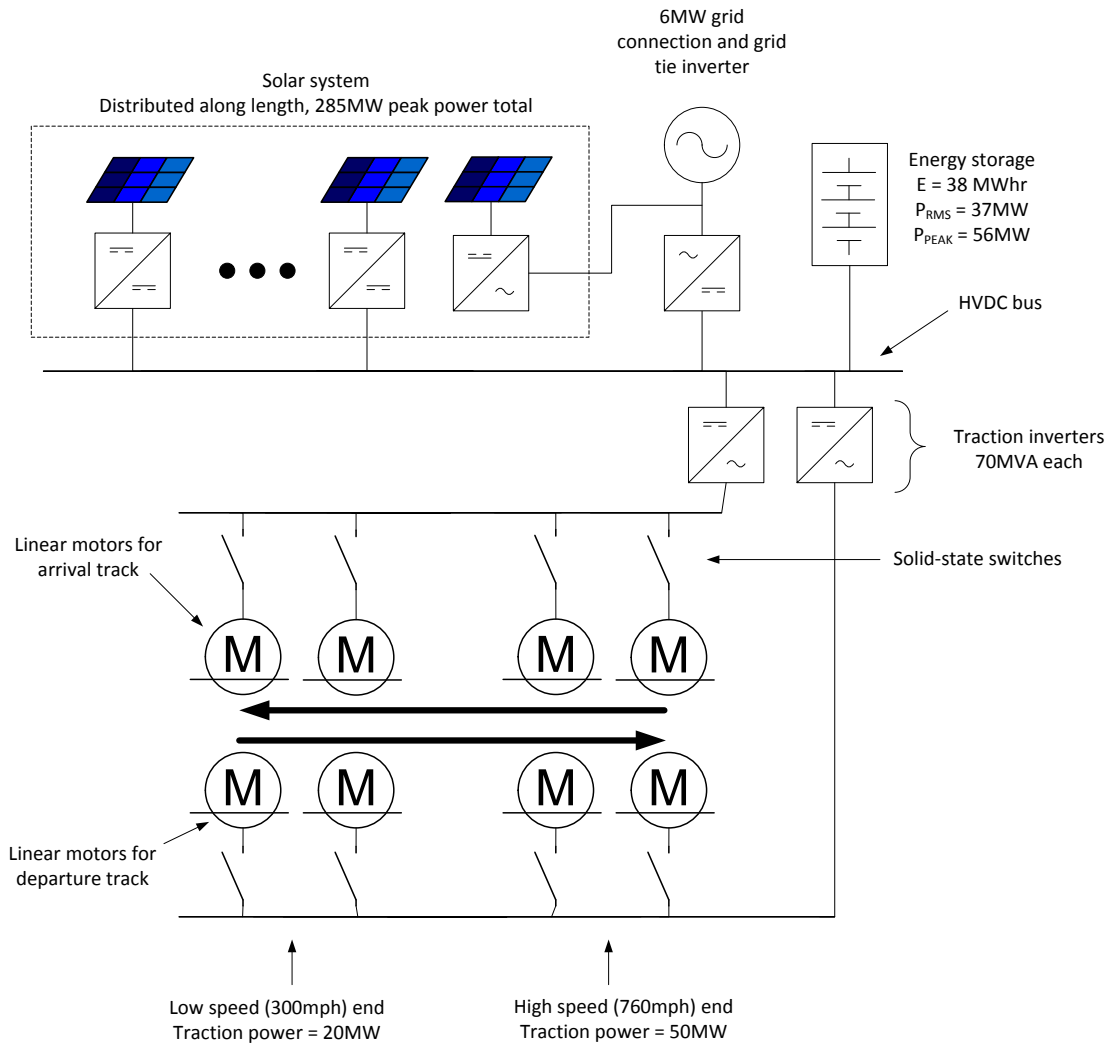


Figure 22. Linear accelerator concept for capsule acceleration and deceleration between 300 and 760 mph (480 and 1,220 kph).

4.3.1. Capsule Components (Rotor)

The rotor of the linear accelerators is very simple - an aluminum blade 49 ft (15 m) long, 1.5 ft (0.45 m) tall, and 2 in. (50 mm) thick. Current flows mainly in the outer 0.4 in. (10 mm) of this blade, allowing it to be hollow to decrease weight and cost.

The gap between the rotor and the stator is 0.8 in. (20 mm) on each side. A combination of the capsule control system and electromagnetic centering forces allows the capsule to safely enter, stay within, and exit such a precise gap.

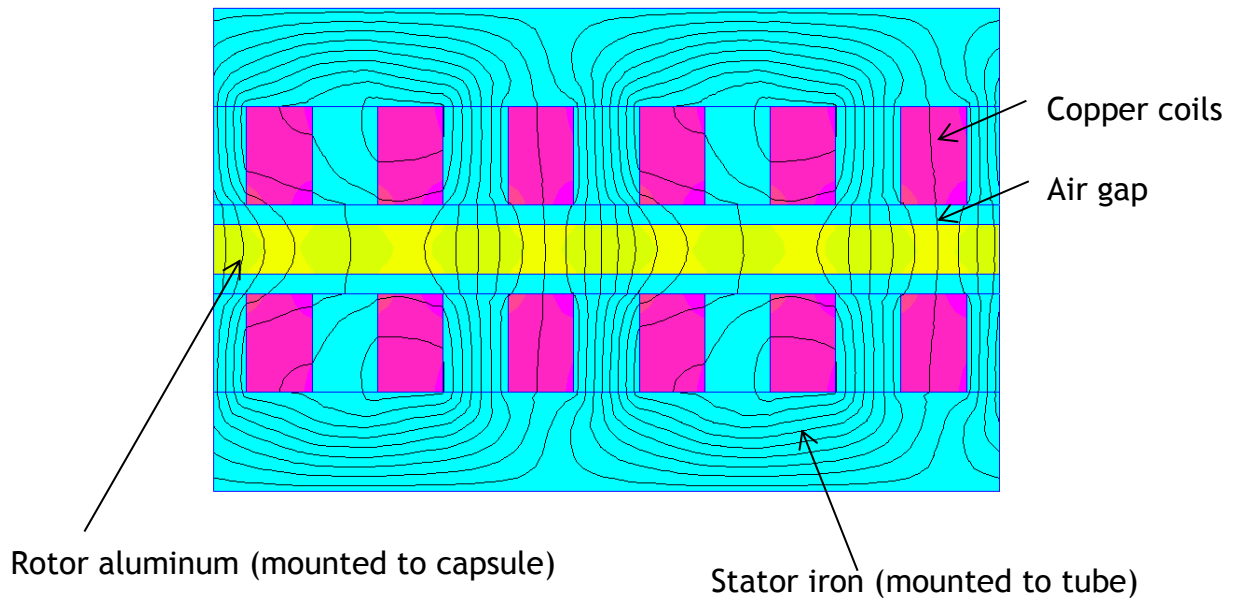


Figure 23. Magnetic field strength inside linear induction motor

4.3.2. Tube Components (Stator)

The stator is mounted to the bottom of the tube over the entire 2.5 miles (4.0 km) it takes to accelerate and decelerate between 300 and 760 mph (480 and 1,220 km). It is approximately 1.6 ft (0.5 m) wide (including the air gap) and 4.0 in. (10 cm) tall, and weighs 530 lb/ft (800 kg/m).

Laid out symmetrically on each side of the rotor, its electrical configuration is 3-phase, 1 slot per pole per phase, with a variable linear pitch (1.3 ft or 0.4 m maximum). The number of turns per slot also varies along the length of the stator, allowing the inverter to operate at nearly constant phase voltage, which simplifies the power electronics design. The two halves of the stator require bracing to resist the magnetic forces of 20 lb_f/ft (300N/m) that try to bring them together.

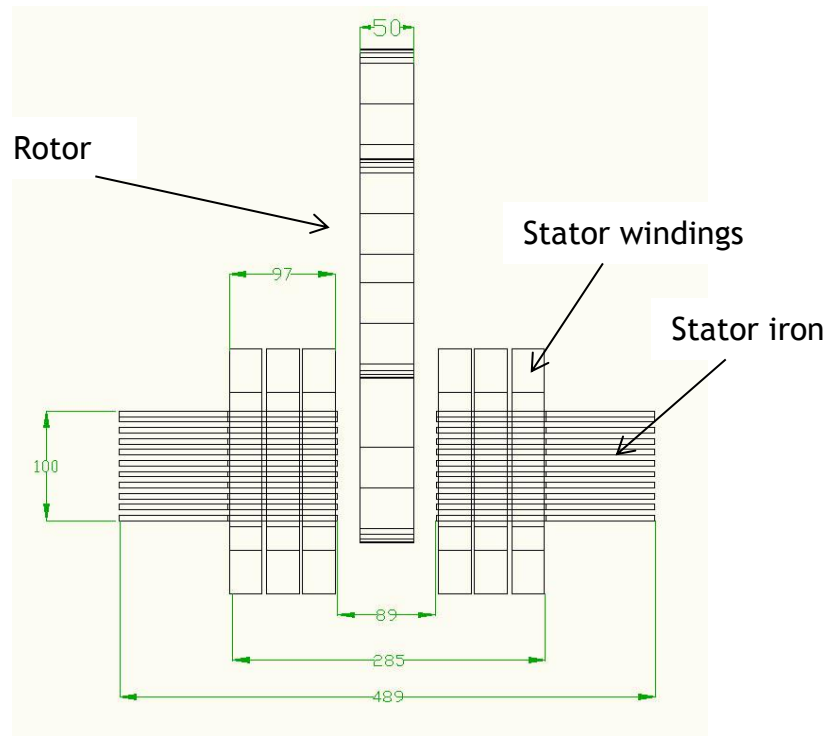


Figure 24. Cross section of rotor inside stator

4.3.3. Energy Storage Components

Energy storage allows this linear accelerator to only draw its average power of 8,000 hp (6 MW) (rather than the peak power of 74,000 hp or 55 MW) from its solar array.

Building the energy storage element out of the same lithium ion cells available in the Tesla Model S is economical. A battery array with enough power capability to provide the worst-case smoothing power has a lot of energy - launching 1 capsule only uses 0.5% of the total energy - so degradation due to cycling is not an issue. With proper construction and controls, the battery could be directly connected to the HVDC bus, eliminating the need for an additional DC/DC converter to connect it to the propulsion system.

4.3.4. Cost

As described above, the propulsion elements on the capsule are limited to the rotor and not expected to cost any more than \$3 million USD for the overall system. The bulk of the propulsion cost is for the stator elements connected to the track and for the inverters to drive the stator. All tube-side propulsion costs together for all linear accelerators add up to \$140 million USD.

This cost is roughly divided as followed:

- Stator and structure materials = 54%

- Power electronics (traction inverters, grid tie inverters) = 33%
- Energy storage = 13%

The solar array and associated electronics provide the required average power of 28,000 hp (21 MW) and are expected to cost approximately \$210 million USD.

4.3.5. Propulsion for Passenger Plus Vehicle System

Compared to the passenger-only capsule, the passenger plus vehicle capsule weighs more, requires a more powerful compressor, and has 50% higher total drag. This increases both the peak and continuous power requirements on the propulsion system, so that the Hyperloop now consumes an average of 66,000 hp (49 MW). However, there is still more than enough solar power available on the wider tubes (122,000 hp or 91 MW, on average) to provide this.

The expected total cost for this larger propulsion system is \$691 million USD, divided as follows:

- 66,000 hp (49 MW) (yearly average requirement) solar array: \$490 million USD
- Propulsion system total: \$200 million USD
 - o Stator and structure materials = 47%
 - o Power electronics = 37%
 - o Energy storage = 16%

4.4. Route

The Hyperloop will be capable of traveling between Los Angeles and San Francisco in approximately 35 minutes. This requirement tends to size other portions of the system. Given the performance specification of the Hyperloop, a route has been devised to satisfy this design requirement. The Hyperloop route should be based on several considerations, including:

1. Maintaining the tube as closely as possible to existing rights of way (e.g., following the I-5).
2. Limiting the maximum capsule speed to 760 mph (1,220 kph) for aerodynamic considerations.
3. Limiting accelerations on the passengers to 0.5g.
4. Optimizing locations of the linear motor tube sections driving the capsules.
5. Local geographical constraints, including location of urban areas, mountain ranges, reservoirs, national parks, roads, railroads, airports, etc. The route must respect existing structures.

For aerodynamic efficiency, the speed of a capsule in the Hyperloop is typically:

- 300 mph (480 kph) where local geography necessitates a tube bend radii < 1.0 mile (1.6 km)
- 760 mph (1,220 kph) where local geography allows a tube bend > 3.0 miles (4.8 km) or where local geography permits a straight tube.

These bend radii have been calculated so that the passenger does not experience inertial accelerations that exceed 0.5g. This is deemed the maximum inertial acceleration that can be comfortably sustained by humans for short periods. To further reduce the inertial acceleration experienced by passengers, the capsule and/or tube will incorporate a mechanism that will allow a degree of 'banking'.

The Hyperloop route was created by the authors using Google Earth.

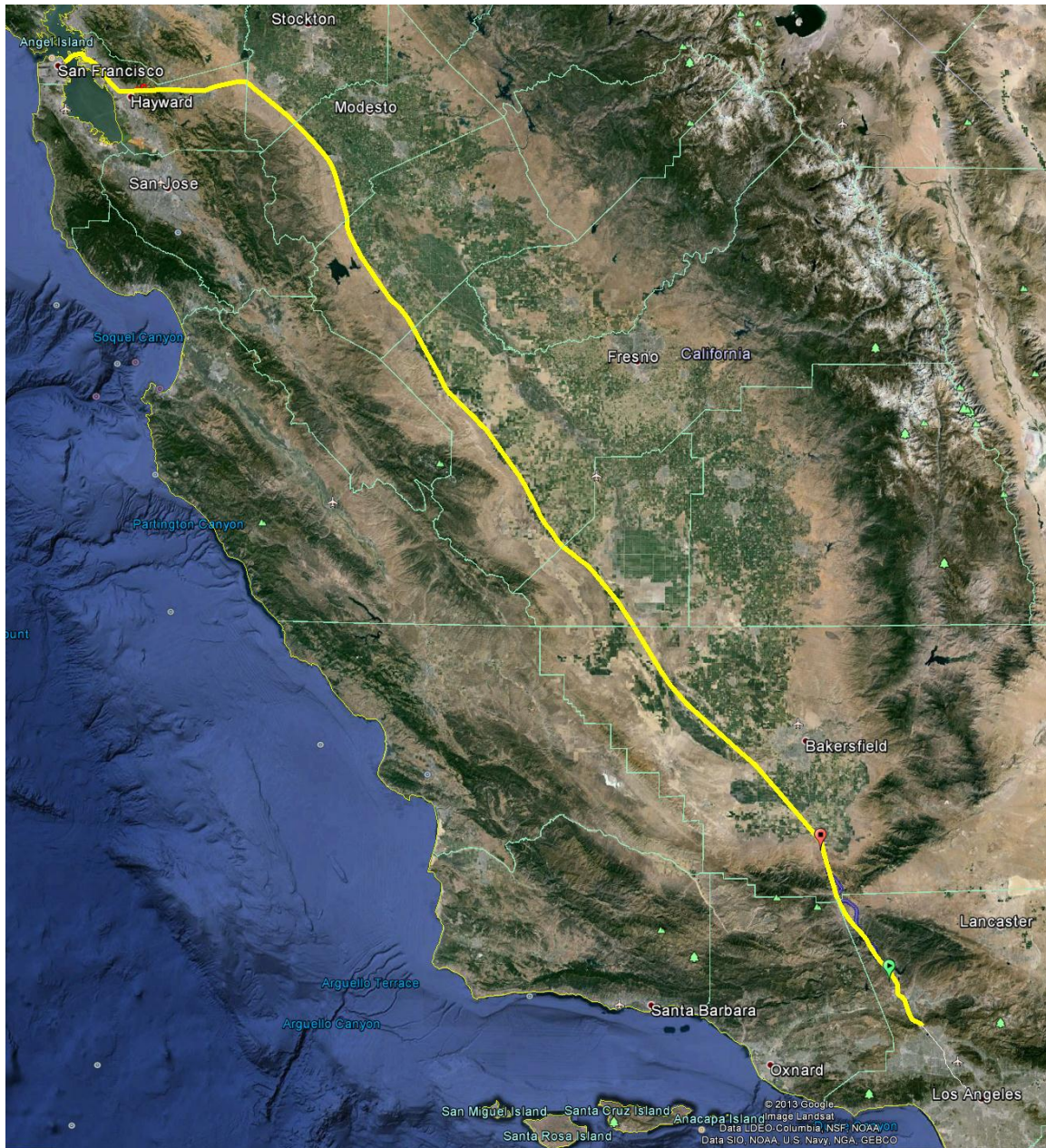


Figure 25. Overview of Hyperloop route from Los Angeles to San Francisco.

4.4.1. Route Optimization

In order to avoid bend radii that would lead to uncomfortable passenger inertial accelerations and hence limit speed, it is necessary to optimize the route. This can be achieved by deviating from the current highway system, earth removal, constructing pylons to achieve elevation change or tunneling.

The proposed route considers a combination of 20, 50, and 100 ft (6, 15, and 30 m, respectively) pylon heights to raise and lower the Hyperloop tube over geographical obstacles. A total tunnel length of 15.2 miles (24.5 km) has been

included in this optimization where extreme local gradients ($>6\%$) would preclude the use of pylons. Tunneling cost estimations are estimated at \$50 million per mile (\$31 million per km). The small diameter of the Hyperloop tube should keep tunneling costs to a far more reasonable level than traditional automotive and rail tunnels.

The route has been divided into the following sections:

- Los Angeles/Grapevine - South and North
- I-5
- I-580/San Francisco Bay

Summary

- 300 mph (480 kph) for the Los Angeles Grapevine South section at 0.5g.

Total time of 167 seconds

- 555 mph (890 kph) for the Los Angeles Grapevine North section at 0.5g.

Total travel time of 435 seconds

- 760 mph (1,220 kph) along I-5 at 0.5g.

Total travel time of 1,518 seconds

- 555 mph (890 kph) along I-580 slowing to 300 mph (480 kph) into San Francisco.

Total travel time of 2,134 seconds (35 minutes)

The speed (Figure 26) along the Hyperloop and distance (Figure 27) as a function of time summarize the route.

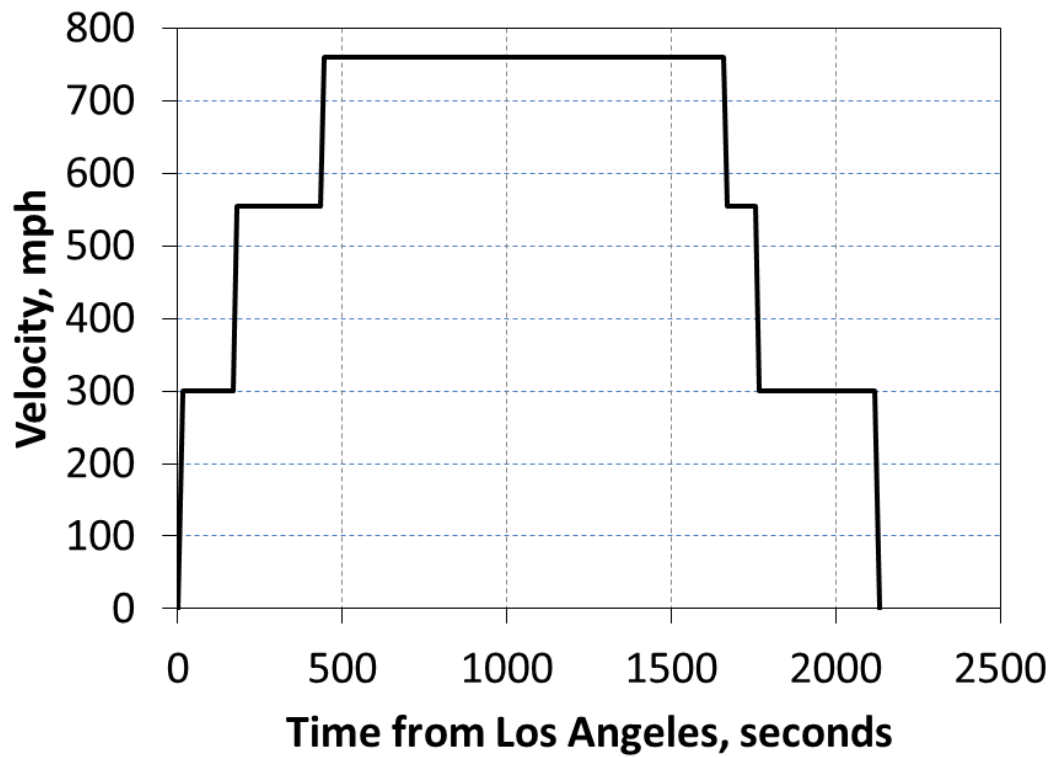


Figure 26. Speed of capsule as a function of time from Los Angeles departure.

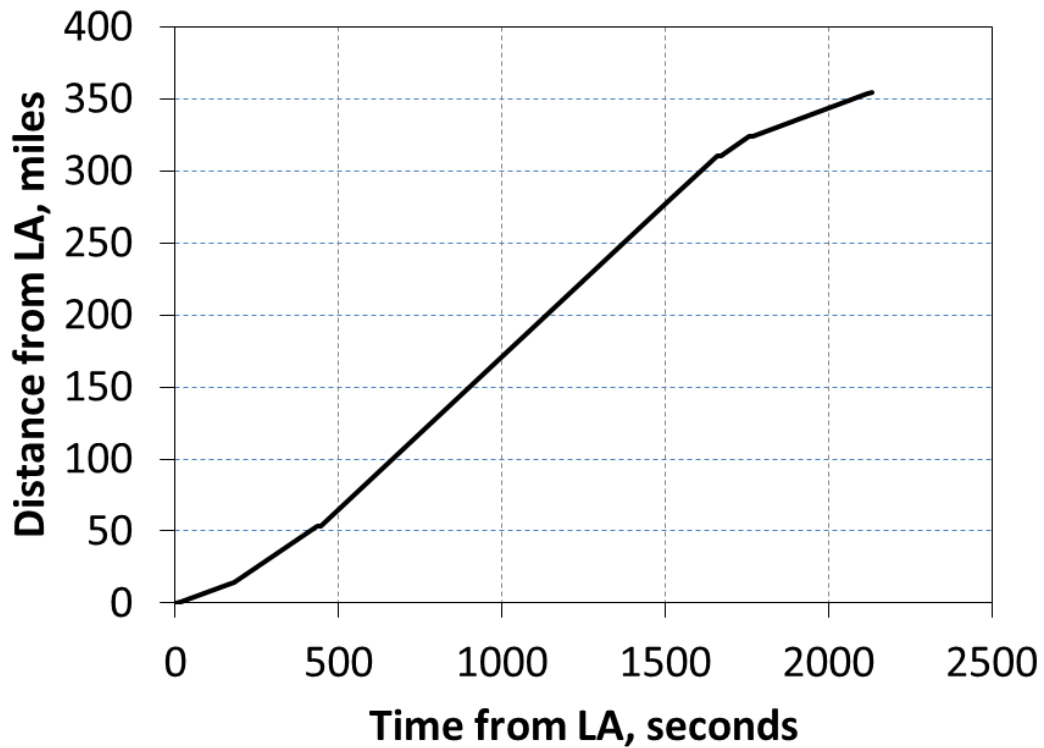


Figure 27. Distance of capsule as a function of time from Los Angeles departure.

4.4.1.1. Los Angeles/Grapevine - South

Visualization - The preliminary route is shown in yellow. Bend radii are shown in red. The green dashed line delineates the north/south Grapevine definition in this document.

Route - Follows I-5 through Santa Clarita and Castaic.



Figure 28. Los Angeles/Grapevine South Section of proposed Hyperloop route.

Table 3. Los Angeles/Grapevine South data at 300 mph (480 kph).

Criteria	0.5g Acceleration
Min. bend radius at 300 mph (483 kph)	2.28 miles (3.67 km)
Section Distance	13.4 miles (21.6 km)
Journey time	167.6 seconds
Tunnel distance	1.0 miles (1.61 km)
No. of 20 ft (6 m) pylons	563
No. of 50 ft (15 m) pylons	80
No. of 100 ft (30 m) Pylons	12
Additional length Required	1.20 miles (1.93 km)

4.4.1.2. Los Angeles/Grapevine – North

- Visualization -* The preliminary route is shown in yellow. Bend radii are shown in red. The green dashed line delineates the north/south Grapevine definition in this document.
- Route -* Significant deviation from I-5 in order to increase bend radius and develop straight sections.

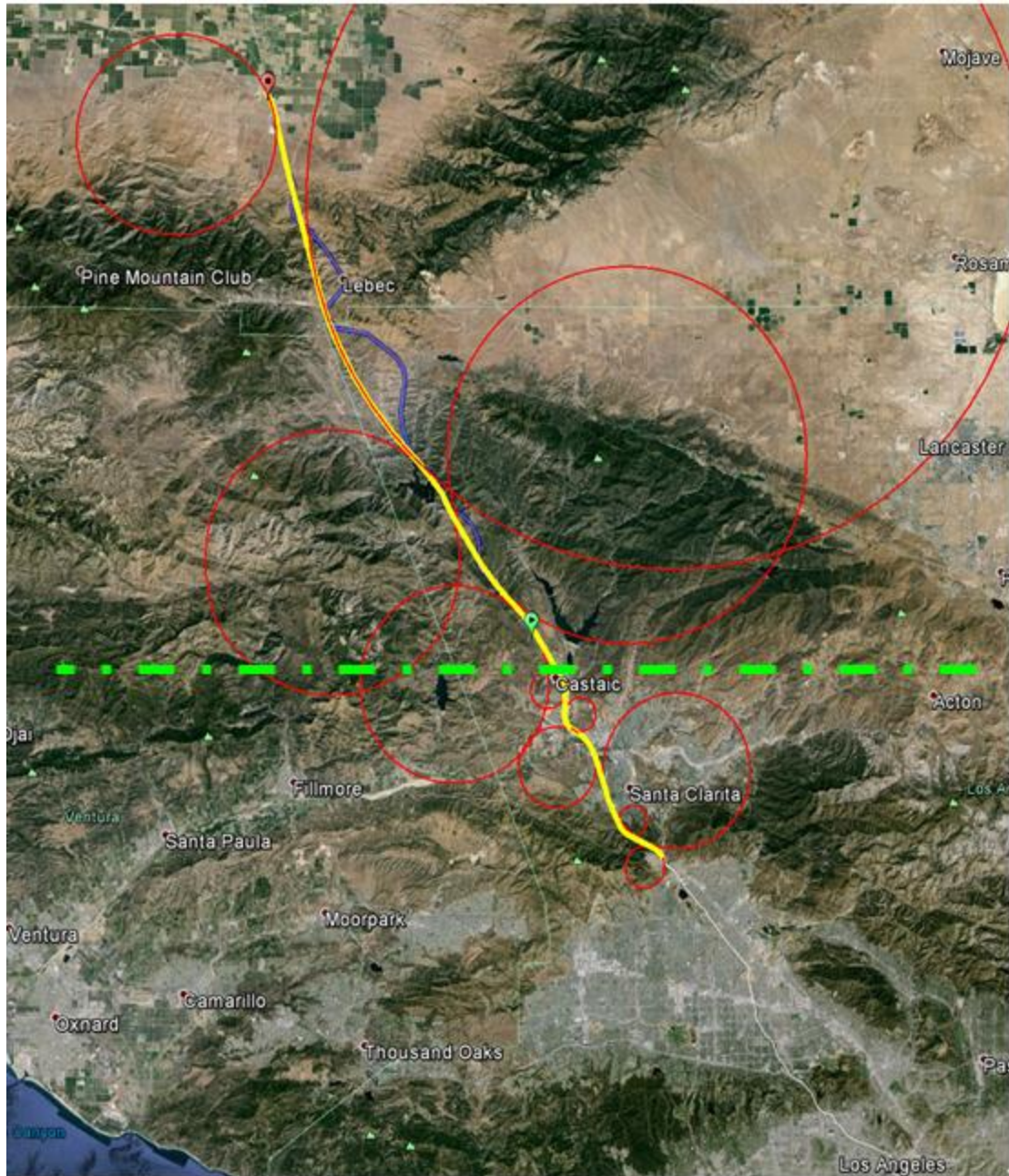


Figure 29. Los Angeles/Gravevine North Section of proposed Hyperloop route.

Table 4. Los Angeles/Grapevine North data at 555 mph (890 kph).

Criteria	0.5g Acceleration
Min. bend radius at 555 mph (890 kph)	7.80 miles (12.6 km)
Distance	40.0 miles (64.4 km)
Journey time	267.4 seconds
Tunnel distance	10.7 miles (17.2 km)
No. of 20 ft (6 m) Pylons	492
No. of 50 ft (15 m) Pylons	260
No. of 100 ft (30 m) Pylons	795
Additional length required	24 miles (38.6 km)

4.4.1.2. Center Section of I-5

Visualization - The preliminary route is shown in yellow. Bend radii are shown in red.

Route - Follows I-5 to minimize land/right of way purchase costs.

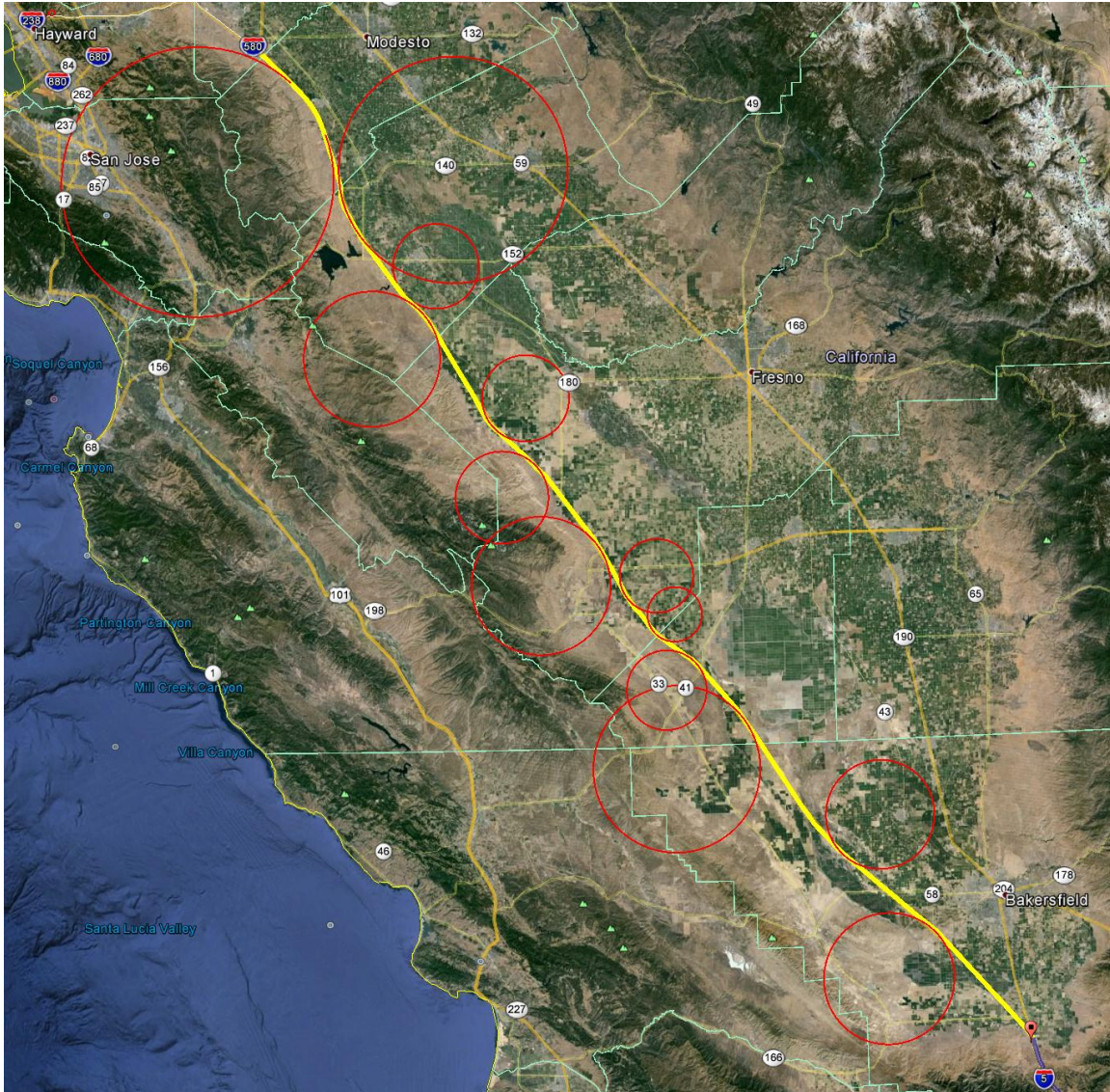


Table 5. I-5 Section data at 760 mph (1,120 kph).

Criteria	0.5g Acceleration
Min. bend radius at 760 mph (1,220 kph)	14.6 miles (23.5 km)
Distance	227 miles (365 km)
Journey time	1,173.0 seconds
Tunnel distance	0 miles (0 km)
No. of 20 ft (6 m) pylons	10,930
No. of 50 ft (15 m) pylons	1,056
No. of 100 ft (30 m) pylons	0
Additional length required	14 miles (22.5 km)

4.4.1.3. I-580/San Francisco Bay

Visualization - The preliminary route is shown in yellow. Bend radii are shown in red.

Route - Follows I-580 to minimize land/right of way purchase costs. Deviation from I-580 West of Dublin in order to develop straight sections.

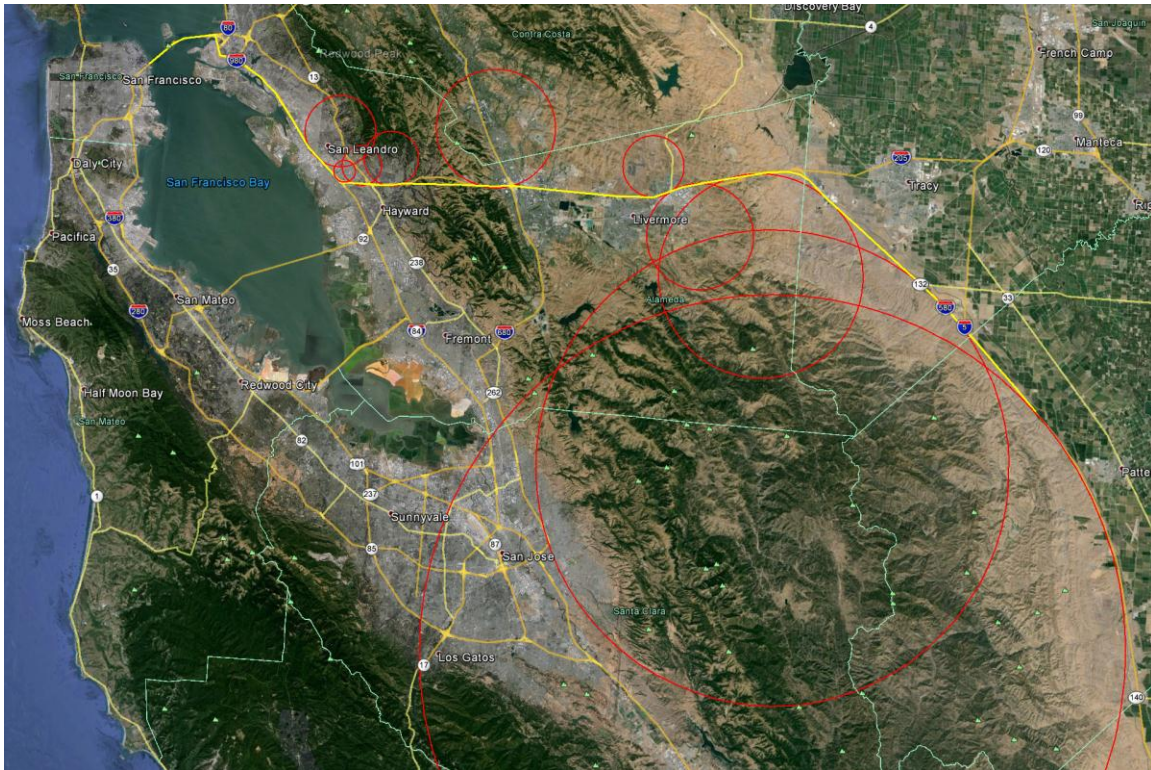


Figure 31. I-580/San Francisco Bay Section of proposed Hyperloop route.

Table 6. I-580/San Francisco Bay Section data at 300, 555, and 760 mph (480, 890, and 1,120 kph, respectively).

Criteria	0.5g Acceleration
Min. bend radius at 300 mph (480 kph)	2.28 miles (3.67 km)
Min. bend radius at 555 mph (890 kph)	7.80 miles (12.55 km)
Min. bend radius at 760 mph (1,220 kph)	14.6 miles (23.5 km)
Distance	73.9 miles (119 km)
Journey time	626.0 seconds
Tunnel distance	3.5 miles (5.6 km)
No. of 20 ft (6 m) pylons	2,783
No. of 50 ft (15 m) pylons	775
No. of 100 ft (30 m) pylons	159
Additional length required	5.7 miles (9.2 km)

4.4.3. Station Locations

The major stations for Hyperloop are suggested based on high traffic regions between major cities. The largest cities by metro population in California according to 2010 to 2012 estimates from various sources (Table 7) are considered for station locations.

Table 7. Largest cities in California by 2013 population.

City	Population (millions)
Los Angeles	18.1
San Francisco/San Jose	8.4
San Diego	3.1
Sacramento	2.6
Fresno	1.1

Stations at these major population centers are considered for Hyperloop. One additional traffic corridor to consider is between Los Angeles, California and Las Vegas, Nevada with a metro population of 2.1 million. Significant traffic is present through this corridor on a weekly basis.

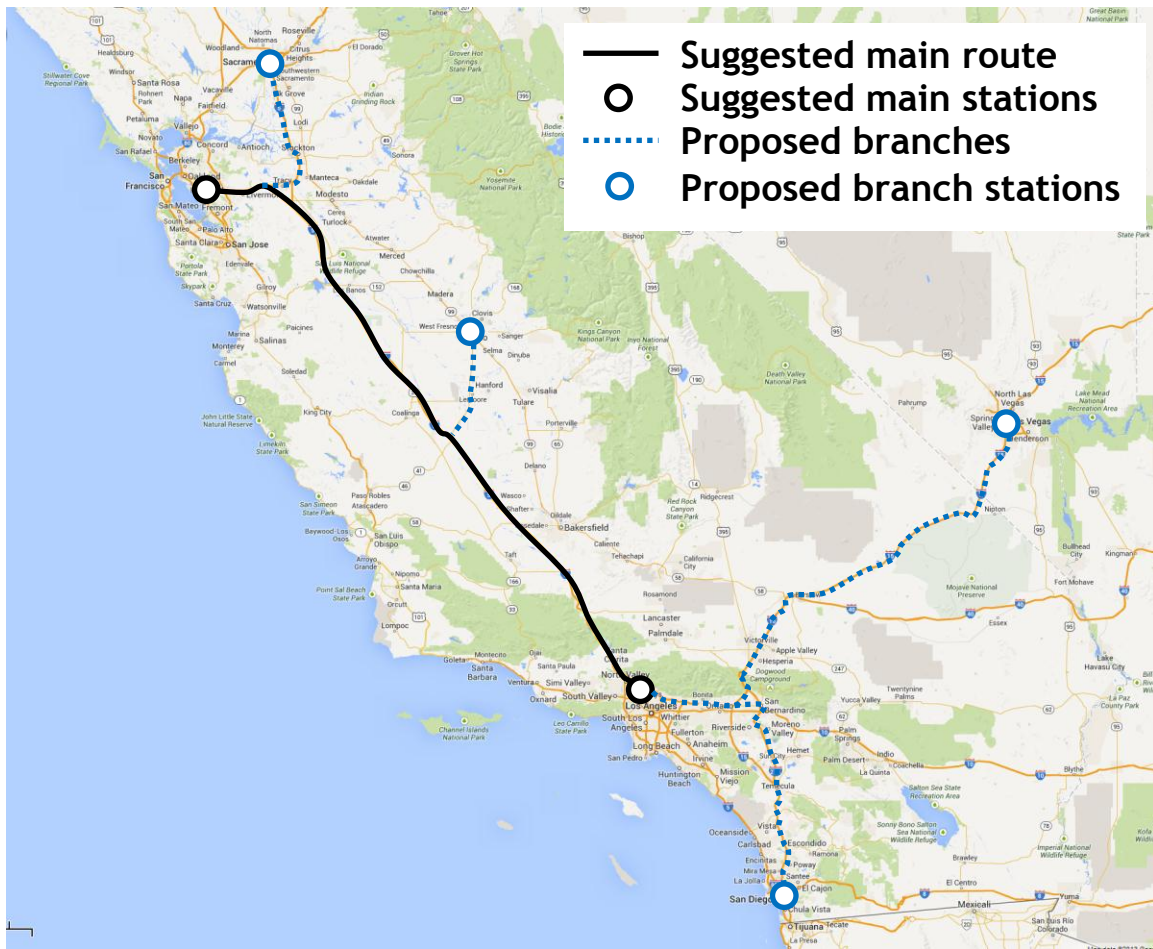


Figure 32. Suggested Hyperloop route map (map courtesy of Google Maps).

The traffic between Los Angeles, California and San Francisco/San Jose, California is estimated to be at least 6 million travelers per year. This possibly represents the busiest corridor of travel in California. Travel along this corridor is anticipated to increase with completion of the Hyperloop due to both decreased travel time and decreased travel cost.

Additional Hyperloop stations are suggested at the following major population centers:

1. San Diego, California:
 - a. Connects to Los Angeles, California main station.
 - b. Capsule departures every 5 minutes.
 - c. Transports around 3 million people per year.
2. Las Vegas, Nevada:
 - a. Connects to Los Angeles, California main station.
 - b. Uses a portion of the San Diego branch route near Los Angeles and tube branches near San Bernardino, California.
 - c. Capsule departures every 8 minutes.

- d. Transports around 1.8 million people per year.
- 3. Sacramento, California:
 - a. Connects to San Francisco, California main station.
 - b. Uses a portion of the main route near San Francisco and tube branches near Stockton, California.
 - c. Capsule departures every 15 minutes.
 - d. Transports around 1 million people per year.
- 4. Fresno, California:
 - a. Connects to both San Francisco, California and Los Angeles, California main stations.
 - b. Los Angeles bound travelers:
 - i. Uses the main route closer to San Francisco plus a small branch along State Route 41 near Fresno.
 - ii. Capsule departures every 15 minutes.
 - iii. Transports around 1 million people per year.
 - c. San Francisco bound travelers:
 - i. Uses the main route closer to Los Angeles plus a small branch along State Route 41 near Fresno.
 - ii. Capsule departures every 30 minutes.
 - iii. Transports around 0.5 million people per year.

4.5. Safety and Reliability

The design of Hyperloop has been considered from the start with safety in mind. Unlike other modes of transport, Hyperloop is a single system that incorporates the vehicle, propulsion system, energy management, timing, and route. Capsules travel in a carefully controlled and maintained tube environment making the system is immune to wind, ice, fog, and rain. The propulsion system is integrated into the tube and can only accelerate the capsule to speeds that are safe in each section. With human control error and unpredictable weather removed from the system, very few safety concerns remain.

Some of the safety scenarios below are unique to the proposed system, but all should be considered relative to other forms of transportation. In many cases Hyperloop is intrinsically safer than airplanes, trains, or automobiles.

4.5.1. Onboard Passenger Emergency

All capsules would have direct radio contact with station operators in case of emergencies, allowing passengers to report any incident, to request help and to receive assistance. In addition, all capsules would be fitted with first aid equipment.

The Hyperloop allows people to travel from San Francisco to LA in 30 minutes. Therefore in case of emergency, it is likely that the best course of action would

be for the capsule to communicate the situation to the station operator and for the capsule to finish the journey in a few minutes where emergency services would be waiting to assist.

Typical times between an emergency and access to a physician should be shorter than if an incident happened during airplane takeoff. In the case of the airplane, the route would need to be adjusted, other planes rerouted, runways cleared, airplane landed, taxi to a gate, and doors opened. An emergency in a Hyperloop capsule simply requires the system to complete the planned journey and meet emergency personnel at the destination.

4.5.2. Power Outage

The vast majority of the Hyperloop travel distance is spent coasting and so the capsule does not require continuous power to travel. The capsule life support systems will be powered by two or more redundant lithium ion battery packs making it unaffected by a power outage. In the event of a power outage occurring after a capsule had been launched, all linear accelerators would be equipped with enough energy storage to bring all capsules currently in the Hyperloop tube safely to a stop at their destination. In addition, linear accelerators using the same storage would complete the acceleration of all capsules currently in the tube. For additional redundancy, all Hyperloop capsules would be fitted with a mechanical braking system to bring capsules safely to a stop.

In summary, all journeys would be completed as expected from the passenger's perspective. Normal travel schedules would be resumed after power was restored.

4.5.2. Capsule Depressurization

Hyperloop capsules will be designed to the highest safety standards and manufactured with extensive quality checks to ensure their integrity. In the event of a minor leak, the onboard environmental control system would maintain capsule pressure using the reserve air carried onboard for the short period of time it will take to reach the destination. In the case of a more significant depressurization, oxygen masks would be deployed as in airplanes. Once the capsule reached the destination safely it would be removed from service. Safety of the onboard air supply in Hyperloop would be very similar to aircraft, and can take advantage of decades of development in similar systems.

In the unlikely event of a large scale capsule depressurization, other capsules in the tube would automatically begin emergency braking whilst the Hyperloop tube would undergo rapid re-pressurization along its entire length.

4.5.3. Capsule Stranded in Tube

A capsule becoming stranded in the Hyperloop tube is highly unlikely as the capsule coasts the majority of the distance at high speed and so there is no propulsion required for more than 90% of the journey.

If a capsule were somehow to become stranded, capsules ahead would continue their journeys to the destination unaffected. Capsules behind the stranded one would be automatically instructed to deploy their emergency mechanical braking systems. Once all capsules behind the stranded capsule had been safely brought to rest, capsules would drive themselves to safety using small onboard electric motors to power deployed wheels.

All capsules would be equipped with a reserve air supply great enough to ensure the safety of all passengers for a worst case scenario event.

4.5.4. Structural Integrity of the Tube in Jeopardy

A minor depressurization of the tube is unlikely to affect Hyperloop capsules or passengers and would likely be overcome by increased vacuum pump power. Any minor tube leaks could then be repaired during standard maintenance.

In the event of a large scale leak, pressure sensors located along the tube would automatically communicate with all capsules to deploy their emergency mechanical braking systems.

4.5.5. Earthquakes

California is no stranger to earthquakes and transport systems are all built with earthquakes in mind. Hyperloop would be no different with the entire tube length built with the necessary flexibility to withstand the earthquake motions while maintaining the Hyperloop tube alignment.

It is also likely that in the event of a severe earthquake, Hyperloop capsules would be remotely commanded to actuate their mechanical emergency braking systems.

4.5.6. Human Related Incidents

Hyperloop would feature the same high level of security used at airports. However, the regular departure of Hyperloop capsules would result in a steadier and faster flow of passengers through security screening compared to airports. Tubes located on pylons would limit access to the critical elements of the system. Multiple redundant power sources and vacuum pumps would limit the impact of any single element.

4.5.7. Reliability

The Hyperloop system comprising all infrastructure, mechanical, electrical, and software components will be designed so that it is reliable, durable, and fault tolerant over its service life (100 years), while maintaining safety levels that match or exceed the safety standard of commercial air transportation.

4.6. Cost

The total cost of the Hyperloop passenger transportation system as outlined is less than \$6 billion USD (Table 8). The passenger plus vehicle version of Hyperloop is including both passenger and cargo capsules and the total cost is outlined as \$7.5 billion USD (Table 9).

Table 8. Total cost of the Hyperloop passenger transportation system.

Component	Cost (million USD)
Capsule	54 (40 capsules)
Capsule Structure & Doors	9.8
Interior & Seats	10.2
Compressor & Plumbing	11
Batteries & Electronics	6
Propulsion	5
Suspension & Air Bearings	8
Components Assembly	4
Tube	5,410
Tube Construction	650
Pylon Construction	2,550
Tunnel Construction	600
Propulsion	140
Solar Panels & Batteries	210
Station & Vacuum Pumps	260
Permits & Land	1,000
Cost Margin	536
Total	6,000

Table 9. Total cost of the Hyperloop passenger plus vehicle transportation system.

Component	Cost (million USD)
Cargo Capsule	30.5 (20 capsules)
Capsule Structure & Doors	5.5
Interior & Seats	3.7
Compressor & Plumbing	6
Batteries, Motor & Electronics	4
Propulsion	3
Suspension & Air Bearings	5.3
Components Assembly	3
Passenger Only Capsule	40.5 (30 capsules)
Capsule Structure & Doors	7.4
Interior & Seats	7.6
Compressor & Plumbing	8.2
Batteries, Motor & Electronics	4.5
Propulsion	3.8
Suspension & Air Bearings	6
Components Assembly	3
Tube	7,000
Tube Construction	1,200
Pylon Construction	3,150
Tunnel Construction	700
Propulsion	200
Solar Panels & Batteries	490
Station & Vacuum Pumps	260
Permits & Land	1,000
Cost Margin	429
Total	7,500

5. Conclusions

A high speed transportation system known as Hyperloop has been developed in this document. The work has detailed two versions of the Hyperloop: a passenger only version and a passenger plus vehicle version. Hyperloop could transport people, vehicles, and freight between Los Angeles and San Francisco in 35 minutes. Transporting 7.4 million people each way every year and amortizing the cost of \$6 billion over 20 years gives a ticket price of \$20 for a one-way trip for the passenger version of Hyperloop. The passenger only version of the Hyperloop is less than 9% of the cost of the proposed passenger only high speed rail system between Los Angeles and San Francisco.

An additional passenger plus transport version of the Hyperloop has been created that is only 25% higher in cost than the passenger only version. This version would be capable of transporting passengers, vehicles, freight, etc. The

passenger plus vehicle version of the Hyperloop is less than 11% of the cost of the proposed passenger only high speed rail system between Los Angeles and San Francisco. Additional technological developments and further optimization could likely reduce this price.

The intent of this document has been to create a new open source form of transportation that could revolutionize travel. The authors welcome feedback and will incorporate it into future revisions of the Hyperloop project, following other open source models such as Linux.

6. Future Work

Hyperloop is considered an open source transportation concept. The authors encourage all members of the community to contribute to the Hyperloop design process. Iteration of the design by various individuals and groups can help bring Hyperloop from an idea to a reality.

The authors recognize the need for additional work, including but not limited to:

1. More expansion on the control mechanism for Hyperloop capsules, including attitude thruster or control moment gyros.
2. Detailed station designs with loading and unloading of both passenger and passenger plus vehicle versions of the Hyperloop capsules.
3. Trades comparing the costs and benefits of Hyperloop with more conventional magnetic levitation systems.
4. Sub-scale testing based on a further optimized design to demonstrate the physics of Hyperloop.

Feedback is welcomed on these or any useful aspects of the Hyperloop design. E-mail feedback to hyperloop@spacex.com or hyperloop@teslamotors.com.

Appendix F: SpaceX Hyperloop Competition Rules as of 10/20/2015

SpaceX Hyperloop Pod Competition Rules and Requirements

August 20, 2015

CONTENTS

1	Introduction	2
2	General Rules	3
3	Preliminary Design Briefing	4
4	Final Design Package	5
5	Design Weekend	7
6	Pod Requirements.....	8
7	Pod Loading	10
8	Pod Launch	11
9	Pod Unloading.....	11
10	Top-Level Competition Weekend Judging Criteria.....	12

1 INTRODUCTION

On August 12, 2013, Elon Musk released a [white paper](#) on the Hyperloop, his concept of high-speed ground transport. In order to accelerate the development of a functional prototype and to encourage student innovation, SpaceX is moving forward with a competition to design and build a half-scale Hyperloop Pod. In parallel with the competition, SpaceX will be constructing a sub-scale test track adjacent to its Hawthorne, California headquarters. During Design Weekend in January 2016, entrants will submit and present their Pod designs. On Competition Weekend, scheduled for June 2016, entrants will operate their Pods within the SpaceX test track.

This document outlines the competition logistics and rules and is meant to augment, and in some cases supersede, the initial [competition announcement document](#) released in June 2015. An additional update will be issued with the tube specifications in September 2015.

For an updated competition schedule, visit www.spacex.com/hyperloop.

Note: This competition is a SpaceX event. SpaceX has no affiliation with any Hyperloop companies, including, but not limited to, those frequently referenced by the media.

Any questions or comments can be posted on the Hyperloop Forum at <http://tx.ag/hyperloopforum> (click on "Enroll Now" to join) or submitted to Hyperloop@spacex.com.

2 GENERAL RULES

1. Any entity is welcome to enter the competition by September 15, 2015, and submit the Preliminary Design Briefing in October 2015. However, SpaceX, at its sole discretion, will select the teams that participate in the January 2016 Design Weekend. After submitting their Preliminary Design Briefing, teams will be notified within two weeks whether they have been chosen to participate in Design Weekend.
2. The team structure is flexible, with no minimum number of team members and no maximum number (within reason). If there is any question about eligibility, please email Hyperloop@spacex.com.
3. In addition to hosting the competition, SpaceX may enter a corporate team into the competition, but this team will not be eligible to win any prizes or awards.
4. Competition Weekend Prizes. The full prize package structure will be released later this year, but, at a minimum:
 - Cash prizes (amounts TBD) for the first, second, and third-place teams.
 - People's Choice Award, where the attendees vote for the coolest feature/design.
 - SpaceX, at its own discretion, may award prizes to teams (student and non-student) with any design features that SpaceX deems especially innovative with regard to design, safety, efficiency, and performance. SpaceX estimates it will award 5 to 10 of these innovation awards.
5. Design Weekend Prizes: See Section 5.
6. At SpaceX's discretion, Pod teams may be allowed to test their Pods on the test track before Competition Weekend.
7. Pods must meet the requirements provided in Section 6 and any future requirements released by SpaceX.
8. SpaceX, at its sole discretion, may allow or disallow entrants to access the test track.
9. **No human (or animal) shall ride in any Pod or other transportation device used within the test track during this competition or during any pre-competition access.**
10. The judging panel will be composed primarily of SpaceX engineers, Tesla Motors engineers, and university professors.
11. Determinations of the judging panel are final, and entrants may not protest results.
12. Competition Weekend is scheduled for June 2016, but the exact date will be determined at a later date.

3 PRELIMINARY DESIGN BRIEFING

This Preliminary Design Briefing package shall consist of a PowerPoint slide deck (in PDF format) of no more than 30 slides, which will include:

1. Description of team and updated list of all associated team members and advisors
2. Reiteration of whether team intends to build a Pod or just present a design at Design Weekend
3. Top-level design description for pod (or subsystem). At a minimum, this should include, where applicable:
 - a. Estimated Pod dimensions
 - b. Estimated Pod mass by subsystem
 - c. Estimated Pod power consumption by subsystem
 - d. Pod navigation mechanism
 - e. Pod levitation mechanism (if any)
 - f. Pod propulsion mechanism (if any)
 - g. Pod braking mechanism
 - h. Pod stability mechanisms (e.g. attitude and lateral motion)
4. List and description of any stored energy on the Pod (e.g. pressure vessels, batteries)
5. List of hazardous materials, if any
6. Top-level description of safety features

With their **Preliminary Design Briefing**, teams shall include a signed **Competitor Entry Agreement** that will be provided to teams who complete the Intent to Compete form on www.spacex.com/hyperloop by September 15, 2015.

Preliminary Design Briefings and signed Competitor Entry Agreement should be submitted to Hyperloop@spacex.com by 5pm PT October 22, 2015. In the subject line, write “Pod Competition Preliminary Briefing: TEAM NAME HERE”. Teams may submit only one Preliminary Design Briefing copy; any copies received after the initial submission will not be accepted. Please check your documents carefully before submission. SpaceX will respond to your submission within 48 hours to verify receipt. If you do not receive verification within 48 hours, please re-contact SpaceX at the same email.

The purpose of this briefing is for SpaceX to “sanity check” the design and ensure the entrant is heading in a viable direction. Following the submission, there may be a down-select decision in order to properly manage the number of entrants. SpaceX will notify teams as to whether they have advanced within two weeks of Preliminary Design Briefing submission.

4 FINAL DESIGN PACKAGE

All entrants who have successfully advanced to the Final Design Package phase must upload a completed version of the Final Design Package on the Hyperloop Forum at <http://tx.ag/hyperloopforum> by 5pm PT on December 15, 2015. This is to facilitate uploading any large files. To upload, click on “Submit Final Design Package” in the left-hand navigation. Name your package as “Pod Competition Final Design package: TEAM NAME HERE”. As with the Preliminary Design Briefing, teams may submit only one Final Design Package copy. Please check your documents carefully.

The Final Design Package must consist of:

1. Description of team and updated list of all associated team members and advisors
2. Reiteration of whether team wishes to build a Pod or just present a design at Design Weekend
3. If your team is unable to attend Design Weekend and wishes to present virtually, please indicate so, along with a detailed explanation
4. Design description for Pod (or subsystem). At a minimum, this should include:
 - a. Pod top-level design summary
 - b. Pod dimensions
 - c. Pod mass by subsystem
 - d. Pod payload capability
 - e. Pod materials
 - f. Pod power source and consumption
 - g. Pod navigation mechanism
 - h. Pod levitation mechanism
 - i. Pod propulsion mechanism (if any)
 - j. Pod braking mechanism
 - k. Pod stability mechanisms (e.g. attitude and lateral motion)
 - l. Pod aerodynamic coefficients
 - m. Pod magnetic parameters (if applicable)
5. Predicted Pod thermal profile
6. Predicted Pod trajectory (speed versus distance)
7. Predicted vibration environments
8. Pod structural design cases: at a minimum, this shall include initial acceleration, nominal deceleration, and end-of-tube off-nominal crash
9. Pod production schedule
10. Pod cost breakdown
11. Sensor list and location map
12. Comments on scalability to an operational Hyperloop with respect to:
 - a. System size (increased tube length, tube diameter, and Pod size)
 - b. Cost (both production and maintenance)
 - c. Estimated Pod mass and cost if built full-scale
 - d. Maintenance (e.g. not requiring specialized alignment tools, hot-swappable subsystems)

Additionally, teams intending to build a Pod shall also submit:

1. Loading and unloading logistics plan (see Sections 7 and 9 for details)
 - a. Full descriptions of all Functional Tests (see Sections 7 and 9)
 - b. Full description of Ready-to-Launch checklist/state (e.g. Loop Computer in “Launch Mode” and sending telemetry, Pod hovering at 0.25 inches)
 - c. Full description of Ready-to-Remove checklist/state (e.g. Wheels locked, Power Off)
 - d. Description of how Pod is moved from Staging Area to Ingress Holding Area
 - e. Description of how Pod is moved from Egress Holding Area to Exit Area
2. List and description of any stored energy on the Pod (i.e. pressure vessels, batteries)
3. List of any hazardous materials, if any
4. Preliminary bill of materials, with each line item categorized as “Commercial-Off-The-Shelf (COTS)” or “custom-built”
5. Description of safety features including:
 - a. Mechanisms to mitigate a complete loss of Pod power
 - b. Pod robustness to a tube breach resulting in rapid pressurization
 - c. Fault tolerance of braking, levitation, and other subsystems
 - d. Single point of failures within the Pod
 - e. Recovery plan if Pod becomes immovable within tube
 - f. Implementation of the Pod-Stop command
 - g. A top-down hazard analysis OR a bottom-up Failure Mode and Effects Analysis (FMEA).
6. Component and system test program before the Pod arrives for Competition Weekend
7. Vacuum Compatibility Analysis

Additional fidelity on the individual data items will be made available to teams in October 2015.

5 DESIGN WEEKEND

Design Weekend will take place on January 15 (Friday) and January 16 (Saturday) at Texas A&M University, College Station. The Design Weekend logistics will be released by Texas A&M in September. Some general notes:

- Updates on Design Weekend details will be posted at: <http://engineering.tamu.edu/hyperloop>
- The goal of Design Weekend is for student teams to present their Pod designs, which, after receiving feedback, vetting, and approval to proceed, will be constructed for Competition Weekend. Non-student teams will be invited on a case-by-case basis to participate at SpaceX's discretion.
- Entrants are encouraged to attend in person. For those student teams who are unable to attend in person, we will likely have limited (i.e. 1 or 2) slots for virtual presentations by webcam. If your team is unable to attend Design Weekend and wishes to present virtually, please indicate this in your Final Design Package along with a detailed explanation.
- Entrants who are not interested in building a Pod may still present designs for a Pod, an individual subsystem, or an individual safety feature. As an example of an individual subsystem submission, a team could choose to optimize the Pod's aerodynamics or design the Pod's Service Propulsion System. The purpose of such submission is to receive design feedback and to participate in a fun educational event.
- Entrants will present before a judging panel, which will be composed primarily of SpaceX engineers, Tesla Motors engineers, and university professors.
- While teams are encouraged to begin finding sponsorships now, the primary rewards for Design Weekend participation are access to corporate sponsorships. Select companies invited by SpaceX will be able to use Design Weekend as a platform for selecting teams to sponsor. At their discretion, such companies may contribute funds toward the construction of their sponsored team's Competition Weekend Pod. Entrants who are selected for sponsorship may elect not to be sponsored or receive funds, at their discretion.
- SpaceX, at its own discretion, may award multiple innovation awards (each of which includes a small cash prize) to teams with any design features that SpaceX feels are innovative with regard to safety, efficiency, and performance.

6 POD REQUIREMENTS

The Pod requirements are intentionally broad in order to encourage diversity of design. Feel free to post any questions about Pod requirements to the Hyperloop Forum at <http://tx.ag/hyperloopforum> or email them to Hyperloop@spacex.com.

1. Mass: Less than 11,000 lbm (5,000 kg)
2. Dimensions: Pods shall be less than 14 feet in length. Pods can be any shape with the main requirement being that they fit within the tube. The tube's exact cross-section will be released in September. To provide initial estimates, Pods shall be less than 3.5 feet in width at the base, less than 4.5 feet in maximum width, and less than 3.75 feet in height. When the final tube specifications are released in September, it is possible that these maximum values will change, but they won't decrease.
3. Service Propulsion System: The Pod shall be moveable at low speeds when not in operation, which may be accomplished by physically pushing it (wheels), physically lifting it (even with a dolly), or remotely controlling it. While pushing and lifting are reasonable for Pod loading, it is highly recommended that the remote control be implemented for unloading. Without a remote system, it will be more difficult to guarantee that the Pod reaches the Egress Holding Area in the event it becomes immovable in the Hyperloop tube.
4. Levitation System(s): The mechanism(s) for levitation is up to the entrant and is not actually required. Wheeled vehicles (e.g. an "electric car in a vacuum") can compete, but are unlikely to win prizes.
5. Operational Propulsion System: This is not required (or suggested), as the SpaceX test track will be providing initial linear impulse. However, teams are not prohibited from having a different primary system (e.g. an electric car) or an auxiliary system (to maintain speed during coast).
6. Operational Propulsion Interface: In order to accelerate the Pods, SpaceX will provide a mechanical interface, which will then be accelerated to operational speed. If the Pod chooses to utilize the interface, the Pod will remain attached to the Operational Propulsion Interface during the entire acceleration phase.
7. Braking system: Each Pod must be able to reduce to zero speed in a controlled fashion (i.e. brake). Braking can be done in any reasonable manner, including, but not limited to, brake tabs, wheels, system drag, or onboard propulsion. SpaceX may choose to provide a permanent magnet surface near the end of the main tube to allow for non-contact electromagnetic braking. Braking system actuation must be demonstrated, if feasible, in one of the pre-launch Functional Tests (see Section 7). The braking system, where feasible, shall be at least 1-fault tolerant.
8. Communications: Within the tube, SpaceX will provide a secure 2.4 GHz WiFi network for all command, data and video communications. Ability to send and receive data and commands (through a GUI created by the entrants) must be demonstrated during Functional Tests.
9. Telemetry: At a minimum, the telemetry stream must include the following data (at a minimum speed of 1 hz):
 - a. Position within tube (X, Y, and Z)
 - b. Velocity within tube (X, Y, and Z)

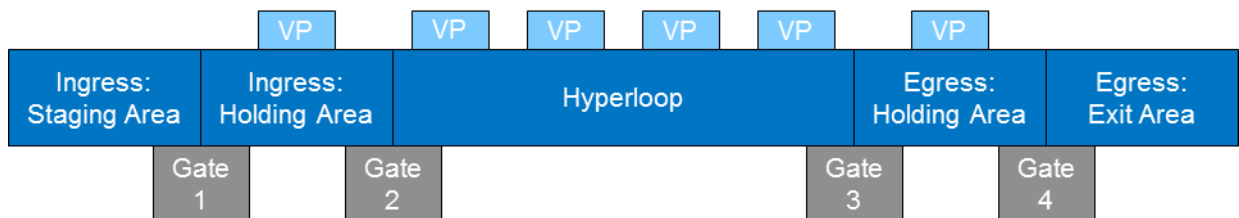
- c. Acceleration within tube (X, Y, and Z)
 - d. Vehicle attitude (roll, pitch, and yaw)
 - e. Pod pressure (only applicable if Pod has any pressurized sections)
 - f. Temperature from at least two points on the Pod
 - g. Power consumption
10. Vibration Environments: SpaceX will provide a self-contained flight data recorder to monitor dynamic environments. After the flight, SpaceX engineers will use this data as part of the judging criteria. Pods must accommodate the unit, which will weigh less than one pound. The interface will be released in late 2015.
11. Pod-Stop Command: Through a remote command, Pods must be able to be commanded to stop safely. The physical mechanism for stopping can, but does not have to be, the same as the Pod's standard braking mechanism.

7 POD LOADING

The Pod loading sequence is as follows. Please note that, since every Pod will have unique features, all teams are required to submit a Pod loading and unloading plan as part of their Final Design Package:

1. Before loading, the Team Captain will give a 15-minute Safety and Logistics briefing to the Judging Panel and Hyperloop Test Director (a SpaceX or Tesla employee), which includes a description of their Pod Design, Pod-handling safety, and the loading/unloading process. The Hyperloop Test Director will also lead a safety and technical inspection of the physical Pod. The loading cannot proceed until the Hyperloop Test Director approves.
2. Pod will be transported via road to the Hyperloop Staging Area. Pods will be lifted, via a SpaceX-provided crane if necessary, onto the Staging Area, an open-air flat surface 20 feet in length.
3. On the Staging Area platform, Pods will perform Functional Test A, which will include a demonstration of power-up.
4. When Functional Test A is complete, Gate 1 will open and the Pod will be moved into the Ingress Holding Area using the Pod's Service Propulsion. The Holding Area is an enclosed airlock 20 feet in length.
5. On the Holding Area platform, the Pod will be physically connected to the Mechanical Propulsion Interface. This is not applicable if the Pod is not using the Hyperloop's Operational Propulsion System (e.g. an electric car). Once connected, Functional Test B will be performed, which may include vehicle hovering.
6. Gate 1 will then be closed and Functional Test C will be performed. This includes the demonstration of a continuous communications link.
7. The Holding Area will be depressurized to operating pressure.
8. At operating pressure, Functional Test D will be performed.

Functional Diagram (not to scale) of the Test Track. VP refers to Vacuum Pumps.



Summary of Pre-Launch Functional Tests

Test ID	Location	Suggested Duration (min)	Suggested Items
A	Staging Area	5	Power-on, 2-way communications
B	Holding Area (Gate 1 open; Gate 2 closed)	5	Levitation
C	Holding Area (Gate 1 & 2 closed)	2	Communications
D	Holding Area (vacuum)	5	Levitation

8 POD LAUNCH

1. Once the Pod has passed Functional Test D, Gate 2 will be opened.
2. The Pod will then go through its Pre-Launch procedures, which places it in “Ready-to-Launch” mode.
3. The entrant will then signal the Hyperloop Test Director that it is Ready-to-Launch.
4. The Hyperloop Test Director will activate the Operational Propulsion System.
 - a. If the Pod is not using the Operational Propulsion System, Step 4 will be skipped.
5. Launch!
6. Upon launch, the Pod will undergo three phases of “flight”:
 - a. Acceleration Phase: The Pod is accelerated through its mechanical interface to the Operational Propulsion Interface. Once the Pod has been accelerated to speed, the Operational Propulsion Interface will stop, freeing the Pod.
 - b. Coast Phase: The Pod coasts down the main Hyperloop section.
 - c. Deceleration Phase: The Pod brakes itself, coming to rest in the Egress Holding Area.

9 POD UNLOADING

1. The Pod is responsible for reaching the Egress Holding Area, an enclosed airlock that is a minimum of 40 feet in length. SpaceX will likely provide a backup system to ensure the Pod reaches the Egress Holding Area, (i.e. a remote pull-cart), but the teams should not rely upon this system.
2. Once in the Egress Holding Area, Gate 3 will be closed.
3. The Egress Holding Area will then be pressurized.
4. Once at pressure, the Pod will perform a safety test before approaching Gate 4, known as Functional Test E, in order to verify that it is safe to proceed. If the Pod requires manual movement from Egress Holding Area to Exit Area, the test must also verify that the Pod is safe to approach.
5. When the Hyperloop Test Director deems the operation as safe, Gate 4 will be opened.
6. The Pod will then be moved into the Exit Area, an open-air flat surface 20 feet in length.
7. The Pod will be placed into a safe powered-down “Ready-to-Remove” state.
8. The Pod will then be removed from the Exit Area via crane or other method.

10 TOP-LEVEL COMPETITION WEEKEND JUDGING CRITERIA

Category 1: Final Design and Construction	Points
Overall quality of construction	100
Overall cost of materials (normalized per payload mass)	100
Levitation system	75
Braking system	75
Ability to economically scale	50
Power consumption (normalized per payload mass)	50
Payload capability (as % of overall mass)	50
Category 1 Total	500
Category 2: Safety and Reliability	
Structural margins of safety and design cases	100
Pod-Stop command	100
Safety in operations	50
Fault tolerance of braking system	50
Fault tolerance of levitation systems	50
Fault tolerance of other systems	50
Loss of power contingency	50
Tube breach contingency	50
Category 2 Total	500
Category 3: Performance in Operations	
Efficiency of transport from Staging Area to Ingress Holding Area	100
Efficiency of Functional Tests	100
Efficiency of connection to the Operational Propulsion Interface	100
Efficiency of transport from Egress Holding Area to Exit Area	100
Pod is removed from the tube without requiring tube pressurization	100
Category 3 Total	500
Category 4: Performance in Flight	
Total distance Pod travels	200
Minimization of system drag	200
Functionality of Pod braking/deceleration system	200
Tightness of lateral control around Hyperloop center-line	100
Attitude control system	100
Comfort of ride (per measured vibration environment)	100
Reliability of data stream and DAQ software	100
Category 4 Total	1000
Total Points Possible	2500

Note: Objective figures of merit for categories will be released with tube specifications.

Appendix G: SpaceX Hyperloop Competition Tube Specifications as of 10/20/2015

SpaceX Hyperloop Test-Track Specification

Revision 1.0

October 20, 2015

CONTENTS

1	Introduction	2
2	Structural	3
3	Propulsion System and Interface.....	8
4	Power	13
5	Communications.....	13
6	Navigation Aids	14
7	Environments	16

1 INTRODUCTION

On August 12, 2013, Elon Musk released a [white paper](#) on the Hyperloop, his concept of high-speed ground transport. In order to accelerate the development of a functional prototype and to encourage student innovation, SpaceX is moving forward with a competition to design and build a Hyperloop Pod. In parallel with the competition, SpaceX will be constructing a sub-scale test track adjacent to its Hawthorne, California headquarters. During Design Weekend in January 2016, entrants will submit and present their Pod designs. On Competition Weekend, scheduled for Summer 2016, entrants will operate their Pods within the SpaceX test track.

This document contains the technical specifications for the test track that SpaceX will build to support Competition Weekend. As this is the first Hyperloop ever built, it is likely that small changes will occur during the construction process.

Note: This competition is a SpaceX event. *SpaceX has no affiliation with any Hyperloop companies, including, but not limited to, those frequently referenced by the media.*

Any questions or comments should be submitted to Hyperloop@spacex.com or can be posted on the Hyperloop Forum at <http://tx.ag/hyperloopforum> (click on “Enroll Now” to join).

2 STRUCTURAL

The test track will be an approximately 1-mile-long steel tube with a 6-foot outer diameter, fitted with an aluminum sub-track and rail mounted to a concrete fill bed. At the tube's egress door, there is a 12-foot-long "foam pit" to help mitigate the {hopefully non-occurring} case of a Pod braking system failure. The tube sections will rest on concrete cradles, reinforced with steel and fitted with PTFE slip bearings.

The parameters of the Hyperloop test track are:

- Material: ASTM A1018 Grade 36
- Outer diameter: 72.0 inches
- Inner diameter: 70.6 inches
- Wall thickness: 0.70 inches
- Length: 1 mile (approximate)
- Subtrack material: Aluminum 6101-T61
- Subtrack roughness: 125 RMS with potential for occasional surface scratches up to 0.008"
- Subtrack thickness: 1.0" for first and last 200 feet; 0.5" for remainder of tube
- Rail Material: Aluminum 6061-T6
- Internal Pressure: 0.02 – 14.7 PSI

In order to support various types of propulsion systems, compressors (if applicable), and outer mold lines, the Pod team may select the tube's operating pressure from the range given above.

All critical dimensions and tolerances are outlined on the drawing on the next page. Please note that the latest drawing revision will always supersede notes in this specification. These notes below are for reference only.

- The flatness profile per unit square is 0.04". This means that local undulations of the plate as installed will be 0.04" or less over a 15" x 15" square.
- The maximum variation of the top plane of the track relative to the theoretical center point of the tube is +/-0.4". Important to note is that this variation does not mean you could have an abrupt step, as the maximum slope of the track in the longitudinal direction is limited to 0.04" per foot.
- Maximum slope of the track in the lateral direction is covered by the parallelism callout and will be 0.06" per subtrack plate.
- See drawing for smoothness values for pipe section joint and helical pipe weld.

Four important open items to be decided after Design Weekend:

- SpaceX is attempting to widen the subtrack from 12" to 15" in order to give teams larger levitation surfaces. However, that widening is not definitive and thus, two drawings are shown.
- SpaceX has not decided the final flushness of the aluminum to the concrete. In the drawings, it is shown as flush, but it might be elevated as high as resting on the concrete.
- SpaceX is still working on optimizing the overall plate lengths and installation gaps. The current baseline is a gap pitch of every 12.5 feet with a maximum gap size of 0.1" to 0.125". We will strive to get the gap size down to 0.05" for the first several hundred feet of the track. Gaps may

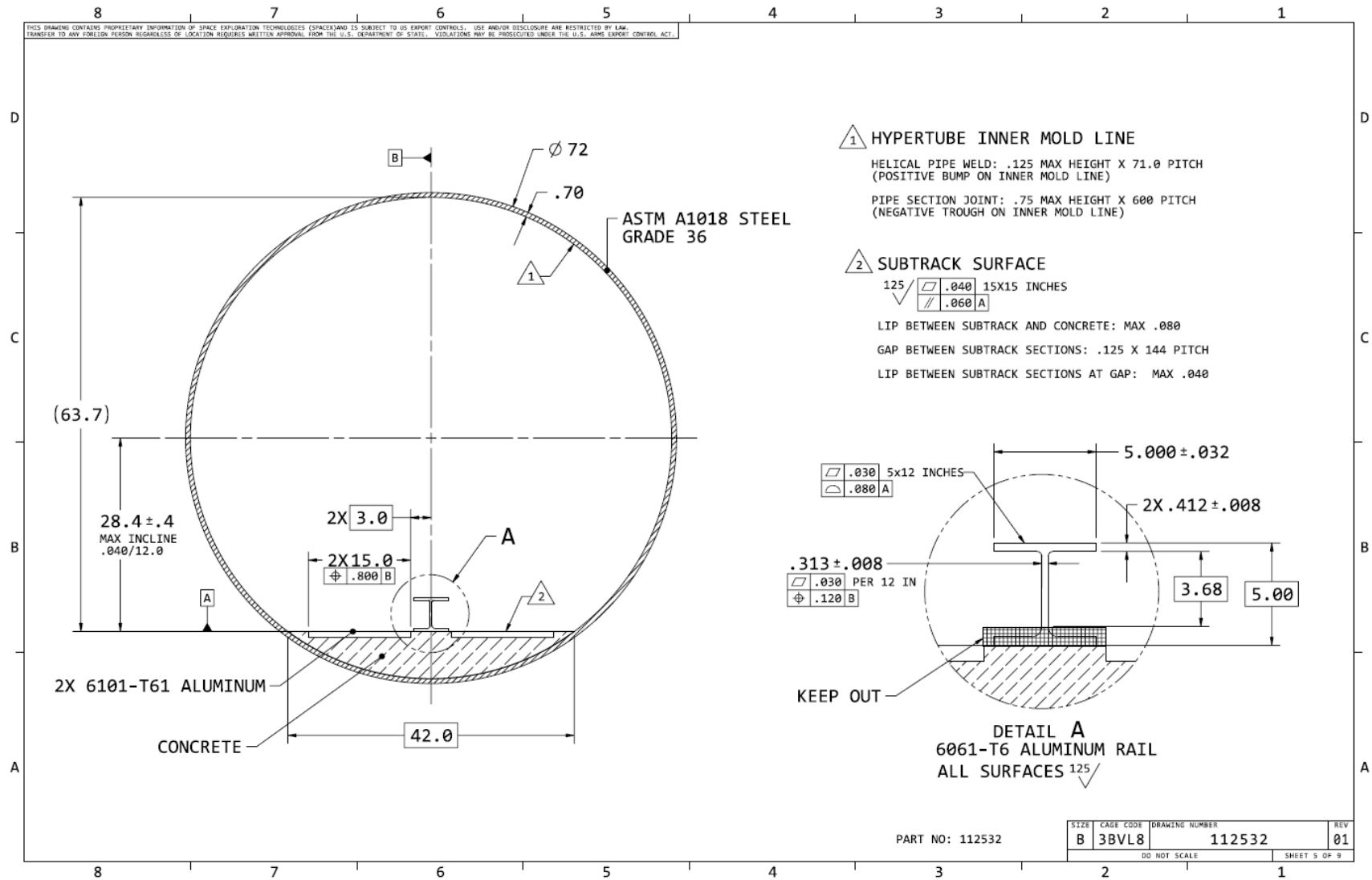
or may not be filled with a non-conductive flexible filler. Maximum steps in height between plates on the track will be limited to 0.04" or less.

- The shape of the central rail is baselined as an I-Beam shape, but see note on Page 7.

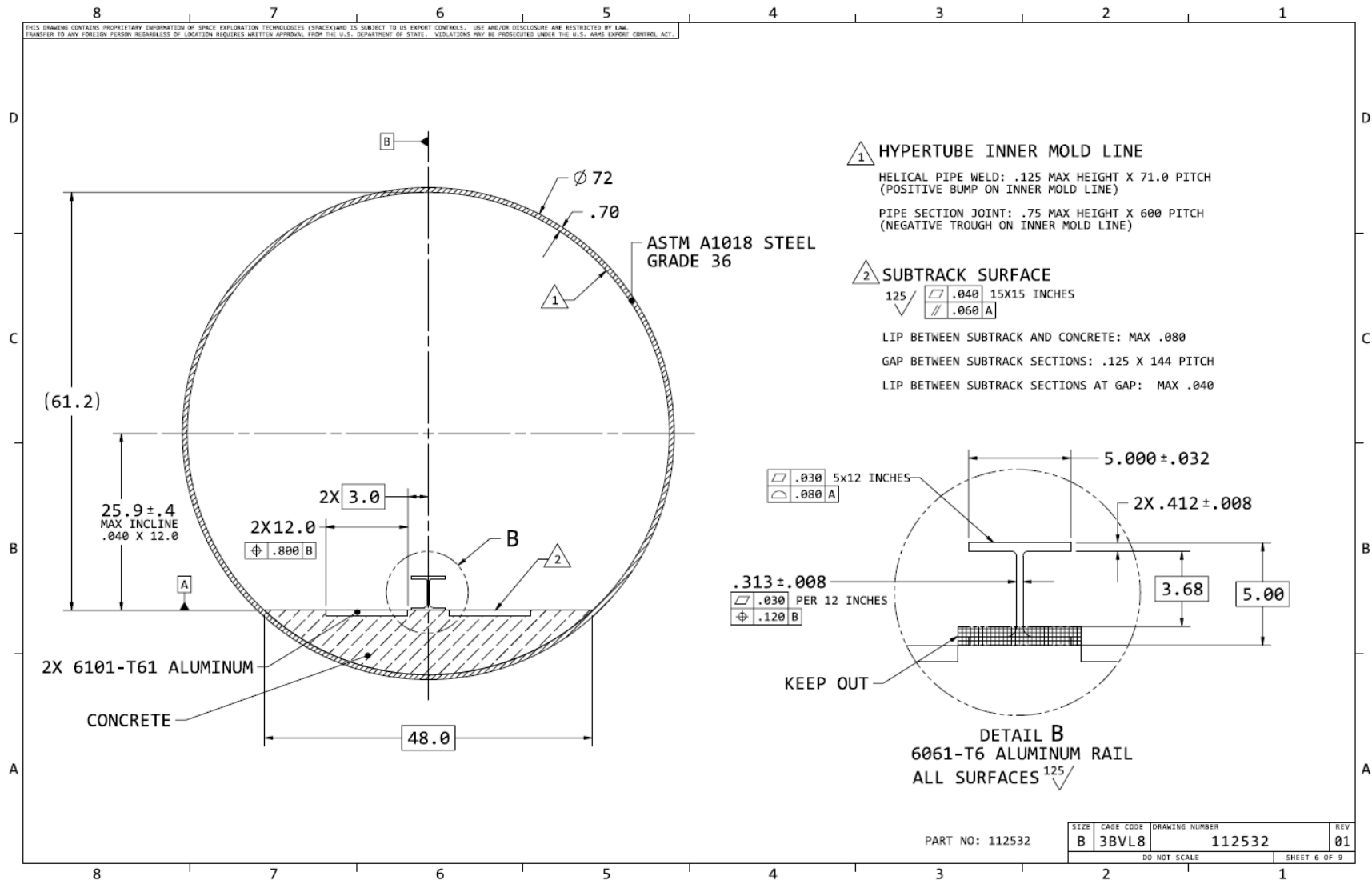
The test track has been designed to be flexible and to allow competitors to implement, at a minimum, the following three types of levitation/suspension:

1. **Wheels:** The concrete (and aluminum) flat sections along the outside allow for a good wheel surface and aluminum rail(s) allow for horizontally oriented wheels, as implemented on certain roller coasters.
2. **Air Bearings:** The aluminum plate allows for a much smoother and flatter surface than the steel tube itself. The rail(s) can be used for lateral control, either through side-mounted bearings or wheels.
3. **Magnetic levitation:** Several forms of magnetic levitation require a conductive non-magnetic surface (e.g. copper or aluminum). The sub-track allows for magnetic levitation and the rail(s) allow for lateral control.

Subtrack: Aluminum subtrack (30" total surface width) with central rail (all dimensions in inches)

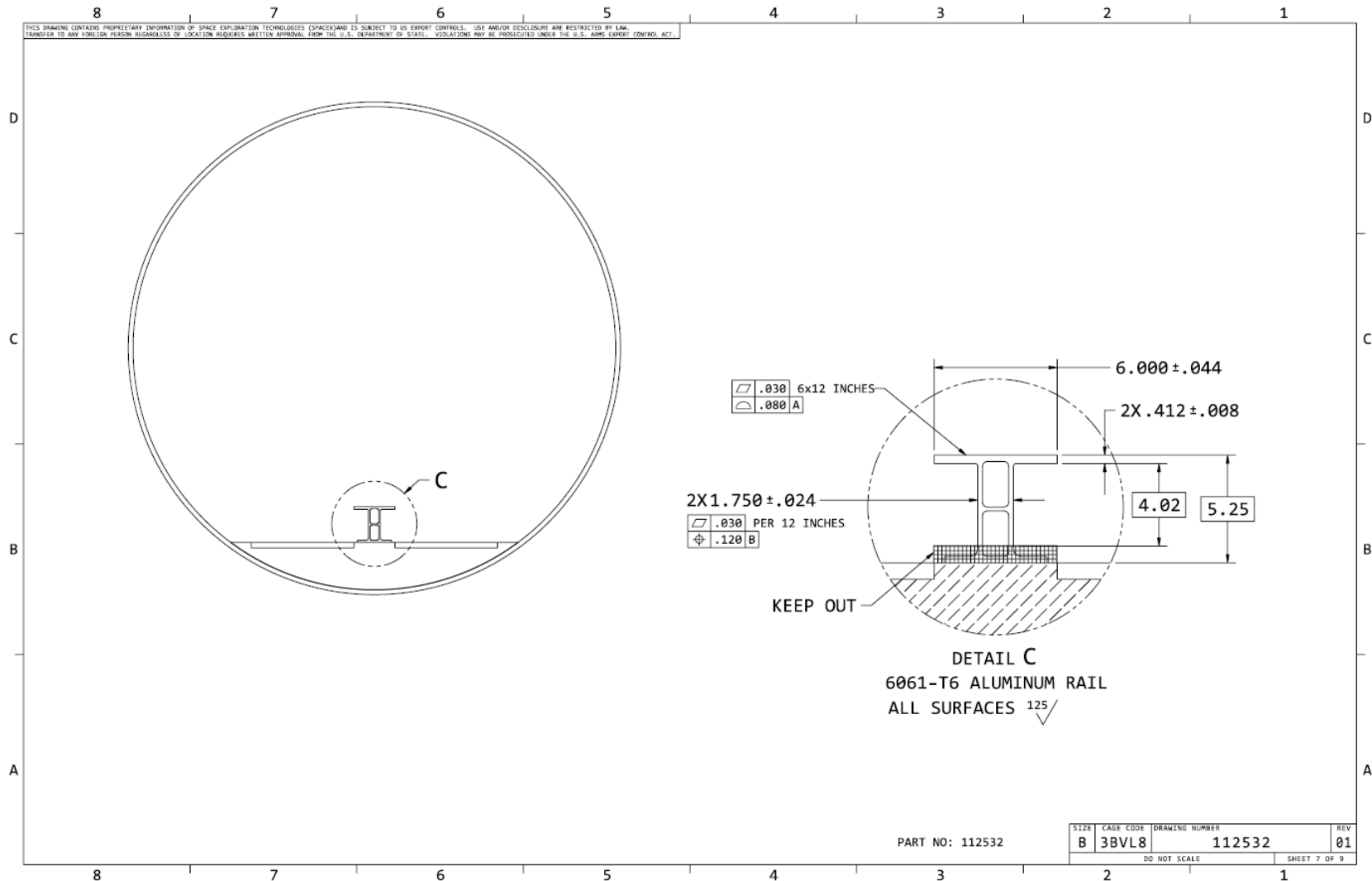


Subtrack: Aluminum subtrack (24" total surface width) with central rail (all dimensions in inches)



Potential Alternative Central Rail

The baselined central rail is currently an I-beam shape, but SpaceX is considering a custom rail shape to give teams more flexibility and surface area. This alternative rail detail "C" would directly replace the rail detail "A" or "B" in the previous specifications of the drawing.



3 PROPULSION SYSTEM AND INTERFACE

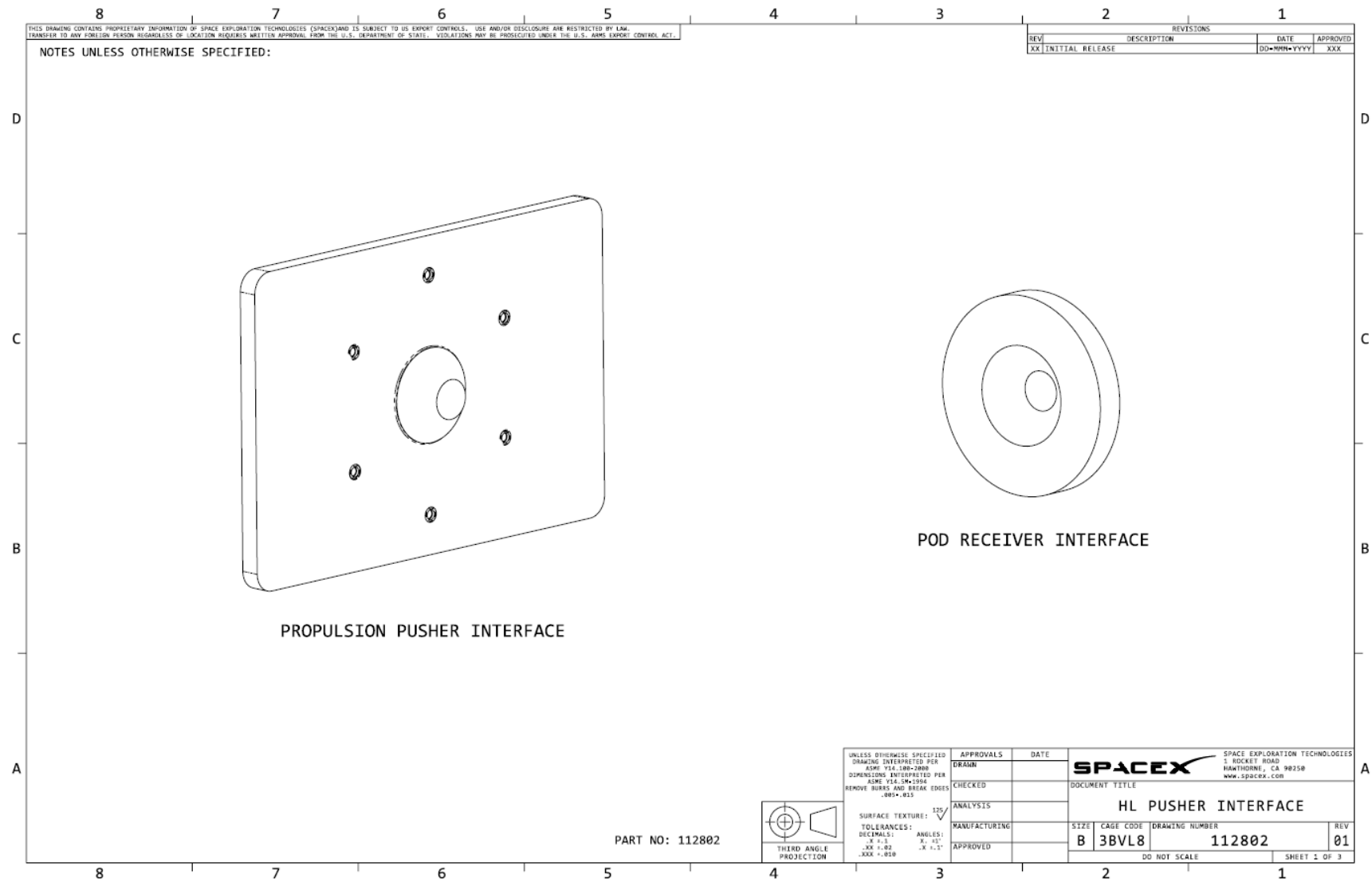
The test track will not be fitted with a structurally integrated propulsion system. Instead, teams have 3 options with regards to initial propulsion:

1. *On-Pod Propulsion System.* This can take for the form of a drive train for wheels, magnetic repulsion, or compressed gas (stored or from turbine). For all cases, entrants can specify the tube's operating pressure to help optimize their system.
2. *Off-Pod Propulsion System.* Teams can work with SpaceX to create their own system, which we can integrate into the tube for that Pod's specific run. This option only applies to very specific Pod designs.
3. *SpaceX Pusher.* SpaceX will construct a high-power wheeled vehicle and attach an interface plate to the front, which can then push Pods up to speed.
 - a. The Propulsion Pusher Interface consists of a flat pusher plate with a centering cone, which will be laterally centered in the tube. See diagrams on the next three pages.
 - b. The height of the cone center can be adjusted, in 2.0-inch increments, between 8 and 20 inches above the concrete, as specified by each Pod team.
 - c. The Interface will float up to 1.0-inch vertically to accommodate levitation after contact.
 - d. For teams interested in a non-standard pusher interface, there are 6 quarter inch inserts in a 6 inch diameter circle on the SpaceX cone side of the interface. Teams may choose to manufacture and bring both sides of their pusher/pod interface joint and mount their pusher side to the SpaceX interface prior to competition. Pre-coordination is required with SpaceX prior to building a custom launch mount. In general, these shall have a weight less than 10 lbs, a length less than 12 inches from the surface of the plate, and the team shall bring their own fastening hardware.
 - e. Maximum displacement for the acceleration profile is 800 feet.
 - f. Each Pod acceleration profile will have to be approved by SpaceX, on a case-by-case basis. Representative pusher acceleration values are shown in the table on the next page. It is very likely that Pods are started at lower values of acceleration than shown in the table.
 - g. Each Pod utilizing this pusher will have to demonstrate mass distributions and separation dynamics to ensure a straight push with limited separation moment.
 - h. Maximum velocities will be determined based on final Pod designs and will be capped in order to make the Judging Criteria fair amongst Pods of different masses.
 - i. The SpaceX Pusher specification will likely not be finalized until early 2016. Thus, Pod teams who utilize this system do face the risk of small interface modifications, and thus should ensure their mechanical interface remains flexible.

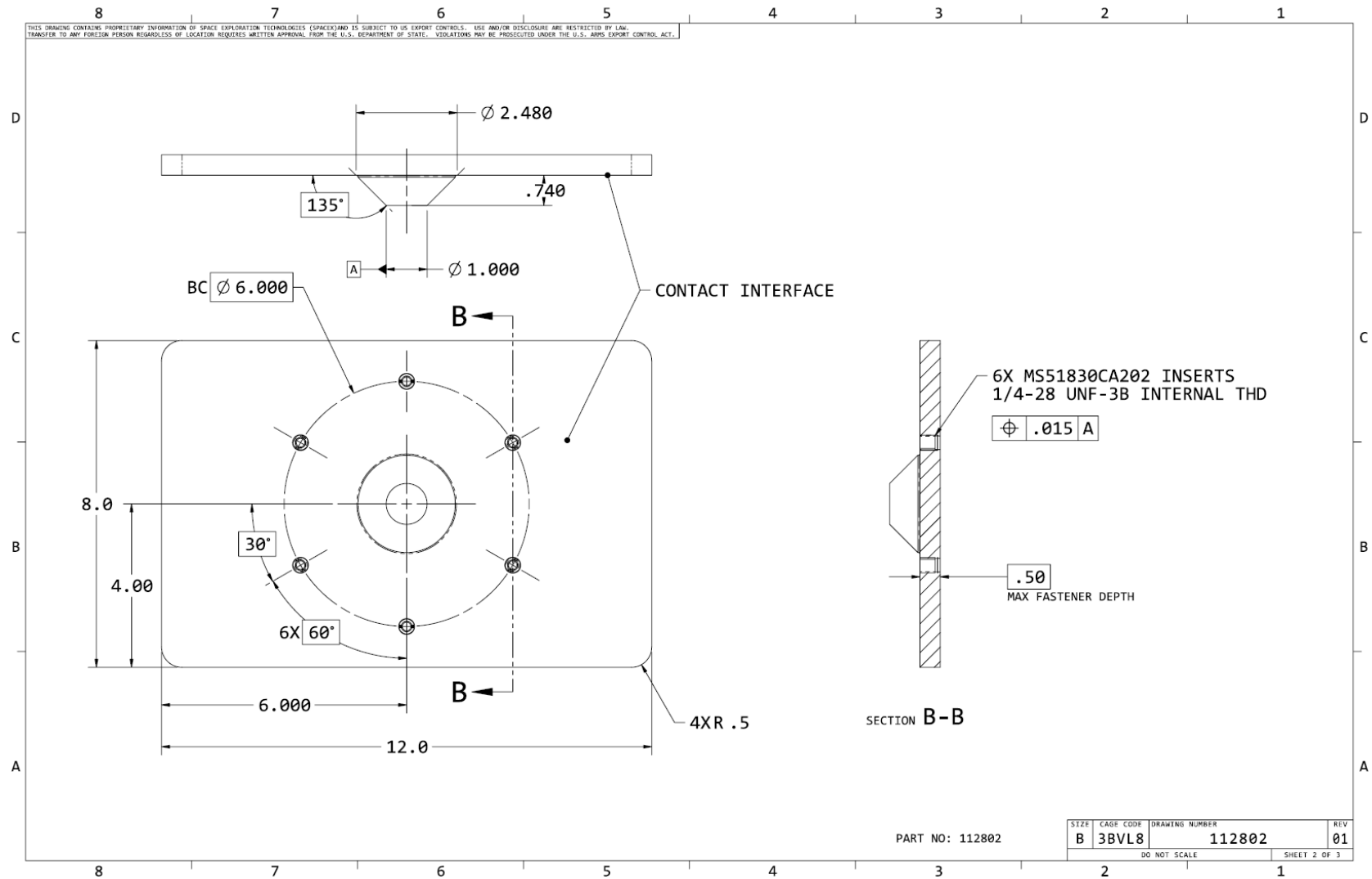
Representative pusher acceleration values

Pod Mass (kg)	Pod Mass (lbm)	Pod Acceleration (g)
250	550	2.4
500	1100	2.0
750	1650	1.7
1000	2200	1.5
1500	3300	1.2
2000	4400	1.0
2500	5500	0.9
3000	6600	0.8
4000	8800	0.6
5000	11000	0.5

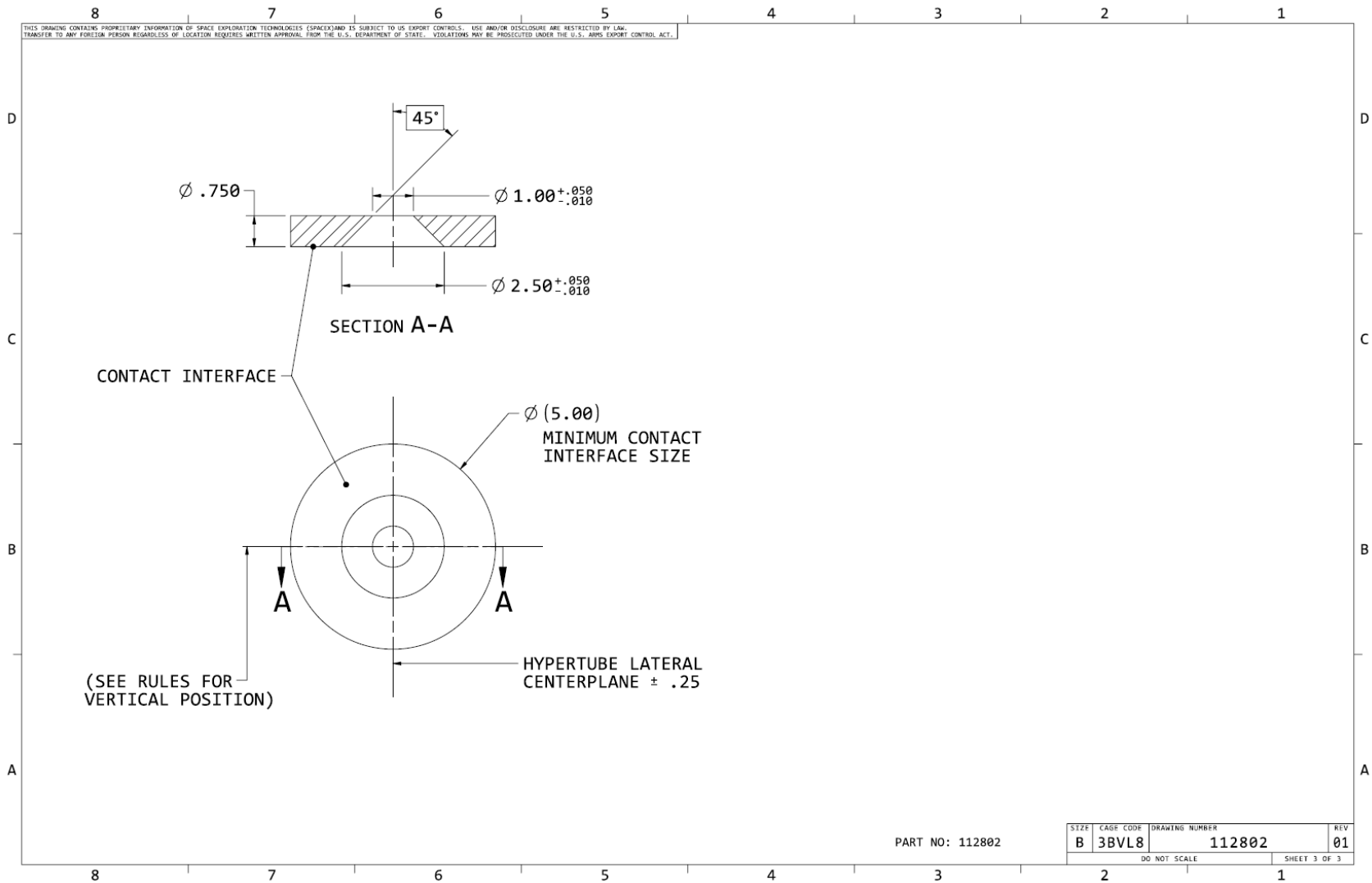
Pusher Interface (1 of 3) (all dimensions in inches)



Pusher Interface (2 of 3) (all dimensions in inches)



Pusher Interface (3 of 3) (all dimensions in inches)



4 POWER

In general, Pod power shall be provided on the Pod itself and there is no auxiliary electric rail in the test track. However, for the pre-launch phases, SpaceX will provide a quick-disconnect electrical umbilical, known as the Hyperloop Power Umbilical. It will be a standard electrical connector with a lanyard release mechanism. The specific capacities and connector-type for the power provided will be released after subsequent feedback is received from teams building Pods for Competition Weekend. Reasonable supplies would be:

- 240 VAC at up to 60 A (single phase, 60 hz)
- 110 VAC at up to 60 A (single phase, 60 hz)
- 28 VDC at up to 100 A

5 COMMUNICATIONS

SpaceX will provide four Access Points (AP's):

1. External to the tube at the entrance (AP_EXT_ENTER)
2. Internal to the tube at the entrance (AP_INT_ENTER)
3. External to the tube at the exit (AP_EXT_EXIT)
4. Internal to the tube at the exit (AP_INT_EXIT)

The external AP's are meant for connections by the ground support teams or any auxiliary Pod testing. The internal AP's will be fitted with directional antennas to beam the signal the length of the tube in order to support standard WiFi receive hardware.

The client (Pod) side WiFi requirements are:

- Support either or both 2.4/5 GHz bands (dual band client)
- WPA2/AES capable client
- PSK authentication
- SSID will be determined by SpaceX and communicated to Pod team before Competition
- Supports either static or DHCP (IP/Subnet will be provided Prior to Competition)
- Flat network (i.e. one subnet)

For transmit connectivity, Pod teams may select any method/hardware they would like. A known solution is to install an AP on the Pod itself; as an example, while large, the [Cisco IW3700](#) would meet the necessary power levels.

Roaming between wireless access points mid-flight (i.e. from AP_INT_ENTER to AP_INT_EXIT) will be allowed, but the specifics will have to be discussed with the SpaceX team.

6 NAVIGATION AIDS

Every 100 feet, a 2-inch wide reflective circumferential stripe will be applied to the inner circumference of the tube. The stripes will be located on the upper 180° of the tube (“9 PM to 3 PM”). The stripe material will consist of [Reflective Tape in Fluorescent Red-Orange Color](#) (P/N 75050060534).

At 1,000 feet from the end of the tube, the upper 180° of the tube will be split into two 90° sections. The right side of the tube will continue to use the same Fluorescent Red-Orange tape. The left side of the tube will use [Reflective Fluorescent Lime-Yellow tape](#) (P/N 75050060518) for the remainder of the tube. The pattern on both sides of the tube will be the same, color will be the only difference.

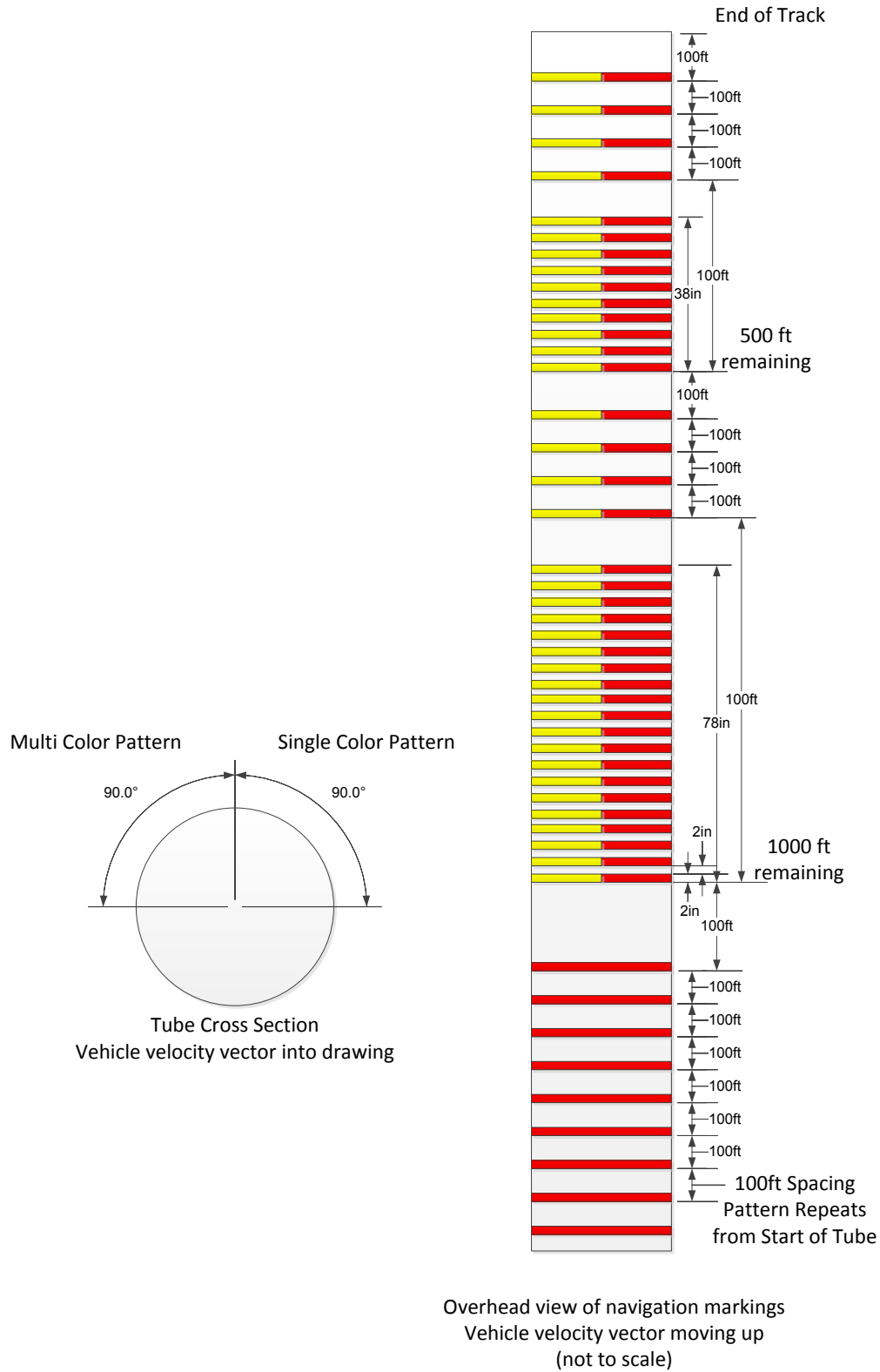
At 1,000 feet, a pattern of twenty 2-inch wide stripes separated by 2-inch “blank sections” of the underlying steel tube will be applied as a “1,000 feet left” marker for the Pods. The entire installation is thus 78 inches long.

Similarly, at 500 feet from the end of the tube, a pattern of ten 2-inch wide stripes separated by 2-inch “blank sections” of the underlying steel tube will be applied as a “500 feet left” marker for the Pods. The entire installation is thus 38 inches long.

The entire interior of tube will be illuminated throughout at standard room levels using standard “white” floodlighting from directly above the track. Based on Design Weekend feedback, it is possible that this is changed to narrow-band illumination. Soon after Design Weekend, full lighting specifications (and reflectivity data for the steel) will be released.

See next page for depiction of optical markings.

Summary of Optical Markings



7 ENVIRONMENTS

SpaceX will provide a self-contained environments measurement system to be used for measuring the dynamics environment, temperature and pressure. The logger to be used is the [Mide Slam Stick X Aluminum](#). A 3D model for the Aluminum version of the logger is available on the product website.



7.1 Concept of Operations

1. SpaceX official installs activated logger on test vehicle in the Ingress Staging Area of the track.
2. Test is performed.
3. SpaceX official uninstalls logger in the Egress Exit Area portion of the track
4. SpaceX official extracts logged content and stores with other test artifact files.

7.2 Installation

Teams will provide a logger mount point on the chassis of their vehicle. The mount point shall consist of three holes threaded for a 4-40 bolt. The holes must be at least a ¼ inch deep. The logger bolts shall be torqued to 6in-lbs. The logger shall be aligned with the X axis pointing out the front of the vehicle within 10° of the nominal direction of travel, parallel to the track. The Y axis shall point out the port side of the vehicle, the Z axis out the top of the vehicle. The plane formed by the X and Y axis must be parallel to the plane of the track within 5° at all times. This mount point may not be isolated from the chassis in any way that would alter the acceleration measured at the logger when compared to the acceleration experienced by the chassis. The mounting location on the vehicle shall be accessible while the vehicle is in the Ingress Staging Area of the track for an operator to use a torque wrench to install the logger.

7.3 Data Availability

Logged test data is available to teams for their vehicle by request.